12-2002

Statistical Mechanical Models of Adsorption and Diffusion of Fluids in Crystalline Nanoporous Materials

Mithun Ramdas Kamat
University of Tennessee - Knoxville

To the Graduate Council:

I am submitting herewith a thesis written by Mithun Ramdas Kamat entitled "Statistical Mechanical Models of Adsorption and Diffusion of Fluids in Crystalline Nanoporous Materials." I have examined the final electronic copy of this thesis for form and content and recommend that it be accepted in partial fulfillment of the requirements for the degree of Master of Science, with a major in Chemical Engineering.

Dr. David J. Keffer, Major Professor

We have read this thesis and recommend its acceptance:

Dr. Paul D. Frymier, Dr. Brian J. Edwards, Dr. Mary Leitnaker

Accepted for the Council:
Carolyn R. Hodges

Vice Provost and Dean of the Graduate School

(Original signatures are on file with official student records.)

To the Graduate Council:

I am submitting herewith a thesis written by Mithun Ramdas Kamat entitled "Statistical Mechanical Models of Adsorption and Diffusion of Fluids in Crystalline Nanoporous Materials". I have examined the final electronic copy of this thesis for form and content and recommend that it be accepted in partial fulfillment of the requirements for the degree of Master of Science, with a major in Chemical Engineering.

Dr. David J. Keffer

We have read this thesis and
recommend its acceptance:

Dr. Paul D. Frymier

Dr. Brian J. Edwards

Dr. Mary Leitnaker

Accepted for the Council:

Dr. Anne Mayhew

Vice Provost and Dean of
Graduate Studies

(Original signatures are on the file with official student records.)

STATISTICAL MECHANICAL MODELS OF ADSORPTION AND DIFFUSION OF FLUIDS IN CRYSTALLINE NANOPOROUS MATERIALS

A Thesis

Presented for the

Master of Science Degree

The University of Tennessee, Knoxville

Mithun Ramdas Kamat

December 2002

DEDICATION

This thesis is dedicated to my dear and loving family. My parents, Mrs. Archana R. Kamat and Mr. Ramdas K. Kamat for their continued support, and to my younger brother, Ashish who has been my best friend all these years

ACKNOWLEDGEMENTS

First and foremost, I would like to express my deep gratitude and sincere appreciation to my advisor and guru Dr. David Keffer for his encouragement and support. This thesis would not have been possible without his constant inputs and suggestions. His generous spirit breathes throughout these pages. I am grateful to have had the opportunity to work with such a brilliant, sincere, and a truly dedicated chemical engineer these past two years. I would also like to thank him for his support during the time I had undertaken a co-op assignment during the final stages of this thesis.

I would also like to thank my other committee members including Dr. Paul Frymier, Dr. Brian Edwards, and Dr. Mary Leitnaker for their comments and advice.

Also, I am grateful to Dr. Charlie Moore, who introduced me to process control and for helping me become aware of and think through many ideas I had not previously considered.

Special thanks are due to the departmental secretaries, Ms. Betty Frazier and Ms. Susan Seymour for their pleasant demeanor and excellent handling of the office work.

Finally, I acknowledge the love and support of my friends, Ms. Vidhya Iyer and Mr. M. Rajkumar. Their friendship has been invaluable to me, and I thank them for their constant encouragement, especially during the final stages of this thesis.

ABSTRACT

Statistical mechanical analytical theories are developed to model adsorption and diffusion of single component and binary fluids in crystalline nanoporous materials. The theory provides insight into the molecular level mechanisms governing the behavior of adsorbed molecules. The theory predicts diffusivities, adsorption isotherms, and heats of adsorption as functions of temperature, pressure, and composition.

Molecular dynamics simulations have identified localized adsorption sites within the adsorbent lattice. In this work, a lattice model of adsorption is developed using an extension of the Quasi-Chemical Approximation Theory. The theory demonstrates that competing entropic and energetic effects dictate the placement of molecules within the lattice sites. The lattice theory is completely general and predictive in nature, and requires very few parameters to characterize the system.

A lattice model of diffusion is developed. The theory yields a self-diffusion coefficient, which is a function of (i) temperature, (ii) adsorbate density, (iii) adsorbate size, (iv) the adsorbate-adsorbate energetic interaction, and (v) the adsorbate-pore energetic interaction. The theory incorporates no fitting parameters and is generalizable to nanoporous materials with three-dimensional porous networks (e.g. Zeolite Y) and one-dimensional porous networks (e.g. $AlPO_4$-5).

The analytical theory is tested with molecular dynamics simulations. Comparisons are presented between the results predicted by the theory and simulations. The agreements and discrepancies between the two approaches are discussed. The theory requires only a minute on a desktop PC to generate the results as against hours of parallel supercomputer time required by the simulations.

This thesis presents an analytical molecular level theory that can be integrated into macroscopic process level simulators to (i) investigate new adsorbents, (ii) generate thermodynamic properties and transport properties in the adsorbed phase, and (iii) establish the principles of adsorption and diffusion in the macroscopic level using fundamentals of molecular physics and statistical mechanics.

TABLE OF CONTENTS

LIST OF FIGURES

LIST OF TABLES

Part 1

Introduction

This thesis investigates the adsorptive and diffusive properties of fluids in crystalline nanoporous materials using fundamentals of statistical mechanics. An analytical theory is developed to describe the phenomenon of adsorption and diffusion of fluids confined in nanopores. The generalized theory is presented in Parts 2 and 3. Parts 2-5 of this thesis contain the appropriate literature survey and a complete list of references pertinent to the particular study. This part provides a general overview of the status of the ongoing research in this field and the motivation for this work.

1.1 INTRODUCTION TO NANOPOROUS MATERIALS AND THEIR APPLICATIONS

The chemical industry has been increasingly examining different nanoporous materials as potential adsorbents in various applications. Nanoporous materials are attractive to the chemical industry due to a number of properties. As the name suggests, these materials have porous networks having dimensions on the order of one nanometer. One example of nanoporous materials is molecular sieves. Molecular sieves include silicates, aluminosilicates, aluminophosphates, and other various compositions. Zeolites, commonly used in the industry are a subset of molecular sieves, which include silicates and aluminosilicates. Figures (1 and 2) show two different types of molecular sieves – Zeolite Na-Y and $AlPO_4$-5. Zeolite Na-Y has a three-dimensional porous network whereas AlPO5 has a one-dimensional porous network.

The nanoporous materials have a large surface area per unit volume. Hence they find applications in the catalyst industry. Furthermore, different fluids adsorbed in the nanopores have different diffusivities due to the relative pore size and energetic interactions. Hence, these materials can effectively cause separation of fluid mixtures. Also, some molecular sieves, particularly zeolites, can facilitate ion exchange. This property is utilized in the softening of water.

1.2 MOTIVATION

Historically, molecular level simulations have been employed to investigate the phenomena of adsorption and diffusion in nanoporous materials. The simulations provide structural and transport properties of fluids adsorbed in nanoporous materials. The simulations also provide important insight into the physical mechanisms within the nanoporous adsorbent structure. However, the simulations are not predictive in nature. In other words, we still need to conduct simulations and experiment each time a new adsorbent-adsorbate system is investigated. Furthermore, the simulations are computationally inefficient and require a lot of parallel supercomputing effort. A predictive analytical theory that is completely generalizable and can be extended to various adsorbate-adsorbent systems will eliminate the above shortcomings. Furthermore, the theory would be easy to integrate into the industrial level process simulators unlike the computationally expensive simulations. Such a theory could also provide a better physical understanding of the system within the context of the molecular level mechanisms. This thesis presents a generalized predictive lattice theory that can describe the behavior of adsorbed molecules within confined geometries. The theory assumes a static lattice composed of different types of sites. The theory is very fundamental in nature and uses the principles of basic statistical mechanics. The theory demonstrates that competing energetic and entropic effects dictate the placement of molecules within the adsorbent pores. The theory requires only a minute on a desktop PC to generate all the thermodynamic as well as transport properties.

1.3 SYNOPSIS

In Part 2, "A generalized analytical theory for adsorption of fluids in nanoporous materials", the predictive lattice theory of adsorption is developed. The theory is presented in a very general form using principles of statistical mechanics. We develop the partition function, which is used to generate the thermodynamic properties (for instance, adsorption isotherms, total energy, Helmholtz free energy). We demonstrate the capabilities of the theory by generating thermodynamic and transport properties for

randomly chosen lattice parameters. Methane data is used for adsorbate properties because we needed a small, spherical molecule, which would provide simple radial adsorbate-adsorbate interaction potential for illustration purposes.

In Part 3, "An analytical theory for diffusion of fluids in crystalline nanoporous materials", we use the results generated by our lattice adsorption theory, and develop a lattice diffusion model to predict self-diffusivity. Our diffusion model assumes blocking species, and models diffusivity as a function of the activation barrier that these species provide to lattice diffusion. The mean diffusivity is a function of temperature, composition and adsorbate-adsorbate interactions.

In Part 4, "Agreement between the analytical theory and molecular dynamics simulations for adsorption and diffusion of fluids in crystalline nanoporous materials", we provide a comparison of our theory with Molecular Dynamics Simulations for single component methane in Zeolite Na-Y. Simulations have identified that the Zeolite Na-Y structure consists of two different types of sites with different maximum occupancies. Hence, Na-Y was an ideal candidate for a first comparison of our theory as it can be easily visualized as a lattice composed of two types of sites.

In Part 5, "A predictive model for adsorption and diffusion of fluids in nanoporous materials: Extension to binary mixtures", we extend the lattice theory for binary fluids. Using a completely generalized lattice model, we predict the thermodynamic and transport properties for both the components as functions of loading, temperature and composition. Some of the lattice parameters are randomly chosen whereas others are obtained from the comparison study explained in Part 4.

In Part 6, "Conclusions and Future Work", I draw some general observations from this work. Future work in this area is also discussed. The theory is presently developed for single component and binary mixtures. Some of the directions for future work are suggestions to extend the comparison studies for different geometries, and incorporate more complex qualitative functionality observed at extremely non-ideal conditions.

APPENDICES

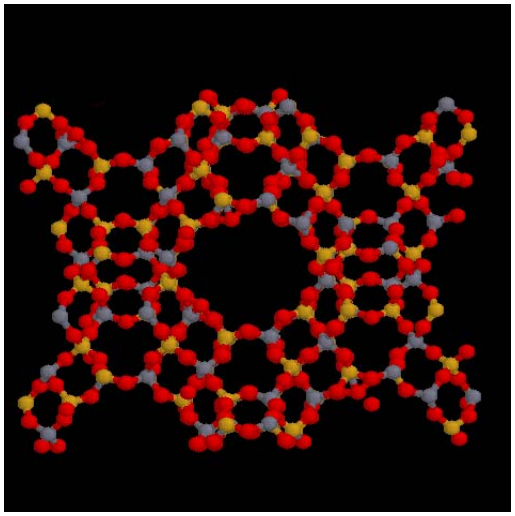

Figure 1: A three-dimensional porous network of Zeolite Na-Y.

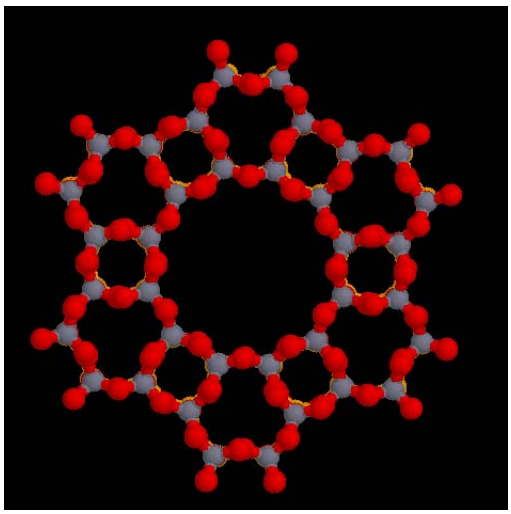

Figure 2: A one-dimensional porous network of $AlPO_4$-5

Part 2

A Generalized Analytical Theory for Adsorption of Fluids In Nanoporous Materials

ABSTRACT

An analytical theory is presented for the adsorption of fluids confined in zeolites, molecular sieves, and other nanoporous materials. The theory takes advantage of the localized adsorption sites within a zeolite and develops a statistical mechanical lattice model of adsorption. The theory is completely generalized and can be used to model the lattice of adsorption sites within any arbitrary zeolite. The theory also has the advantage of requiring very few parameters: it requires only four parameters to describe the adsorbent, which can be obtained from a potential energy map of the adsorbent. No molecular dynamics simulations are required for parameterization. The theory incorporates both the atomistic structure of the adsorbent and the fundamental physical mechanisms, both of which dictate the behavior of fluids confined in nanoporous materials. Finally the theory has the practical advantage of computational efficiency. The theory can generate a complete isotherm in approximately one minute on a desktop PC (300MHz), compared with tens of CPU hours of supercomputer or parallel cluster time necessary to perform the molecular dynamics simulations required to generate a few points of the same isotherm.

2.1 INTRODUCTION

2.1.1 Background

A substantial body of research on the behavior of fluids confined in nanoscale spaces has been conducted using molecular-level computer simulations. The goal of the simulation work has been to define the fundamental mechanisms for adsorption and diffusion in nanoporous materials.[1-84] The state of the research has matured to the point where the fundamental mechanisms are relatively well understood. It has been established that competing energetic and entropic effects dictate the placement of adsorbates within the nanoporous material [1-3, 6]. This placement is a function of the atomistic structure of the adsorbent, the size of the localized adsorption sites and the energetic well depth. [31]

However, due to the vast range of nanoporous materials—molecular sieves, zeolites, and MCM-type materials, the results for different systems often give seemingly contradictory results. For example, the diffusivity of methane may increase with methane loading in one nanoporous adsorbent, decrease with loading in a second, and show a maximum in a third absorbent [85,86,87]. The loading dependence of the diffusivity is of course dictated by the energetic and entropic landscape of the nanoporous environment. A unifying theory that incorporates the differences in the nanoporous environment would be able to show that the seemingly contradictory results in the literature are in fact manifestations of the same underlying physical mechanisms.

Technology transfer to industry of this body of simulation knowledge is somewhat limited by the fact that the simulations are computationally expensive. A predictive theory will reduce the computational requirement in obtaining, for example an adsorption isotherm, from hours of supercomputer usage to a few minutes on a desktop PC. Furthermore, the theory can be efficiently used for each new nanoporous material to be considered as an absorbent for a particular process. Additionally, a predictive theory can be easily integrated into industry standard finite-element process simulators, which

would demonstrate that the results indicated by molecular-level simulations do in fact have the suggested ramifications in a macroscopic chemical process.

2.1.2 Objective

The objective of the proposed work is to develop a predictive theory of adsorption in nanoscopically confined pore spaces.

2.1.3 Theory

Simulations of fluids adsorbed in zeolites and other molecular sieves have identified localized adsorption sites. Because these sites are localized, they can be described by an adsorption lattice. The lattice of adsorption sites is distinct from and located within the pore space defined by the crystal lattice of the adsorbent. Shifting from a continuum to a lattice model provides two major benefits. First, it drastically reduces computational time. Second, lattice models may have analytical solutions, which all but eliminates computational effort.

Several lattice models of adsorption have been proposed in the literature. Van Tassel et. al. [36] have introduced a lattice model for the adsorption of small molecules in zeolite NaA. Snurr et al. [14] have presented a lattice model for adsorption of benzene in silicalite. We provide a generalized model for the adsorption of any compound within any arbitrary zeolite.

Our predictive theory of adsorption and diffusion in nanoscopically confined pore spaces is a lattice model. We use standard statistical mechanics to develop the partition functions for the adsorbate molecules. From the partition functions, we can directly obtain the desired thermodynamic and transport properties. The nanoporous environment is determined by (i) adsorption site volume, (ii) adsorption site energetic well depth, (iii) lattice connectivity, (iv) and lattice spacing. These four factors are distinct for each combination of adsorbate and adsorbent but can be calculated without molecular dynamics simulations. All that is required is a potential energy map of the pore space

[31]. Thus, by minimizing the number of parameters required in the model, we make it more accessible to broader usage.

2.2. THEORY

The lattice model uses a generalization of the quasi-chemical approximation to account for adsorbate-adsorbate interactions. The quasi-chemical approximation is the simplest approximation that will still allow for adsorbate clustering within the pore, a phenomenon, which is critical to obtaining correct isotherms, transport properties, and phase change (e.g. capillary condensation).

The theory results in a system of highly nonlinear algebraic equations. In some cases, these equations must be solved numerically. However, the numerical solution to a small system of nonlinear algebraic equations can be accomplished in a few minutes on a desktop PC, as compared to days of computation time on a supercomputer, required to perform the analogous molecular dynamics simulations. To complicate matters, the system of equations is extremely stiff and a numerical technique must be specifically developed to account for the unique boundary conditions and scaling issues imposed by the functional form of the partition function. We suspect that it is the extreme difficulty in solving these equations that has prevented the theory from being exploited to date. In developing the theory, the bulk of our time is involved in creating a numerical algorithm that would solve the stiff equations efficiently and reliably.

2.2.1 One type of site

Consider an arbitrary lattice with connectivity (in other words, coordination number), c, with sites separated by distance, ℓ. The sites have a well-depth of $U_{AP}(x)$, where this is the potential energy due to adsorbate-pore interactions. $U_{AP}(x)$ may be a function of x, the occupancy of the site, where in a zeolite or molecular sieve x typically takes on values of 1 or 2. (The sites are small and cannot accommodate more than 1 or 2

adsorbates.) The sites have volume, V_S. The four parameters—c, ℓ, $U_{AP}(x)$, and V_S—completely characterize the lattice.

Consider a pure fluid adsorbing in the nanoporous material. The adsorbate is completely characterized by a given potential. In our case, we use the Lennard-Jones 6-12 potential

$$U_{LJ}(r) = 4\varepsilon\left[\left(\frac{\sigma}{r}\right)^{12} - \left(\frac{\sigma}{r}\right)^{6}\right] \tag{1}$$

Here, we require two additional parameters: σ, the molecule diameter and ε, the well depth of adsorbate-adsorbate interactions. Generally these Lennard-Jones parameters are obtained from the literature [88]. With this potential we specify the adsorbate-adsorbate potential energy due to adsorbates in neighboring sites (an intersite interaction), w_x, as

$$w_x = U_{LJ}(\ell) \tag{2}$$

The adsorbate molecule is assumed spherical such that the volume of the adsorbate is

$$V_A = \frac{\pi}{6}\sigma^3 \tag{3}$$

In the case where a site can hold more than one adsorbate, we have additionally, an intrasite adsorbate-adsorbate interaction, w_i. Since the sites sit next to each other, we assume that the potential in equation (1) is at a minimum, yielding a value of

$$w_i = U_{LJ}(r_{min}) = \varepsilon \tag{4}$$

The partition function for the system is composed of three factors: (i) the configurational degeneracy, (ii) the intrasite partition function, and (iii) energetic interactions due to neighboring atoms. In our model, we include only nearest neighbor interactions. In the simplest case, where we have only one type of site, which has a maximum occupancy of one adsorbate, the partition function in the canonical ensemble, takes the form:

$$Q(N,M,T) = \sum_{\text{configurations}} g(N,M) q(T)^N e^{-N_{11}\frac{w_x}{kT}} \tag{5.a}$$

Where N is the number of adsorbates, M is the number of sites, and T is the temperature, $g(N,M)$ is the configurational degeneracy, $q(T)$ is the intrasite partition function, and N_{11} is the number of neighbors of sites each with occupancy one. N_{11} is the only term that contributes to intersite interaction energy, since the other neighbor pairs, namely N_{00}, N_{01}, and N_{10} all contain empty sites.

In the more general case, where we retain one type of site but allow the sites to have arbitrary maximum occupancy, $m_s \geq 1$, we have the following analogous partition function

$$Q(N,M,T) = \sum_{\text{configurations}} g(N,M) \prod_{x=1}^{m_s} q(x,T)^{x \cdot n_s(x)} e^{-\sum_{x=1}^{m_s}\sum_{y \geq x}^{m_s} N_{xy}\frac{w_x}{kT}} \tag{5.b}$$

where $n_s(x)$ is the number of sites with occupancy x, and the product, $(x \cdot n_s(x))$ is the number of adsorbates in sites with occupancy x. The summation in the exponent includes all possible combinations of occupancies of neighboring sites with non-zero contributions to the intersite energy, avoiding double counting of N_{xy} and N_{yx}.

The intrasite partition function is given the form

$$q(x,T) = \left(\frac{V_S - xV_A}{x\,\Lambda^3} \right) e^{-\frac{x(x-1)}{2}\frac{w_i}{kT}} \tag{6}$$

where Λ is the thermal de Broglie wavelength. The factor $\frac{x(x-1)}{2}$ gives the correct number of intrasite adorbate-adsorbate interactions for any arbitrary occupancy, including one.

The next objective is to obtain the configurational degeneracy, $g(N,M)$, all number of neighbor pairs, N_{xy}, and all number of sites with occupancy x, $n_s(x)$, as a function of the known canonical ensemble variables, N, M, and T, as well as the 4 parameters that describe the lattice, and the 2 parameters that describe the adsorbate. There is no analytical solution for the general case, even when the maximum site occupancy, m_s, equals one, except at a $N/M = 0.5$. Therefore we must use an approximation.

The first approximation one might use in obtaining the configurational degeneracy is the Bragg-Williams approximation, which says that the adsorbate are randomly distributed, despite the fact that for non-zero w_x, this will not be true [89]. A physical manifestation of the Bragg-Williams approximation is that the adsorbates cannot cluster within the pore. Since, we have seen from simulations that adsorbate clustering in zeolites is important, we cannot use the Bragg-Williams approximation.

The next simplest approximation is the quasi-chemical approximation [90]. In the quasi-chemical approximation, neighboring pairs are counted independently—double counting some combinations, then reweighted to give the proper total number of states in the configurational degeneracy. This theory, while algebraically obtuse to manipulate, does yield adsorbate clustering. It is the theory we expand upon and use in this work.

For the simple case where we have one type of site, $N_T = 1$ and maximum occupancy $m_s = 1$, it can be shown that the configuration degeneracy is given by [90]

$$g(N,M) = \left(\frac{M!}{N!(M-N)!} \right)^{1-c} \frac{\left(\frac{cM}{2} \right)!}{N_{00}! \frac{N_{01}}{2}! \frac{N_{10}}{2}! N_{11}!} \tag{7.a}$$

The factor of ½ is inserted in some of the factorials to avoid double counting. Here, the maximum term approximation is used to remove the summation from the partition function. Additionally, in order to obtain the weighting factor, we maximize $g(N,M)$ with respect to the independent neighbor variables, N_{01}. We solve for N_{01} at the maximum and substitute it back into $g(N,M)$ to obtain the weighting factor. (See below for a discussion of determining independence among the various N_{xy}.)

It is a non-trivial excercise in combinatorics to show that for an arbitrary maximum occupancy, m_s, the configuration degeneracy of the quasi-chemical approximation can be written as

$$g(N,M) = \left(\frac{M!}{\prod_{x=0}^{m_s} n_s(x)!} \right)^{1-c} \frac{\left(\frac{cM}{2} \right)!}{\prod_{x=0}^{m_s} \prod_{y=0}^{m_s} \frac{N_{xy}}{(2-\delta_{xy})}!} \tag{7.b}$$

where δ_{xy} is the Kronecker delta function, which is unity for $x = y$ and zero otherwise.

At this point we require equations to obtain (i) all number of neighbor pairs, N_{xy}, and (ii) all number of sites with occupancy x, $n_s(x)$. These equations take five forms. First, we have symmetry relations of the form:

$$N_{xy} = N_{yx} \qquad \text{for all } x \neq y \tag{8.a}$$

Second, we have a site balance:

$$M = \sum_{x=0}^{m_s} n_s(x) \tag{8.b}$$

Third, we have an adsorbate balance:

$$N = \sum_{x=1}^{m_s} x \cdot n_s(x) \tag{8.c}$$

Fourth we have balances on the number of neighbors, which have the form

$$\frac{c \cdot n_s(x)}{2} = \sum_{y=0}^{m_s} \frac{N_{xy}}{(2-\delta_{xy})} \qquad \text{for } 0 \le x \le m_s \tag{8.d}$$

The linear algebraic constraints in equations (8.a) through (8.d) are not sufficient to define all of the variables. For example, in the case where $m_s = 1$, the set of unknown variables is $\{n_s(0), n_s(1), N_{00}, N_{01}, N_{10}, N_{11}\}$, so that we have six unknowns. In terms of constraints, we have one symmetry equation (8.a), one site balance (8.b), one adsorbate balance (8.c), and two neighbor balances (8.d), giving a total of five equations. We lack one equation.

In the case where $m_s = 2$, the set of unknown variables is $\{n_s(0), n_s(1), n_s(2), N_{00}, N_{01}, N_{02}, N_{10}, N_{11}, N_{12}, N_{20}, N_{21}, N_{22}\}$, so that we have twelve unknowns. In terms of contraints, we have three symmetry equation (8.a), one site balance (8.b), one adsorbate balance (8.c), and three neighbor balances (8.d), giving a total of eight equations. We lack four equations.

The final step of the quasi-chemical approximation, is to take all variables, not defined by the above constraints and minimize the partition function with respect to them. So that, in the case where $m_s = 1$, the remaining equation is:

$$\left(\frac{\partial \ln Q}{N_{01}}\right)_{N,M,T} = 0 \tag{9.a}$$

For the case where $m_s = 2$, the remaining equations are

$$\left(\frac{\partial \ln Q}{N_{01}}\right)_{N,M,T} = 0 \;,\; \left(\frac{\partial \ln Q}{N_{02}}\right)_{N,M,T} = 0 \;,\; \left(\frac{\partial \ln Q}{N_{12}}\right)_{N,M,T} = 0 \;,\; \left(\frac{\partial \ln Q}{n_s(2)}\right)_{N,M,T} = 0 \tag{9.b}$$

What remains is a system of algebraic equations (six for $m_s = 1$ and twelve for $m_s = 2$) which must be solved simultaneously to yield the partition function. Once these variables are known, we know the partition function and we can extract thermodynamics properties from it per usual procedure.

For the simplest cases, the system of equations has an analytical solution. For more complicated systems, we were generally unable to obtain analytical solutions. In those cases, we used numerical techniques to find the roots. (See the Numerical Methods Section below.) Here, we present, analytical solutions for three simple cases.

For $N_T = 1,\ m_s = 1,\ w_x = 0$ (no intersite adsorbate-adsorbate interactions)

$$n_s(0) = M - N, \qquad n_s(1) = N, \qquad \text{and} \qquad N_{xy} = \frac{1}{(1+\delta_{xy})}\frac{c}{M} n_s(x) n_s(y) \quad (10.a)$$

This is the standard qausi-chemical approximation without adsorbate interaction.

For $N_T = 1,\ m_s = 1,\ w_x \neq 0$ (non-zero intersite adsorbate-adsorbate interactions)

$$n_s(0) = M - N, \qquad n_s(1) = N,$$

$$N_{01} = \frac{cM + \sqrt{(cM)^2 - 4(1-a)c^2 N(M-N)}}{2(1-a)} \quad (10.b)$$

$$N_{00} = \frac{c}{2} n_s(0) - \frac{1}{2} N_{01}, \qquad N_{10} = N_{01}, \qquad N_{11} = \frac{c}{2} n_s(1) - \frac{1}{2} N_{01}$$

where $a = e^{-\frac{w_x}{kT}}$.

This is the standard qausi-chemical approximation with adsorbate interactions.

For $N_T = 1,\ m_s = 2,\ w_x = 0$ (no intersite adsorbate-adsorbate interactions)

$$n_s(2) = \frac{-\left(-n + \frac{q(1)^2}{q(2)^2}(n-m)\right) + \sqrt{\left(-n + \frac{q(1)^2}{q(2)^2}(n-m)\right)^2 - \left(1 - \frac{q(1)^2}{q(2)^2}\right)n^2}}{2\left(1 - \frac{q(1)^2}{q(2)^2}\right)}$$

$$n_s(0) = M - n_s(1) - n_s(2), \qquad n_s(1) = N - 2n_s(2), \tag{10.c}$$

$$N_{xy} = \frac{1}{(1+\delta_{xy})}\frac{c}{M} n_s(x) n_s(y)$$

For $N_T = 1,\ m_s = 2,\ w_x \neq 0$, we found no analytical solution. We solved the system of equations using a numerical technique.

2.2.2 Two types of sites

Most zeolites and molecular sieves have more than one type of site. Even in these cases, the lattice sites are still localized and can be solved using a lattice model. We now extend the theory to an arbitrary lattice with two types of sites, $N_T = 2$. This lattice is described by a connectivity matrix, $\underline{\underline{c}}$, where

$$\underline{\underline{c}} = \begin{bmatrix} c_{11} & c_{12} \\ c_{21} & c_{22} \end{bmatrix} \tag{11}$$

where each of these elements, c_{ij}, describes the number of sites of type j connected to a site of type i. Specifying the connectivity in this way specifies the relative number of sites of Types 1 and 2, M_1 and M_2.

As an example consider the lattice schematic in Figure 1. In this case, $\underline{\underline{c}} = \begin{bmatrix} 0 & 3 \\ 2 & 0 \end{bmatrix}$. The number of sites of Type 1 and 2 must obey the relations:

$$\sum_{i=1}^{N_T} M_i = M \tag{12.1}$$

and a neighbor balance

$$c_{12}M_1 = c_{21}M_2 \tag{12.2}$$

which determines M_1 and M_2 to be

$$M_1 = \frac{c_{21}}{c_{12} + c_{21}} M \qquad \text{and} \qquad M_2 = \frac{c_{12}}{c_{12} + c_{21}} M \tag{13}$$

The separation between nearest neighbor sites is given by a matrix of distances, $\underline{\underline{\ell}}$. When there are no nearest neighbor sites of type i and j (i.e. $c_{ij} = 0$), the value of ℓ_{ij} is immaterial. As before, the sites have a well depth of $U_{AP,i}(x)$, where this is the potential energy due to adsorbate-pore interactions. $U_{AP,i}(x)$ is now not only a function of x b, the occupancy of the site, but also of site type i. The sites have volume, $V_{S,i}$. As was the case with $N_T = 1$, the four parameters—$\underline{\underline{c}}$, $\underline{\underline{\ell}}$, $\underline{U_{AP}}(x)$, and $\underline{V_S}$—completely characterize the lattice.

We again use an arbitrary pairwise potential to model the adsorbate-adsorbate interactions, evaluating it at $\underline{\underline{\ell}}$ to obtain $\underline{\underline{\underline{w_x}}}$.

The partition function again has the same three factors, a configurational degeneracy, intrasite partition function, and intersite interaction energy, but is extended to account for sites of type i = 1 to N_T:

$$Q(N,M,T) = \sum_{\text{configurations}} g(N,\underline{M}) \prod_{i=1}^{N_T} \left[\prod_{x=1}^{m_{s,i}} q_i(x,T)^{x \cdot n_{s,i}(x)} \right] e^{-\sum_{i=1}^{N_T} \sum_{j \geq i}^{N_T} \sum_{x=1}^{m_{s,i}} \sum_{y^*}^{m_{s,i}} N_{ij,xy} \frac{w_x}{kT}} \tag{14}$$

The summation in the exponential of equation (14) requires two comments. First, the summation includes only combinations of i and j which have nearest neighbors (i.e. $c_{ij} \neq 0$). Second, the index y^* varies. If $i = j$, $y^* \geq x$. If $i \neq j$, $y^* \geq 1$. This way we avoid double counting. Also, notice that the maximum occupancy, $m_{s,i}$, the intrasite partition function, $q_i(x,T)$, and the number of sites with occupancy x, $n_{s,i}(x)$, are now defined for each site of type i. Finally, note that the number of neighbors, $N_{ij,xy}$, now includes four subscripts designating the number of neighbors between sites of type i with occupancy x and sites of type j with occupancy y.

As before, we proceed with an extension to the quasi-chemical approximation in order to formulate the configurational degeneracy. For the connectivity matrix given in equation (11), the general configurational degeneracy is given by

$$g(N,M) = \left[\prod_{\substack{i=1 \\ j \neq i}}^{N_T} \left(\frac{M_i!}{\prod_{x=0}^{m_{s,i}} n_s(x)!} \right)^{1-c_{ij}} \right] \left[\frac{(c_{12}M_1)!}{\prod_{x=0}^{m_{s,i}} \prod_{y=0}^{m_{s,j}} N_{ij,xy}!} \right] \tag{15}$$

This general form would have to be altered to meet particular forms of the connectivity matrix. We proceed with the case of the connectivity matrix given in equation (11).

At this point we require equations to obtain (i) all number of neighbor pairs, $N_{ij,xy}$, and (ii) all number of sites with occupancy x, $n_{s,i}(x)$. These equations take the same five forms as in the single type of site case; however, the number of each constraint varies. We have symmetry relations (8.a), N_T site balances (8.b), one adsorbate balance (8.c), and neighbor balances (8.d) (for our $\underline{\underline{c}}$, numbering $\sum_{i=1}^{N_T}(m_{s,i}+1)$, all but one of which are linearly independent). All remaining unknowns must be determined by minimization of the partition function as was done in Equation (9). For $N_T > 1$, we obtained an analytical solution only for $N_T = 2$, $m_{s,1} = 1$, $m_{s,2} = 1$, and $w = 0$. For all other cases, we employed a numerical solution.

We list the variables and equations for three cases below. For the case where $N_T = 2$, $m_{s,1} = 1$, $m_{s,2} = 1$, and $w \neq 0$, we have twelve unknowns, given in the set: $\{n_{s,1}(0), n_{s,1}(1), n_{s,2}(0), n_{s,2}(1), N_{12,00}, N_{12,01}, N_{12,10}, N_{12,11}, N_{21,00}, N_{21,01}, N_{21,10}, N_{21,11}\}$. We have four symmetry relations of a new form

$$N_{ij,xy} = N_{ji,yx} \tag{16}$$

We have N_T site balances (8.b), one adsorbate balance (8.c), and four neighbor balances (8.d), three of which are linearly independent. These ten equations are supplemented by two additional constraints of the form:

$$\left(\frac{\partial \ln Q}{N_{12,11}}\right)_{N,M,T} = 0 \quad \text{and} \quad \left(\frac{\partial \ln Q}{n_{s,1}(1)}\right)_{N,M,T} = 0 \tag{17}$$

For the case where $N_T = 2$, $m_{s,1} = 1$, $m_{s,2} = 2$, and $w \neq 0$, a similar analysis of variables and constraints yields seventeen unknowns, requiring four constraints of the type shown in Equation (17).

For the case where $N_T = 2$, $m_{s,1} = 2$, $m_{s,2} = 2$, and $w \neq 0$, a similar analysis of variables and constraints yields twenty-four unknowns, requiring seven constraints of the type shown in Equation (17).

Again, once these variables are known, we can formulate the partition function and solve for any thermodynamic variables of interest. We need to point out that, even in the cases where we require numerical solutions for the unknowns, we can still obtain analytical formulae for the thermodynamic properties.

For example the Helmholtz Free Energy, A, given by

$$A = -kT \ln Q \tag{18}$$

can be obtained by solving for numerical values of the unknowns and substituting them into the partition function. Similarly, we can obtain analytical expressions for the total energy, E, (kinetic and potential) and the entropy, S, from

$$E = kT^2 \left(\frac{\partial \ln Q}{\partial T}\right)_{N,\underline{M},\{unknowns\}} \tag{19}$$

and

$$S = \frac{-A + E}{T} \tag{20}$$

We are able to obtain analytical expressions for these quantities because the unknowns are held constant in the differentiation for the energy. Thus we do not need the derivatives of the unknowns; i.e., thus we don't need their functional forms.

The chemical potential must be treated a little differently. The chemical potential is given by

$$\mu = -kT\left(\frac{\partial \ln Q}{\partial N}\right)_{N,T} \tag{21}$$

Many of the unknowns are functions of N. However, since we are obtaining the values of the unknowns numerically, we do not know the analytical functionality of the unknowns on N. This problem can be avoided by grouping our unknowns into two types. The unknowns that we minimize the partition function with respect to, as in equations (9.a), (9.b), and (17) comprise the first group. Let us label the unknowns in the first group generically as $\{n_u\}$. All other unknowns comprise the second group. The variables in the second group can be arranged as functions of the variables in the first group and N. We substitute the functional form of the unknowns of the second group into the partition function, before applying the derivative in equation (21). Then we differentiate with respect to N:

$$\mu = -kT\left[\left(\frac{\partial \ln Q}{\partial N}\right)_{N,T,n_u} + \sum_{\text{unknowns}}\left(\frac{\partial \ln Q}{\partial n_{u,i}}\right)_{N,T,n_{u,j}}\left(\frac{\partial n_u}{\partial N}\right)_{T,n_{u,j}}\right] \tag{22}$$

The first factor in the summation is zero for all i, since we obtained the value of $\{n_u\}$ by minimizing the partition function. Therefore, we don't need the functional form of $\{n_u\}$ in order to obtain $\left(\frac{\partial n_u}{\partial N}\right)_{T,n_{u,j}}$. We remark that the analytical form of the chemical potential obtained in this way depends on which variables were chosen to comprise $\{n_u\}$. Different choices will yield different forms. However, the numerical values will, of course, be the same.

2.3 NUMERICAL METHODS

2.3.1 The Problems

By far the most difficult element of evaluating the theory, once it has been formulated, is solving the system of nonlinear algebraic equations that result from the constraints on the system. Our particular method of solution of these equations, and the reasons behind it, deserve explanation. There are two issues: scaling of the unknowns and stiffness of the equations.

The set of unknowns contains variables that span many orders of magnitudes. For example, the number of sites of type i with occupancy x, $n_{s,i}(x)$, is bound by $0 \le n_{s,i}(x) \le \min(\frac{N}{x}, m_i)$. Since we want to obtain the entire isotherm, we are interested in loadings ranging from $0 \le N \le N_{max}$, where the maximum loading is given by

$$N_{max} = \sum_{i=1}^{N_T} m_{s,i} \cdot M_i \tag{23}$$

Because we have multiple occupancies in a site, in order to obtain a fractional occupancy bounded by zero and unity, we must use the definition

$$\theta = \frac{N}{N_{max}} = \frac{N}{\sum_{i=1}^{N_T} m_{s,i} \cdot M_i} \tag{24}$$

Over this range of loadings, the number of neighbors, $N_{ij,xy}$, changes drastically. $N_{ij,xy}$ is bounded by $0 \le N_{ij,xy} \le c_{ij}M_i$. For example, in a case where $N_T = 2$, $m_{s,1} = 2$, and $m_{s,2} = 2$,

at the start of the isotherm, say $\theta = 10^{-4}$, $\frac{N_{12,00}}{M}$ is near its maximum value (on the order of c_{ij}, e.g. 3 or 4). However, very few sites are doubly occupied; a variable like $\frac{N_{12,22}}{M}$ scales as $n_{s,1}(2)n_{s,2}(2)$. As a result, $\frac{N_{12,22}}{M}$ is frequently twenty to thirty orders of magnitude smaller than $\frac{N_{12,00}}{M}$.

One might think that since $\frac{N_{12,22}}{M}$ is so small, it can be assumed to be zero. However, a closer examination of the constraints where we minimized the partition function (e.g. Equation 17, shows that we take the natural logarithm of the $N_{ij,xy}$, so that if we assume any one of them is zero, the entire equation blows up. In fact, accurately knowing the values of all $N_{ij,xy}$ and $n_{s,i}(x)$ over a range of twenty or thirty orders of magnitude is essential to obtaining a partition function from which accurate thermodynamic properties can be obtained. Since the computers at our disposal run at double precision (sixteen significant figures), it is impossible to directly solve for variables spanning more than sixteen orders of magnitude. Therefore, we need to scale the unknowns.

The second issue is one of stiffness. The equations obtained from minimizing the partition function contain various combinations of natural logarithms of sundry functions of the unknowns. Thus, the constraints quickly become undefined for combinations of $N_{ij,xy}$ which yield negative values of the logarithm argument. Due to this problem, solving the system of equations in the form in which the constraints are obtained over the entire range of the isotherm for arbitrary values of $\underline{\underline{c}}$, $\underline{V_s}$, $\underline{U_{AP}}$, and w_x has proven to be virtually impossible.

2.3.2 The Solution

We have obtained a robust method to solve the system of constraints for arbitrary systems. The algorithm is as follows:

1. Obtain constraints from Equations (8) and (9).
2. Perform a nonlinear transformation of unknowns to scaled unknowns.
3. Formulate the constraints in terms of the scaled unknowns.
4. Solve the constraints in the transformed variables for $w_x = 0$ and $\theta = 10^{-4}$.
5. Select a new value of w_x, incrementally higher than the previous value. Using the converged solution to the unknowns at the previous value of w_x as the initial guess, solve for the unknowns at the new value of w_x. Maintain a loading of $\theta = 10^{-4}$.
6. Loop through step 5 until the desired value of w_x is reached.
7. Select a new value of θ, incrementally higher than the previous value. Using the converged solution to the unknowns at the previous value of θ as the initial guess, solve for the unknowns at the new value of θ.
8. Loop through step 7 until the entire isotherm has been defined.
9. Reverse the nonlinear transformation to obtain the unscaled unknowns.

We selected our scaled variables based on two criteria: (1) the variables should be relatively well-scaled over the entire range of θ, (ii) the nonlinear transformation used to obtain the scaled variables should have a relatively simple reverse transformation. (Otherwise, we would be stuck solving a new system of nonlinear algebraic equations to get the unscaled variables from the scaled variables and we have the same problem of scaling as before.)

The choice of scaled variables and transformation varied for each combination of values of N_T and $\underline{m_s}$, depending upon which unknowns with respect to which we chose

to differentiate the partition function. Most generically, our nonlinear transformation matrix from unscaled variables, x, to scaled variables y had the form:

$$\underline{\ln(y)} = \underline{\underline{A}}\,\underline{\ln(x)} + \underline{b} \tag{25}$$

The values of $\underline{\underline{A}}$ and $\underline{b}$ had to be determined for each combination of N_T and $\underline{m_s}$.

In steps 5 and 7, we used a customized version of the multivariate Newton-Raphson method with a first-order numerical approximation to the partial derivatives needed in the Jacobian. An arbitrary element of the Jacobian was calculated as

$$J_{ij} = \frac{f_i(\{x\}, x_j + h_j) - f_i(\{x\}, x_j - h_j)}{2h_j} \tag{26}$$

where the algorithm iteratively selects the size of the interval over which the partial derivative is approximated, h_j, such that the magnitude of the residual at $x_j + h_j$ and $x_j - h_j$ is within a specified factor of the residual at x_j. (We used a value of 10 for our factor.) This is necessary because the equations are so stiff that fixing h_j to be a constant factor like $10^{-6} x_j$, or worse yet a constant, results in a method that invariably does not converge to the solution at some value of θ, regardless of the goodness of the initial guess (or equivalently the number of increments into which the isotherm is divided).

2.4 RESULTS AND DISCUSSION

In this section, we present results that demonstrate the capabilities of this theory. As mentioned previously, we have selected six different cases by varying the number of types of adsorbate sites and the maximum occupancy of molecules at them. We parameterize the lattice as shown in Table 1 for the six cases, varying N_T and $\underline{m_s}$. We randomly selected values for these parameters for illustration purposes. Exact values could be obtained from a potential energy map of the pore space. The well depth, $\underline{\underline{U_{AP}}}$, is given as a matrix in Table 1, where rows indicate the type of site and columns indicate the occupancy of the site. In this model, sites of Type 2 are assumed to be slightly larger than sites of Type 1. Additionally, sites of Type 1 are assumed to be energetically deeper than sites of Type 2 at occupancy of one adsorbate in each site but less favorable energetically than sites of Type 2 at occupancy of two adsorbates in each site. For the cases with $N_T = 2$, the connectivity matrix defines the relative number of sites via Equation (13). Forty percent of the sites are Type 1 and sixty percent of the sites are Type 2.

Our model observes the behavior of fluids in context of the lattice structure of the adsorbent. It may be easily understood that as the loading is increased, the adsorbate molecules occupy the different adsorbent sites depending on factors such as site volume and well depth. These variations in the occupancy levels of the two types of sites are plotted in Figure (2). Here, we choose to show the occupancy for the case with two types of sites each having a maximum occupancy of two because of its generalized behavior.

Since the connectivity matrix is given by $\underline{\underline{c}} = \begin{bmatrix} 0 & 3 \\ 2 & 0 \end{bmatrix}$, forty percent of the sites are Type1 and sixty percent of the sites are Type 2. This value would vary for each case depending on the maximum occupancy of each type of site in the system. Initially, when no molecules are present, all the sites of Type 1 and 2 have zero occupancy. The total

must sum to unity at all loadings. At any given loading, the distribution of molecules, in the two types of sites with varying occupancy levels, would always sum to unity.

As the loading increases, $n_{s,1}(0)$ and $n_{s,2}(0)$ approach zero. On the other hand, $n_{s,1}(1)$ and $n_{s,2}(1)$ simultaneously increase as all sites are filled with one molecule each. At low loading, we see a preference in both sites for occupancies of Type 1, because there is an energetic and entropic barrier in the intra-site partition function to double occupancy. This leads to the stage near a density of one adsorbate per site when both $n_{s,1}(1)$ and $n_{s,2}(1)$ have attained maximum values. We notice that $n_{s,2}(1)$ reaches a higher value than $n_{s,1}(1)$ at the maximum, a fact clearly understood because sites of Type 2 are more numerous than Type 1. As we continue to fill the sites, $n_{s,1}(2)$ and $n_{s,2}(2)$ increase while $n_{s,1}(1)$ and $n_{s,2}(1)$ decrease. The symmetry of the figure can thus be explained by the phenomenological sequence of the preferential filling of molecules in different types of sites.

In Figure (3), we plot the normalized number of neighbors, $N_{ij,xy}$ for the same case as in Figure (2). (We designate $N_{ij,xy}$ as the number of neighbor interactions between sites of type i with an occupancy of x and sites of type j with an occupancy of y) As adsorbates try to fit into the lattice, at low loadings, the energetically deeper sites of Type 1 start filling first. This causes $N_{12,10}$ to attain higher values than $N_{12,01}$ for any given loading. We observe that both types of sites are first filled with one molecule each. This sort of arrangement appears because there is an entropic advantage to distributing adsorbates between both types of sites. As both types of sites are filled with one molecule each, $N_{12,11}$ increases and reaches a maximum value at half loading, i.e. $n = 1$. $N_{12,12}$ and $N_{12,21}$ interactions are negligible until this point, as can be seen from the graph. As we further increase the loading, these interactions have an increasing effect because the sites are now filled with second molecule. Here, an interesting observation noted is that sites of Type 2 are filled with a second molecule before sites of Type 1 because in moving from occupancy one to occupancy two, there is a steeper energetic penalty in sites of Type 1 than in sites of Type 2. Hence these interactions are not

symmetric. As both types of sites are filled with two molecules, $N_{12,22}$ interactions increase until the full capacity loading is attained. As explained before, it is unfavorable in these cases, under the prevalent assumptions, for any site to be filled with a second molecule with another site being empty due to the entropic effects. Hence, $N_{12,02}$ and $N_{12,20}$ assume insignificant figures at any point of time during the loading.

Thus, having provided a thorough understanding of the present system, our model carries on to predict the thermodynamic properties of the same. Statistical mechanics fundamentals provide the partition functions for the different cases, which are effectively used to calculate these thermodynamic properties. As mentioned previously, our model predicts them for six different cases with various combinations of number of type of sites and maximum occupancy in them. As mentioned previously, the maximum loading capacity in all the six cases would be different. Hence all the figures henceforth would show the variations in thermodynamic properties against fractional loading.

Figure (4) plots the adsorption isotherms as functions of chemical potential for the six different cases. Using the standard quasi-chemical case ($N_T = 1$ and $m_s = 1$) as a reference point, we can explain the features in the other isotherms based on the difference in their adsorbent structure as directed by c, l, U and v. $\underline{\underline{c}}$, $\underline{\underline{\ell}}$, $\underline{U_{AP}}(x)$ and $\underline{V_S}$.

As a short hand, we designate the case with $N_T = 1$ and $m_s = 1$ as the 1-1 case. For $N_T = 2$ (two types of sites), $m_{s,1} = 1$ (sites of Type 1 having a maximum occupancy of 1), and $m_{s,2} = 2$ (sites of Type 2 having a maximum occupancy of 2), we use the notation 2-12. The 1-1 case is a standard quasi-chemical adsorption isotherm, which demonstrates the expected behavior. However, the isotherm in the 1-2 case shows different features. Since singly occupied sites have deeper wells, we see nearly complete adsorption of 1 adsorbate per site before any double occupancy. Thus the adsorption isotherms in the 1-1 and 1-2 case are very similar up to a loading of one adsorbate per site. After that, we see a plateau before the second adsorbate per site filling begins.

The isotherm in the 2-11 case shows less favorable adsorption relative to that of the 1-1 case because the 2-11 case has 40% sites of Type 1 that are the same as in the 1-1 case, but 60% of the sites of Type 2, with shallower energetic wells. The isotherm in the

2-12 case follows that of the 2-11 case up to a loading of approximately 0.9 adsorbates per site, and then we begin to fill 2 adsorbates in sites of Type 2 while there are still a few empty sites of Type 1. This occurs in the 2-12 case (while it does not occur compared with 1-1 and 1-2 case) because this second type of site can more easily accommodate two adsorbates, due to the larger site volume and lesser energetic penalty involved for double occupancy.

The adsorption isotherm of the 2-21 case follows the isotherm of the 2-11 case more closely than that of the 2-12 case because sites of Type 1 are smaller and have a larger energetic penalty to double occupancy than sites of Type 2. The adsorption isotherm of the 2-22 case shows less favorable adsorption compared with that of the 1-2 case at loading below one because we have introduced sites of Type 2, which have shallow wells. However, at high loading, the 2-22 case shows more favorable adsorption because the sites of Type 2 have a smaller barrier to double occupancy.

Figure (5) plots the adsorbate-pore interaction energy for the six different cases. In these plots, and henceforth for the other energy and entropy plots, the properties are plotted against variations in the fractional loading (θ) and not the number of adsorbates per site. The adsorbate-pore interaction energy (a-p interaction energy) in the 1-1 case is constant and is equal to the well depth because there is only one type of site present with single occupancy. The a-p interaction energy of the 1-2 case follows that of the 1-1 case closely up to a fractional loading of around 0.45. Above this loading, the sites are filled with the second adsorbate, which causes an energetic and entropic penalty because of the smaller sites and shallower depths at double occupancy. This leads to a sharp increase in the a-p interaction energy at high loading.

The a-p interactions in the 2-11 case increase in an approximately linear pattern, indicating adsorption in both types of sites. At $\theta = 1$, U_{AP} = -700 K because 40% of the sites which are of type 1 have an energetic well depth of –1000 K and 60% that are of type 2, a well depth of –500 K.

The a-p interaction energy of the 2-12 case follows that of the 2-11 case at low loading. We then see an increase in the a-p interaction as we begin to fill the second

adsorbate in sites of Type 2. This increase is also observed in the 2-21 and 2-22 cases. However, the a-p interactions in the 2-21 case are energetically less favorable than in the 2-12 case because, although both cases involve higher energetic penalties at double occupancy, the sites of Type 1 have a greater energetic and entropic barrier to double occupancy. At $\theta = 1$, the 2-22 case shows the maximum a-p interactions among all the cases because both types of sites at double occupancy have to pay an energetic penalty.

Figure (6) shows the variations in the adsorbate-adsorbate (a-a) interaction energy for the six different cases. The 1-1 case shows an approximately linear curve for the a-a interactions because the adsorbate-adsorbate interaction energy is relatively weaker than adsorbate-pore interaction energy. A larger more attractive value of the a-a interaction would make the curve more non-linear with positive concavity. The slope of the a-a interaction energy in the 1-2 case appears to be very different than that of the 1-1 case at $\theta < 0.5$, primarily because the x-axis is fractional occupancy and not the adsorbate loading. Plotted against loading, the two cases would have a similar a-a interaction up to a loading of one adsorbate per site. We observe a sudden change in slope at the onset of double occupancy in the 1-2 case, due to the intra-site a-a interaction w_i, which has a larger magnitude than the inter-site a-a interaction w_x.

The a-a interaction energy slope in the 2-11 case is also approximately linear but is different and less than that of the 1-1 case. This can be accounted for by the fact that, due to the connectivity between the different types of sites, there are 1.5 bonds per site in systems with one type of site and 1.2 bonds per site for systems with two types of sites. The a-a interaction energy of the 2-12 case has approximately the same slope as in the 2-11 case because the adsorbate distribution is dominated by a-p interaction here. However, the a-a interaction energy of the 2-12 case has a slight kink. The kink is observed due to the barrier encountered by the sites to double occupancy. The kink is more obvious in the a-a interaction energy of the 2-21 case because the 2-21 case has double occupancy of sites of type 1, which have a larger barrier to double occupancy than that of sites of type 2, thus making the transition to double occupancy more abrupt. The a-a interaction energy curve in the 2-22 case has a less negative slope than that of the 1-2

case because of the differences in connectivity and thus the total number of a-a interactions.

Figure (7) plots the total energy for each of the cases. Note that the variations are plotted for fractional occupancy and not the adsorbates per site. The total energy is merely an addition of the adsorbate-adsorbate interaction energy, adsorbate-pore interaction energy and the kinetic energy of the adsorbates. A wide range of behavior is seen for energy of adsorption due to the adsorbent structure (N_T and $\underline{m_s}$). One peculiar observation in several cases is the non-monotonic nature of the curves. We observe local minima for each of these cases, approximately during their transition from single occupancy to double occupancy. This fact can be easily accounted for from our discussions of Figures (5 and 6).

Figure (8) shows the intensive entropic contribution for all the six different cases to the free energy (TS). Entropy (S) has contributions from the system configurational degeneracy contained in Eq. (7.b) and the intra-site partition function in Eq. (6). Entropy decreases with loading as volume per adsorbate decreases. To understand Figure (8), consider the standard quasi-chemical 1-1 case. In this case, the contribution to entropy from intra-site partition function (q) is constant with respect to loading because there is only one adsorbate per site. Therefore, all the entropy is due to the configurational term. This entropy when plotted as an extensive variable has the same shape as the entropy of ideal mixing of a binary solution (where our two components are the occupied and unoccupied sites). This extensive entropy has a maximum at a fractional occupancy of 0.5. The intensive entropy plotted in Figure (8) thus corresponds to this same concept.

The differences in the six entropy curves are due to changes in the intra-site partition function, q, and changes in the lattice configuration. The entropy per molecule of 1-2 case is less than the 1-1 case because we are putting twice as many adsorbates into the same number of sites. Hence the volume per adsorbate is less. Similar reasoning explains the trends in the four cases with two types of sites. The entropy in the cases with two types of sites is greater than that in the one type sites cases because of the greater number of configurations in the two site systems.

In Figure (9), we show the Helmholtz free energy as a function of fractional occupancy for our six adsorbents. We show these principally to demonstrate that the theory is capable of predicting free energies and that the free energy has a functional form based on the molecular-level structure of the adsorbent as characterized by $\underline{\underline{c}}$, $\underline{\underline{\ell}}$, $\underline{U_{AP}}(x)$, $\underline{V_S}$, N_T and $\underline{m_s}$.

2.5 CONCLUSIONS

In this work, we have presented an analytical theory for adsorption of fluids confined in zeolites, molecular sieves, and other nanoporous materials. It predicts the macroscopic thermodynamic properties of fluids. The advantage of this theory is that it takes a minute or so to evaluate an isotherm on a desktop PC, as opposed to tens of CPU hours of molecular dynamics simulations on a supercomputer or parallel cluster.

The theory also has the advantage of requiring very few parameters. The theory requires only four parameters to describe the adsorbent, which can be obtained from a potential energy map of the adsorbent. It requires the selection of an adsorbate pair-wise interaction potential, such as the Lennard-Jones potential.

The theory incorporates the atomistic structure of the adsorbent and also incorporates the fundamental physical mechanisms that dictate the behavior of fluids confined in nanoporous materials.

We are currently in the midst of extending the theory in three directions. We are comparing the theory to simulation and experiment. We are extending the theory to multicomponent fluids. We are obtaining transport properties (i.e. diffusion coefficients) for the model.

REFERENCES

1. Keffer, D., Davis, H.T., McCormick, A.V., "The effect of nanopore shape and loading on adsorption selectivity of a binary mixture" *J. Phys. Chem.* 1996 **100** p. 638-645.
2. Keffer, D., Davis, H.T., McCormick, A.V., "The effect of nanopore shape on the structure and isotherms of adsorbed fluids" *Adsorption* 1996 **2** p. 9-21.
3. Keffer, D., "Molecular Models of Adsorption and Diffusion in Nanoporous Materials", Ph.D. Thesis, University of Minnesota, July, 1996.
4. Keffer, D., McCormick, A.V., Davis, H.T., " Uni-directional and single-file diffusion in $AlPO_4$-5: a molecular dynamics study", *Mol. Phys.* 1996 **87** p. 367-387.
5. Keffer, D., McCormick, A.V., Davis, H.T., "Agreement between Theory and Simulation of Single-file diffusion in a molecular sieve", Proceedings from the XI International Workshop on Condensed Matter Theories, Caracas, Venezuela, June, 1995.
6. Hahn, K. Kärger, J., "Molecular Dynamics Simulations of Single-File Systems", *J. Phys. Chem.*, 1996 100 p. 316-326.
7. Keffer, D., McCormick, A.V., Davis, H.T., "Diffusion and Percolation on Zeolite Sorption Lattices", *J. Phys. Chem.* 1996 **100** p. 967-973.
8. Kono, H., Takasaka, A., "Statistical mechanics calculation of the sorption characteristics of Ar and N2 in dehydrated zeolite 4A by a Monte Carlo method for determining configuration integrals", *J. Phys. Chem.* 1987 **91** p. 4044-4055.
9. Razmus, D.M., Hall, C.K., "Prediction of gas adsorption in 5A zeolites using Monte Carlo simulations", *AIChE J.* 1991 **37** p. 769-779.
10. Van Tassel, P.R., Davis, H.T., McCormick, A.V., "Monte Carlo calculations of adsorbate placement and thermodynamics in a micropore: Xe in NaA", *Mol. Phys.* 1991 **73** p. 1107-1125.
11. Van Tassel, P.R., Davis, H.T., McCormick, A.V., "Monte Carlo calculations Xe arrangement and energetics in the NaA alpha cage", *Mol. Phys.* 1992 **76** p. 411-432.
12. Van Tassel, Phillips, J.C., P.R., Davis, H.T., McCormick, A.V., "Zeolite adsorption site location and shape shown by simulated isodensity surfaces", *J. Mol. Graphics* 1993 **11** p. 180-184,188.
13. Van Tassel, P.R., Davis, H.T., McCormick, A.V., "Open-system Monte Carlo simulations of Xe in NaA" *J. Chem. Phys.* 1993 **98** p. 8919-8928.
14. Van Tassel, P.R., Somers, S.A., Davis, H.T., McCormick, A.V., "Lattice model and simulation of dynamics of adsorbate motion in zeolites" *Chem. Eng. Sci.* 1994 **49** p. 2979-2989.
15. Van Tassel, P.R., Davis, H.T., McCormick, A.V., "New lattice model for adsorption of small molecules and their mixtures in a zeolite micropore", *AIChE J.* 1994 **40** p. 925-934.
16. Van Tassel, P.R., Davis, H.T., McCormick, A.V., "Adsorption simulations of small molecules and their mixtures in a zeolite micropore", *Langmuir* 1994 **10** p. 1257-1267.

17. Soto, J.L., Myers, A.L., "Monte Carlo studies of adsorption in molecular sieves", *Mol. Phys.* 1981 **42** p. 971-983.
18. Woods, G.B., Panagiotopolous, A.Z., Rowlinson, J.S., "Adsorption of Fluids in Model Zeolites" *Mol. Phys.* 1988 **63** p. 49-63.
19. Woods, G.B., Rowlinson, J.S., "Computer Simulations of fluids in zeolites X and Y" *J. Chem. Soc. Faraday Trans. 2* 1989 **85** p. 765-781.
20. Yashonath, S., Thomas, J.M., Novak, A.K., Cheetham, A.K., "The siting, energetics and mobility of saturated hydrocarbons inside zeolitic cages: methane in zeolite Y", *Nature* 1988 **331** p. 601-604.
21. Yashonath, S., Demontis, P., Klein, M.L., "A molecular dynamics study of methane in zeolite NaY", *Chem. Phys. Lett.* 1988 **153** p. 551-556.
22. Demontis, P. Yashonath, S., Klein, M.L., "Location and mobility of benzene in sodium-Y zeolite by molecular dynamics calculations", *J. Phys. Chem.* 1989 **93** p. 5016-5019.
23. Yashonath, S., "A molecular dynamics study of cage-to-cage migration in sodium Y zeolite: Role of surface-mediated diffusion", *J. Phys. Chem.* 1991 **95** p. 5877-5881.
24. Yashonath, S., Demontis, P., Klein, M.L., "Temperature and concentration dependence of adsorption properties of methane in NaY: A molecular dynamics study", *J. Phys. Chem.* 1991 **95** p. 5881-5889.
25. Santikary, P., Yashonath, S., Ananthakrishna, G., "A molecular dynamics study of xenon sorbed in sodium Y zeolite. 1. Temperature and concentration dependence", *J. Phys. Chem.* 1992 **96** p. 10469-10477.
26. Yashonath, S., Santikary, P., "Xenon in sodium Y zeolite 2. . Arrhenius relation, mechanism, and barrier height distribution for cage-to-cage diffusion", *J. Phys. Chem.* 1993 **97** p. 3849-3857.
27. Yashonath, S., Santikary, P., "Diffusion of sorbates in zeolites Y and A: Novel dependence on sorbate size and strength of sorbate-zeolite interaction", *J. Phys. Chem.* 1994 **98** p. 6368-6376.
28. Klein, H. Kirschhock, C., Fuess, H., "Adsorption and diffusion of aromatic hydrocarbons in zeolite Y by molecular mechanics calculation and x-ray powder diffraction", *J. Phys. Chem.* 1994 **98** p. 12345-12360.
29. Gupta, V., Davis, H.T., McCormick, A.V., "Comparison of the ^{129}Xe NMR chemical shift with simulation in zeolite Y", *J. Phys. Chem.* 1996 **100** p. 9824-9833.
30. Gupta, V., Davis, H.T., McCormick, A.V., "^{129}Xe NMR chemical shifts in zeolites: Effect of Loading studied by Monte Carlo simulations", *J. Phys. Chem.* 1997 **101** p. 129-137.
31. Keffer, D., Gupta, V., Kim, D., Lenz, E., Davis, H.T., McCormick, A.V., "A compendium of zeolite potential energy maps" *J. Mol. Graphics* 1996 **14** p. 108-116, 100-104.

32. Nivarthi, S.S., Van Tassel, P.R., Davis, H.T., McCormick, A.V., "Adsorption and energetics of xenon in mordenite: a Monte Carlo simulation study", *J. Chem. Phys.* 1995 **103** p. 3029-3037.
33. Vernov, A.V., Steele, W.A., "Sorption of xenon in zeolite Rho: A thermodynamics/simulation study", *J. Phys. Chem.* 1993 **97** p. 7660-7664.
34. Loriso, A., Bojan, M.J., Vernov, A., Steele, W.A., "Computer simulation studies of ordered structures formed by rare gases sorbed in zeolite Rho", *J. Phys. Chem.* 1993 **97** p. 7665-7671.
35. Snurr, R.Q., June, R.L., Bell, A.T., Theodorou, D.N., "Molecular simulations of methane adsorption in silicalite", *Mol. Sim.* 1991 **8** p. 73-92.
36. Snurr, R.Q., June, R.L., Bell, A.T., Theodorou, D.N., "A hierarchical atomistic/lattice simulation approach for the prediction of adsorption thermodynamics of benzene in silicalite", *J. Phys. Chem.* 1994 **98** p. 5111-5119.
37. Demontis, P., Fois, E.S., Suffriti, G.B., Quartieri, S., "Molecular dynamics studies on zeolites 4. Diffusion of methane in silicalite", *J. Phys. Chem.* 1990 **94** p. 4329-4334.
38. Demontis, P., Suffriti, G.B., Fois, E.S., Quartieri, S., "Molecular dynamics studies on zeolites 6. Temperature dependence of diffusion of methane in silicalite", *J. Phys. Chem.* 1992 **96** p. 1482-1490.
39. Nowak, A.K., Cheetham, A.K., Pickett, S.D., Ramdas, S., "A computer simulation of the adsorption and diffusion of benzene and toluene in the zeolites Theta-1 and silicalite", *Mol. Sim.* 1987 **1** p. 67-77.
40. Vigne-Maeder, F., Jobic H., "Adsorption sites and packing of benzene in silicalite", *Chem. Phys. Lett.* 1990 **169** p. 31-35.
41. Vigne-Maeder, F., Auroux, A., "Potential maps of methane, water, and methanol in silicalite", *J. Phys. Chem.* 1990 **94** p. 316-322.
42. June, R.L., Bell, A.T., Theodorou, D.N., "Molecular Dynamics studies of methane and xenon in silicalite", *J. Phys. Chem.* 1990 **94** p. 8232-8240.
43. June, R.L., Bell, A.T., Theodorou, D.N., "Transition-state studies of xenon and SF_6 diffusion in silicalite", *J. Phys. Chem.* 1991 **95** p. 8866-8878.
44. Goodbody, S.J., Watanabe, K. MacGowan, D., Walton, J.P.R.B., Quirke, N., "Molecular simulation of methane and butane in silicalite", *J. Chem. Soc. Faraday Trans.* 1991 **87** p. 1951-1958.
45. June, R.L., Bell, A.T., Theodorou, D.N., "Molecular Dynamics studies of butane and hexane in silicalite", *J. Phys. Chem.* 1992 **96** p. 1051-1060.
46. Snurr, R.Q., Bell, A.T., Theodorou, D.N., "Prediction of adsorption of aromatic hydrocarbons in silicalite from grand canonical Monte Carlo simulations with biased insertions", *J. Phys. Chem.* 1993 **97** p. 13472-13752.
47. Nicholas, J.B., Trouw, F.R., Mertz, J.E., Iton, L.E., Hopfinger, A.J., "Molecular Dynamics simulation of propane and methane in silicalite", *J. Phys. Chem.* 1993 **97** p. 4149-4163.
48. Vigne-Maeder, F., "Analysis of ^{129}Xe chemical shifts in zeolites from molecular dynamics calculations", *J. Phys. Chem.* 1994 **98** p. 4666-4672.

49. Smit, B. Siepmann, J.I., "Computer simulations of the energetics and siting of n-alkanes in zeolites", *J. Phys. Chem.* 1994 **98** p. 8442-8452.
50. Smit, B., Maesen, T.L.M., "Commensurate 'freezing' of alkanes in the channels of a zeolite" *Nature* 1995 **374** p. 42-44.
51. Bandopadhyay, S., Yashonath, S., "Diffusion anomaly in silicalite and VPI-5 from molecular dynamics simulations', *J. Phys. Chem.* 1995 **99** p. 4286-4292.
52. Yashonath, S., Bandopadhyay, S., "Surprising diffusion behavior in the restricted regions of silicalite", *Chem. Phys. Lett.* 1994 **228** p. 284-288.
53. Heffelfinger, G.S., Pohl, P.I., Frink, L.J.D., "Molecular Dynamics computer simulations of diffusion in porous silicates", *Mater. Res. Soc. Symp. Proc.* 1995 **366** p. 225-230.
54. Antonchenko, V.Y., Ilyin, V.V., Makovsky, N.N., Khryapa, V.M., "Short-range order in cylindrical liquid-filled micropores", *Mol. Phys.* 1988 **65** p. 1171-83.
55. Bratko, D., Blum, L., Wertheim, M.S., "Structure of hard sphere fluids in narrow cylindrical pores", *J. Chem. Phys.* 1989 **90** p. 2752-2757.
56. Carigan, Y.P., Vladimiroff, T., Macpherson, A.K., "Molecular Dynamics of hard spheres III. Hard spheres in an almost spherical container", *J. Chem. Phys.* 1988 **88** p. 4448-4450.
57. Demi, T., "Molecular Dynamics studies of adsorption and transport in micropores of different geometries", *J. Chem. Phys.* 1991 **95** p. 9242-9247.
58. Dunne, J., Myers, A.L., "Adsorption of gas mixtures in micropores: effect of difference in size of adsorbate molecules", *Chem. Eng. Sci.* 1994 **49** p. 2941-2951.
59. Glandt, E.D., "Density distribution of hard-spherical molecules inside small pores of various shapes", *J. Col. Inter. Sci.* 1980 **77** p. 512-524.
60. Groot, R.D., Faber, N.M., van der Eerden, "Hard sphere fluids near a hard wall and a hard cylinder", *Mol. Phys.* 1987 **62** p. 861-874.
61. Han, K.K., Cushman, J.H., Diestler, D.J., "Grand Canonical Monte Carlo simulations of a Stockmayer fluid in a slit micropore", *Mol. Phys.* 1993 **79** p. 537-545.
62. Heinbuch, U., Fischer, J., "Liquid argon in a cylindrical carbon pore: molecular dynamics and Born-Green-Yvon Results", *Chem. Phys. Lett.* 1987 **135** p. 587-590.
63. Jiang, S., Rhykerd, C.I., Gubbins, K.E., "Layering, freezing transitions, capillary condensation, and diffusion of methane in slit carbon pores", *Mol. Phys.* 1993 **79** p. 373-391.
64. Macelroy, J.M.D., Suh, S.H., "Computer simulation of moderately dense hard-sphere fluids and mixtures in microcapillaries", *Mol. Phys.* 1987 **60** p. 475-501.
65. Macelroy, J.M.D., Suh, S.H., "Simulation studies of a Lennard-Jones liquid in micropores", *Mol. Sim.* 1989 **2** p. 313-315.
66. Macpherson, A.K., Carignan, Vladimiroff, T., "Molecular dynamics of hard spheres II. Hard spheres in a spherical cavity", *J. Chem. Phys.* 1987 **87** 1768-1770.
67. Murad, S., Ravi, P., Powles, J.G., "A computer simulation study of fluids in model slit, tubular, and cubic micropores", *J. Chem. Phys.* 1993 **98** p. 9771-9781.

68. Peterson, B.K., Walton, J.P.R.B., Gubbins, K.E., “Fluid behaviour in narrow pores*”, J. Chem. Soc. Faraday Trans. 2* 1986 **82** p. 1789-1800.
69. Peterson, B.K., Gubbins, K.E., “Phase Transitions in a cylindrical pore: Grand canonical Monte Carlo, mean field theory, and the Kelvin equation”, *Mol. Phys.* 1987 **62** p. 215-226.
70. Saito, A., Foley, H.C., “Curvature and parametric sensitivity in models for adsorption in micropores”, *AIChE J.* 1990 **37** p. 429-436.
71. Sarman, S., “The influence of the fluid-wall interaction potential on the structure of a simple fluid in a narrow slit”, *J. Chem. Phys.* 1990 **92** p. 4447-4455.
72. Schoen, M., Rhykerd, C.L., Cushman, J.H., Diestler, D.J., “Slit-pore sorption isotherms by the grand-canonical Monte Carlo method: Manifestations of Hysteresis”, *Mol. Phys.* 1989 **66** p. 1171-1187.
73. Somers, S.A., Davis, H.T., “Microscopic dynamics of fluids confined between smooth and atomically structured solid surfaces”, *J. Chem. Phys.* 1992 **96** p. 5389-5407.
74. Somers, S.A., McCormick, A.V., Davis, H.T., “Superselectivity and solvation forces of a two component fluid adsorbed in nanopores”, J. Chem. Phys. 1993 99 p. 9890-9898.
75. Tan, Z., Gubbins, K.E., “Selective adsorption of simple mixtures in slit pores: A model of methane-ethane mixtures in carbon”, J. Phys. Chem. 1992 96 p. 845-854.
76. Walton, J.P.R.B., Quirke, N., “Capillary condensation: a molecular simulation study”, *Mol. Sim.* 1989 **2** p. 361-391.
77. Page, K.S., Monson, P.A., "Phase equilibrium in a molecular model of a fluid confined in a disordered porous material", *Phys. Rev. E* 1996 **54** p. R29-32.
78. Vuong, T., Monson, P.A., "Monte Carlo calculations of heats of adsorption in heterogeneous solids", *Langmuir* 1996 **12** p. 5425-5432.
79. Fan, Y., Finn, J.E., Monson, P.A., "A Monte Carlo simulation study of adsorption from a liquid mixture at states near liquid-liquid coexistence", *J. Chem. Phys.* 1993 **99** p. 8238-8243.
80. Peterson, B.K., Heffelfinger, G.S., Gubbins, K.E., Van Swol, F., “Layering transitions in cylindrical nanopores”, *J. Chem. Phys.* 1990 **93** p. 679-685.
81. Heffelfinger, G.S., Van Swol, F., Gubbins, K.E., “Liquid-Vapor coexistence in a cylindrical pore”, *Mol. Phys.* 1987 **61** p. 1381-1390.
82. Demontis, P., Suffritti, G.B., “Molecular Dynamics Investigations of the Diffusion of Methane in a Cubic Symmetry Zeolite of Type ZK4”, *Chem. Phys. Lett.* 1994 **223** p. 355.
83. Beezus, A.G., Kiselev, A.V., Lopatkin, A.A., Pham Quang Du, “Molecular statistical calculation of the thermodynamic adsorption characteristics of zeolites using the atom-atom approximation. Adsorption of methane by zeolite NaX”, *J. Chem. Soc. Faraday Trans.* 1978 **74** p. 367-379.
84. Saravanan, C., Jousse, F., Auerbach, S.M., “Modeling the concentration dependence of diffusion in zeolites. III. Testing Mean Field Theory for benzene in Na-Y with simulation”, *J. Chem. Phys.* 1998 **108** p. 2162-2169.

85. Sanborn, M.J., Snurr, R.Q., “Diffusion of binary mixtures of CF sub 4 and n-alkanes in faujasite”, *Sep. Pur. Tech.* 2000 **20** p. 1-13.
86. Eagen, J.A., Anderson, R.B., “Kinetics and equilibrium of adsorption on 4A zeolite”, *J. Coll. Interface. Sci*. 1975 **50** p. 419.
87. Karger. J., Ruthven, D.M., “Diffusion in zeolites and other microporous solids”, Wiley-Interscience, New York, 1992.
88. Hirschfelder, J.O., Curtiss, C.F., Bird, R.B., “Molecular theory of gases and liquids”, Wiley, New York, 1964.
89. Hill, T.L., “ Introduction to statistical thermodynamics”, Addison Wesley Pub. Co., Mass., 1960.

APPENDICES

Nomenclature

SYMBOL	DESCRIPTION	UNITS
a	$\exp(-w_x/kT)$	-
A	Helmholtz free energy	{K/molecule}
$\underline{\underline{c}}$	Connectivity matrix	-
c_{ij}	Number of sites of type j connected to a site of type i	-
E	Total energy	{K/molecule}
$g(N,M)$	Configurational degeneracy of the lattice	-
k	Boltzmann constant	{J/mole/K}
$\underline{\underline{\ell}}$	Matrix of distances between sites	{A}
$m_{s,i}$	Maximum occupancy of sites of type i	-
M_i	Number of sites of types 1	-
$n_{s,i}(x)$	Number of sites of type i with an occupancy of x	-
n_μ	Label of unknowns	-
N	Number of adsorbates	-
$N_{ij,xy}$	Number of neighbors between sites of type i with occupancy x and sites of type j with occupancy y	-
$q_i(x,T)$	Intrasite partition function of sites of type i	-
$Q(N,M,T)$	Partition function of a function of N, M, and T	-
r	Lennard- Jones distance between molecules	{A}
r_{min}	Distance of well minimum	{A}
S	Entropy	{/molecule}
T	Temperature	{K}
$U_{AP,i}(x)$	Well-depth of a site of type i having an occupancy of x	{K}
$U_{LJ}(l)$	Inter-site potential energy obtained from LJ potential	{K}
$U_{LJ}(r)$	Lennard- Jones potential energy	{K}
V_a	Volume of adsorbate	$\{A^3\}$
$V_{S,i}$	Volume of sites of type i	$\{A^3\}$
w_i	Intrasite adsorbate-adsorbate interaction	{K}

$\underline{\underline{w_x}}$	Matrix of adsorbate-adsorbate potential energy due to adsorbates in neighboring sites	{K}
x	Occupancy of a site of type i	-
y	Occupancy of a site of type j	-
ε	Lennard Jones well-depth	{K}
θ	Fractional occupancy	-
δ_{xy}	Kronecker delta function	-
Λ	Thermal deBroglie wavelength	{A}
σ	Molecule diameter	{A}
μ	Chemical potential	{K/molecule}

Table 1: Lattice Parameters

Case	N_T	$\underline{m_s}$	$\underline{\underline{c}}$	$\underline{\underline{\ell}}$ (Å)	$\underline{V_S}$ ($Å^3$)	$\underline{U_{AP}}$ (K)
1	1	[1]	[3]	[4.0]	[78.1]	[-1000]
2	1	[2]	[3]	[4.0]	[78.1]	$\begin{bmatrix} -1000 & -350 \end{bmatrix}$
3	2	[1,1]	$\begin{bmatrix} 0 & 3 \\ 2 & 0 \end{bmatrix}$	$\begin{bmatrix} - & 4.0 \\ 4.0 & - \end{bmatrix}$	[78.1 ,142]	$\begin{bmatrix} -1000 \\ -500 \end{bmatrix}$
4	2	[1,2]	$\begin{bmatrix} 0 & 3 \\ 2 & 0 \end{bmatrix}$	$\begin{bmatrix} - & 4.0 \\ 4.0 & - \end{bmatrix}$	[78.1 ,142]	$\begin{bmatrix} -1000 & - \\ -500 & -350 \end{bmatrix}$
5	2	[2,1]	$\begin{bmatrix} 0 & 3 \\ 2 & 0 \end{bmatrix}$	$\begin{bmatrix} - & 4.0 \\ 4.0 & - \end{bmatrix}$	[78.1 ,142]	$\begin{bmatrix} -1000 & -350 \\ -500 & - \end{bmatrix}$
6	2	[2,2]	$\begin{bmatrix} 0 & 3 \\ 2 & 0 \end{bmatrix}$	$\begin{bmatrix} - & 4.0 \\ 4.0 & - \end{bmatrix}$	[78.1 ,142]	$\begin{bmatrix} -1000 & -350 \\ -500 & -350 \end{bmatrix}$

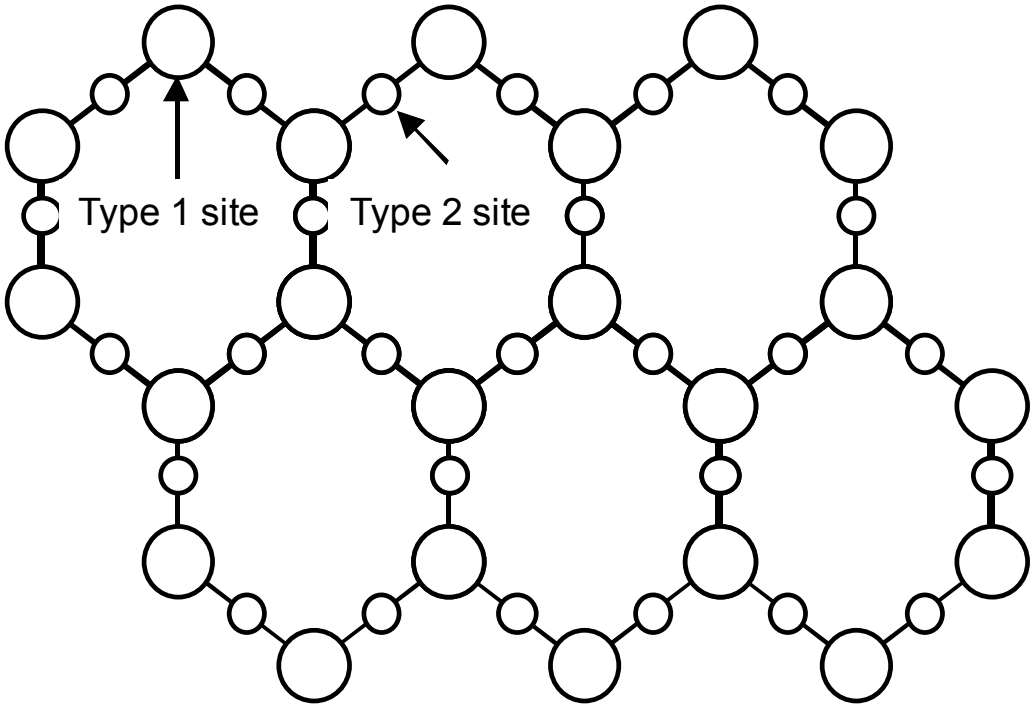

Figure 1: Lattice structure with two types of sites and connectivity matrix $\underline{\underline{c}} = \begin{bmatrix} 0 & 3 \\ 2 & 0 \end{bmatrix}$

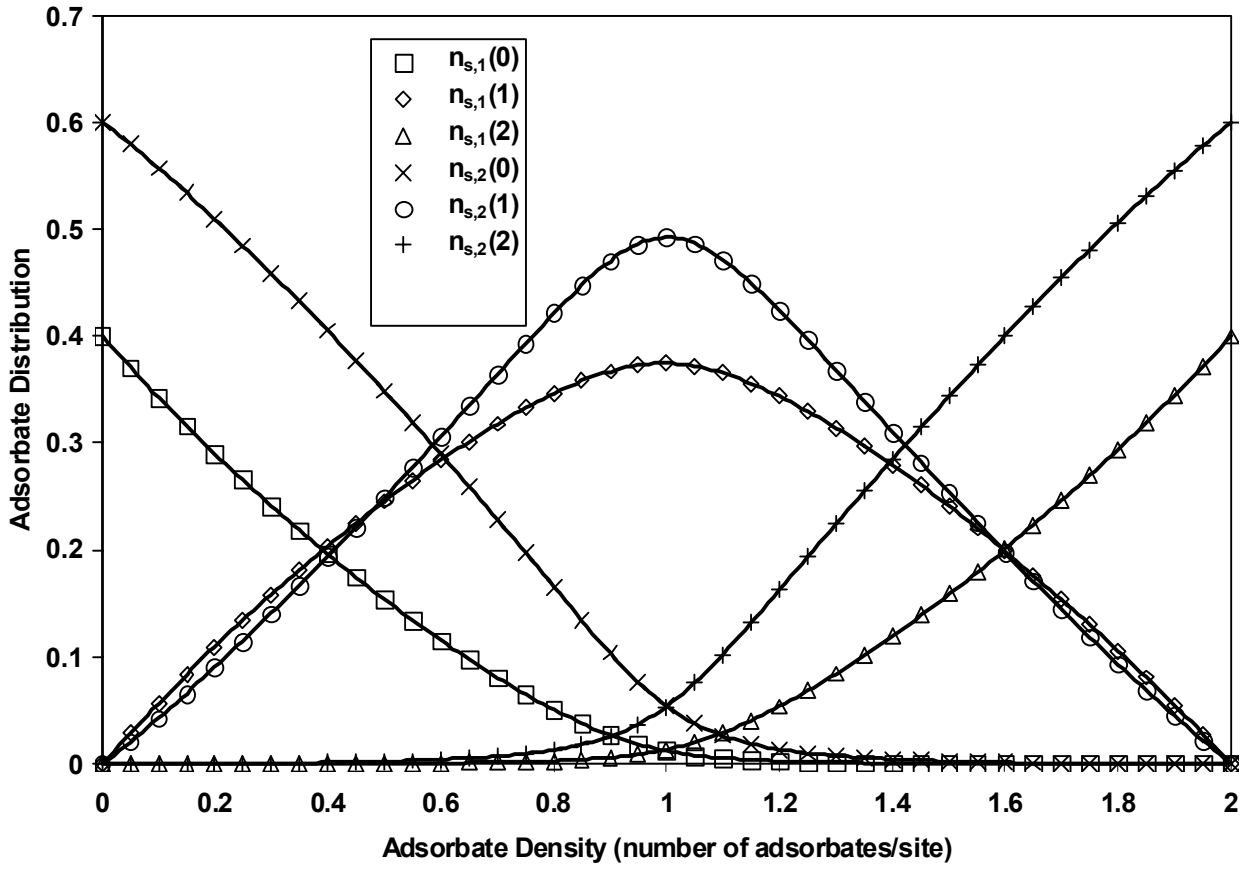

Figure 2: Adsorbate distribution versus adsorbate density for the case where $N_T = 2$, $\underline{m_s} = (2,2)$.

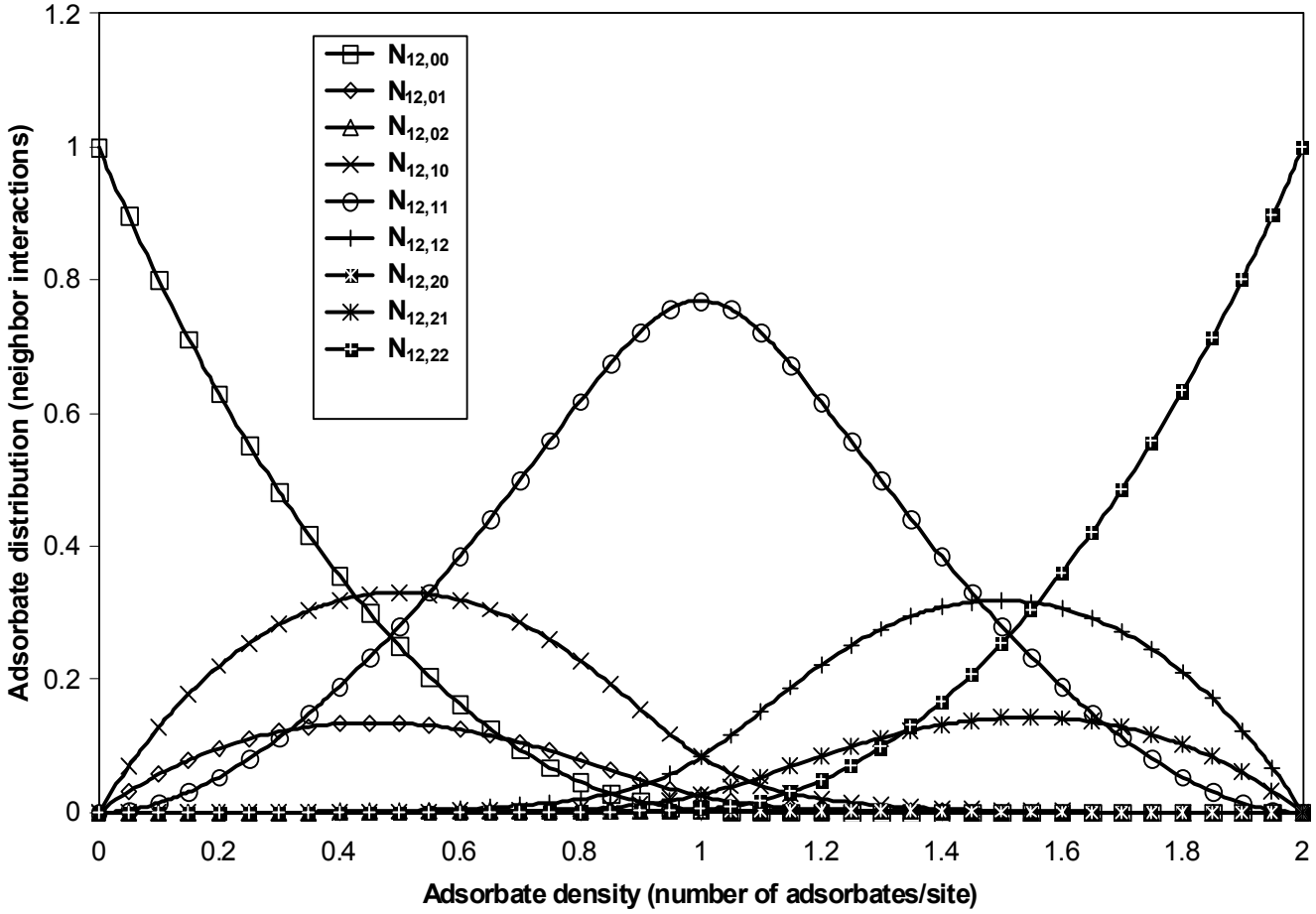

Figure 3: Neighbor distribution versus adsorbate density for the case where $N_T = 2$, $\underline{m_S} = (2,2)$.

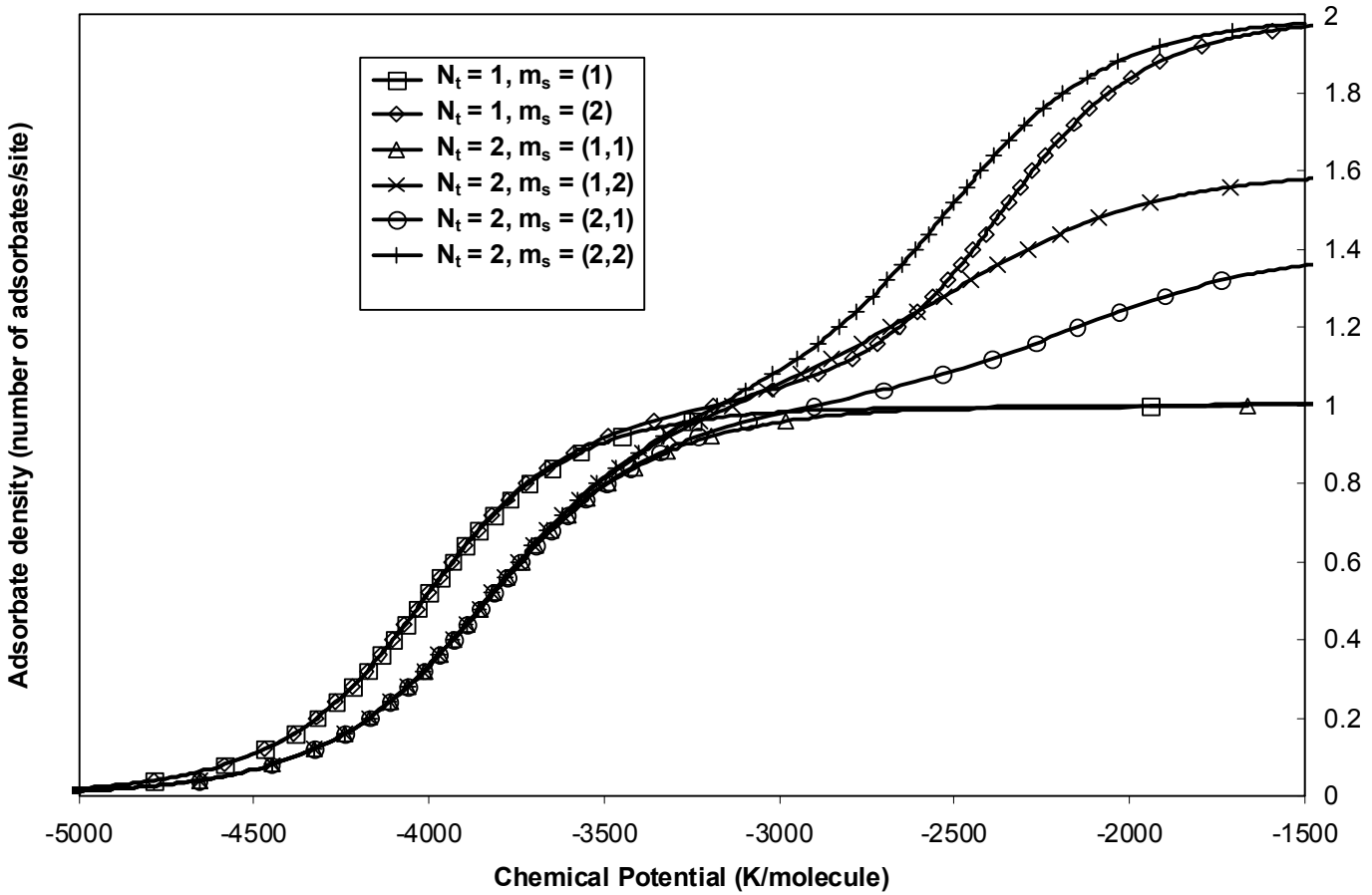

Figure 4: Adsorption isotherms as a function of chemical potential.

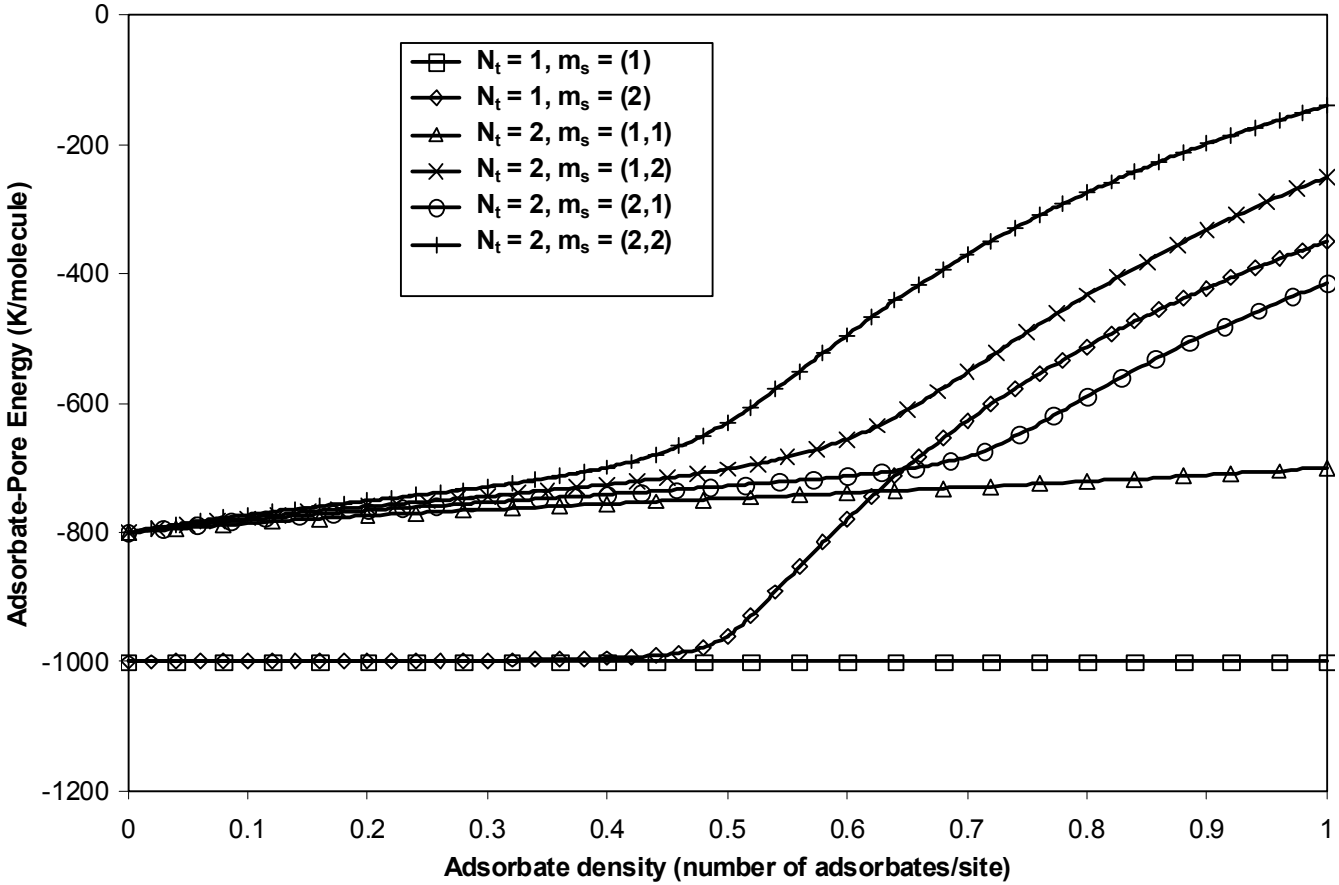

Figure 5: Adsorbate-Pore energy as a function of fractional occupancy.

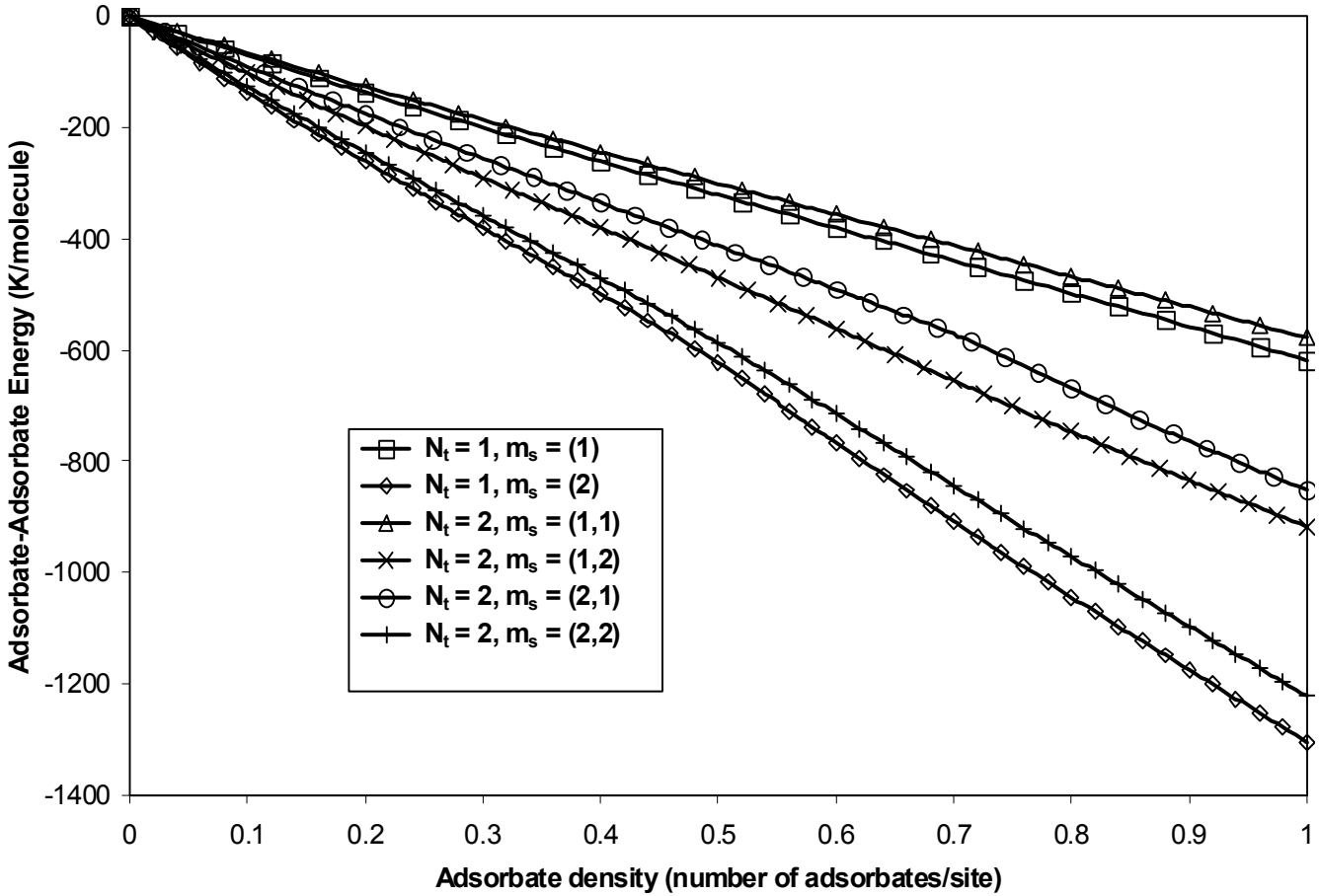

Figure 6: Adsorbate-Adsorbate energy as a function of fractional occupancy.

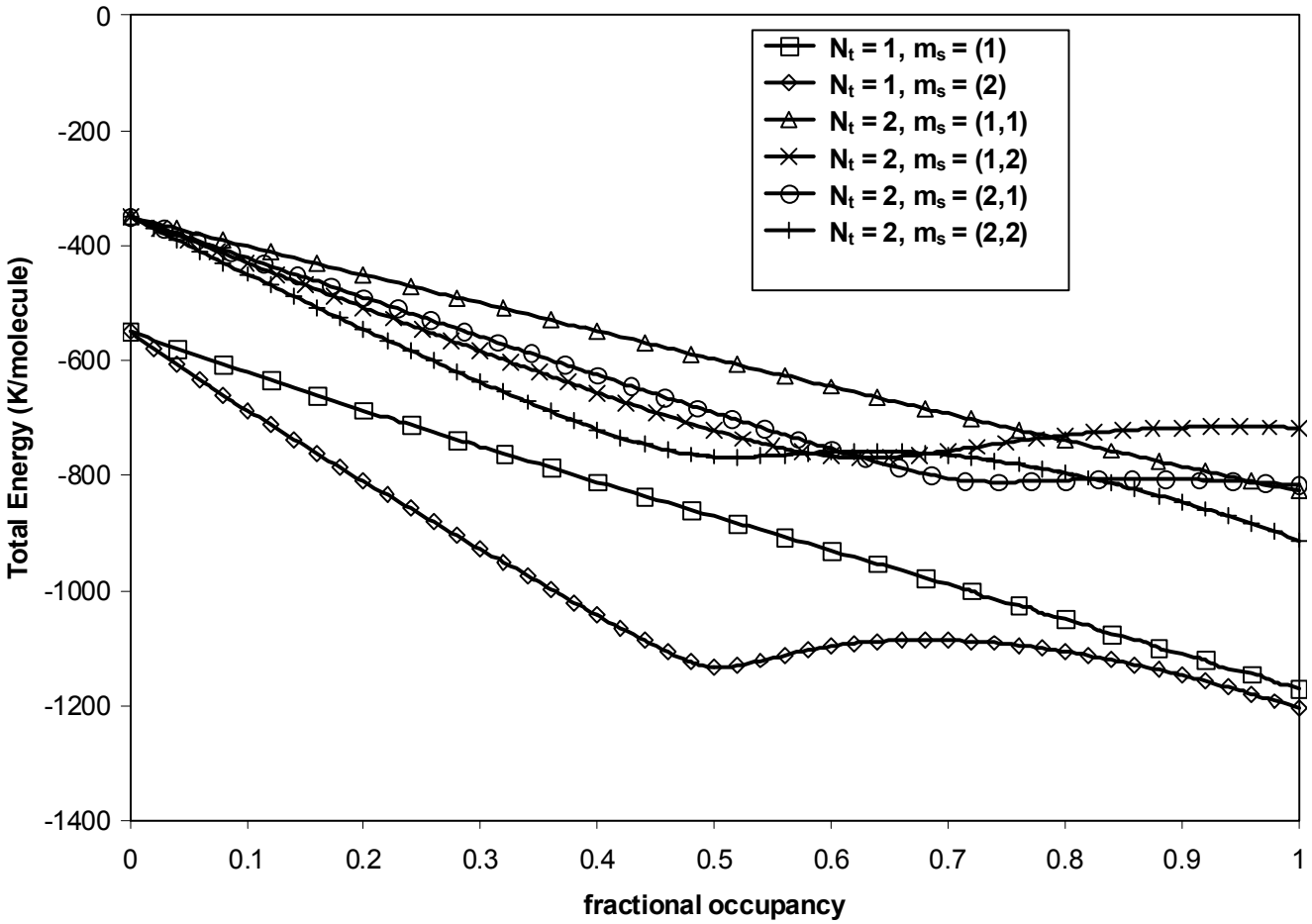

Figure 7: Total energy as a function of fractional occupancy.

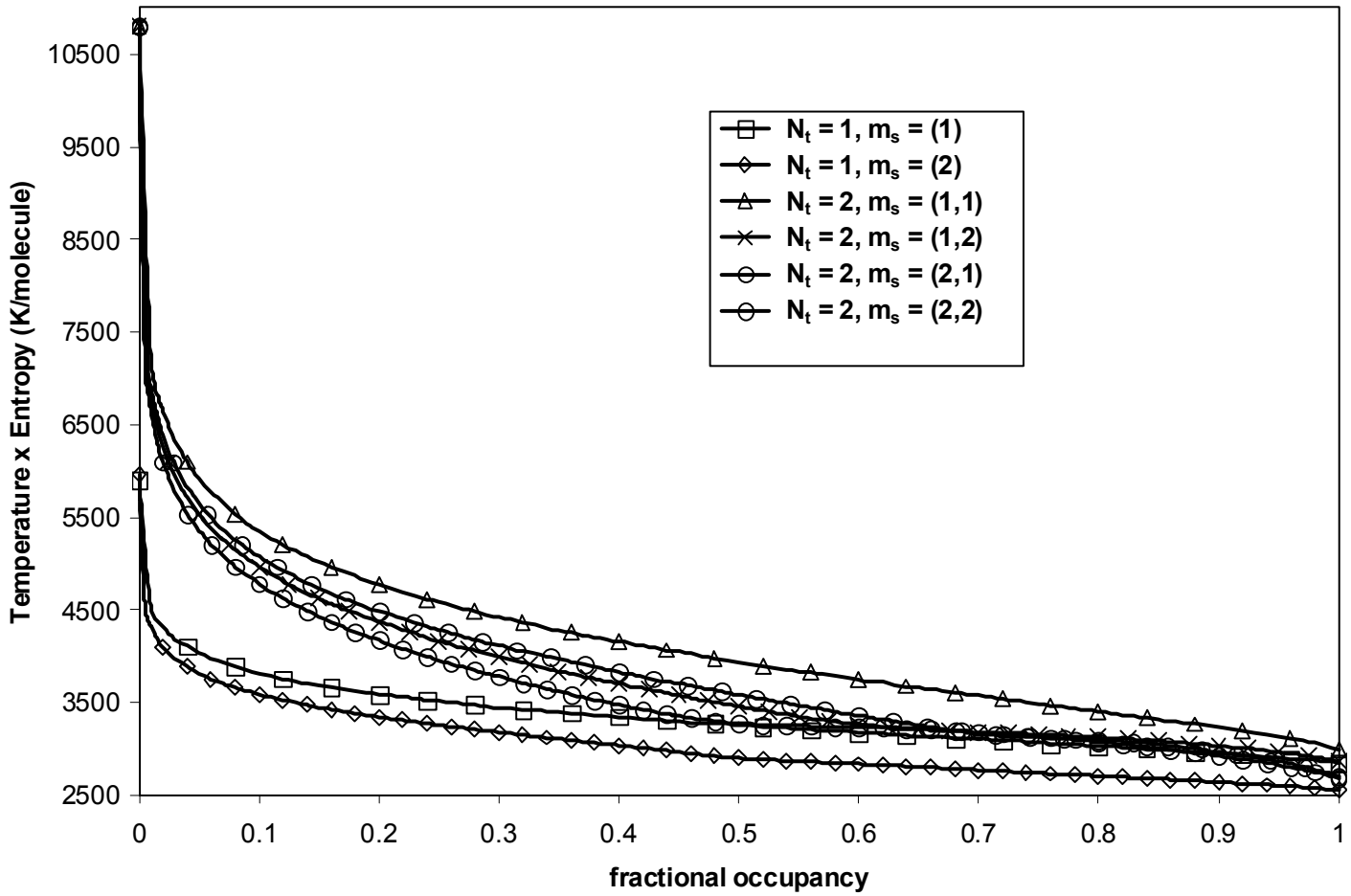

Figure 8: Entropy as a function of fractional occupancy.

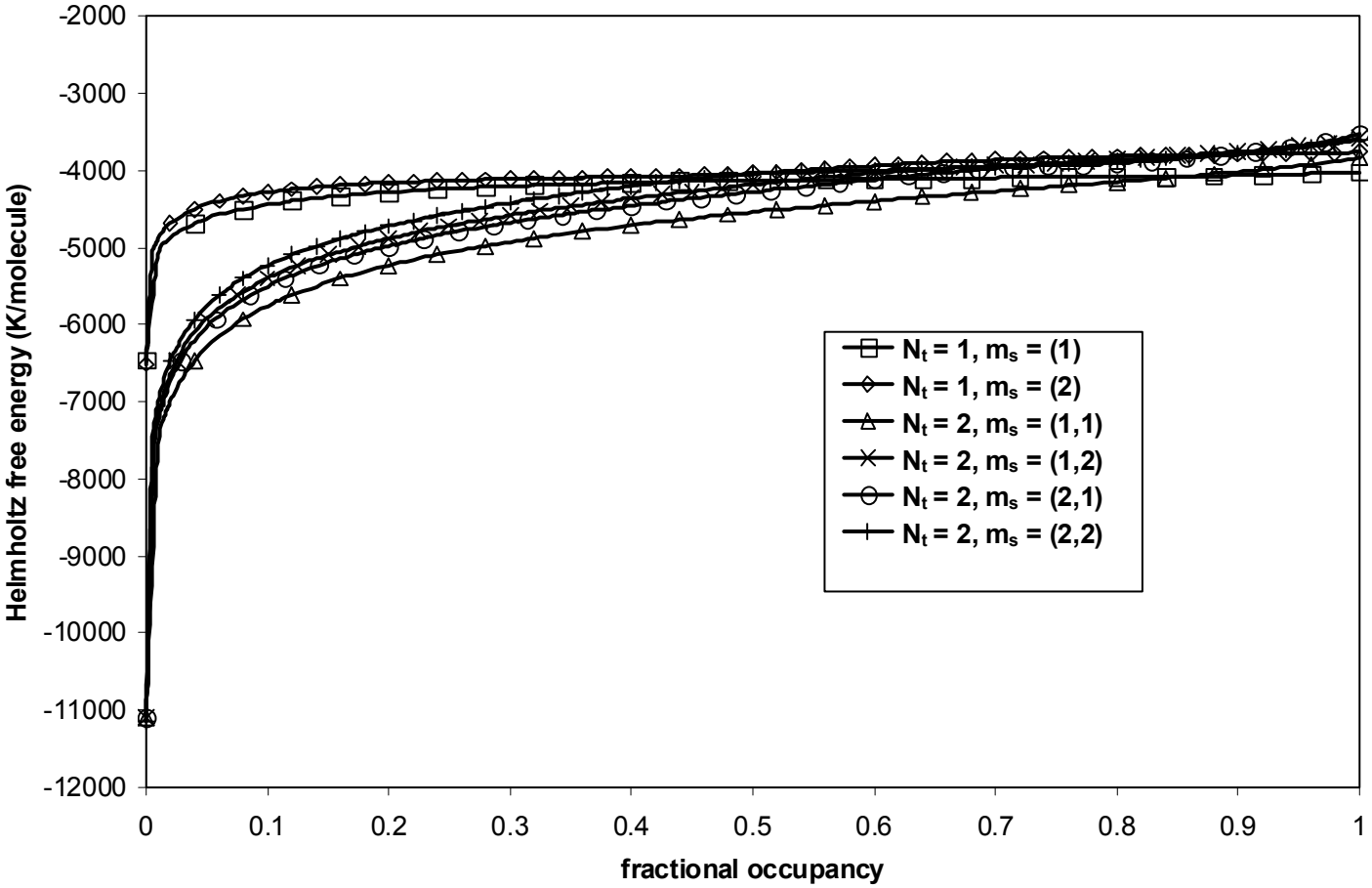

Figure 9: Helmholtz Free energy as a function of fractional occupancy.

Part 3

An Analytical Theory for Diffusion of Fluids in Crystalline Nanoporous Materials

ABSTRACT

An analytical theory for diffusion of fluids in zeolites and other nanoporous materials has been developed. The theory incorporates molecular level information about the nanoporous material, which is obtainable from an energy minimization and does not require molecular dynamics computer simulations. The theory is statistical mechanical in nature and assumes a lattice composed of adsorption sites. The theory yields a self-diffusion coefficient, which is a function of (i) temperature, (ii) adsorbate density, (iii) adsorbate size, (iv) adsorbate-adsorbate energetic interaction, and (v) adsorbate-pore energetic interaction. The theory is generalized and is applicable to nanoporous materials with three-dimensional porous networks (e.g. faujusite) and one-dimensional porous networks (e.g. $AlPO_4$-5).

The theory is self-contained and incorporates no fitting parameters. The theory does not require computational effort beyond a few seconds on a standard personal computer.

3.1 INTRODUCTION

3.1.1 Background

Dynamic molecular-level computer simulations have been employed to study the behavior of fluids in nanoporous materials (e.g. zeolites) during the last fifteen years [1-88]. The primary objective of the simulation work has been to define the fundamental mechanisms for adsorption and diffusion in nanoporous materials. These phenomena play a pivotal role in the catalytic and separation processes that utilize these nanoporous materials [89,90]. The state of the research has matured to the point where it has been well established that competing energetic and entropic effects dictate the placement of adsorbates within the nanoporous material [1-3, 6]. This placement is a function of the atomistic structure of the adsorbent, and the size and energetic well depth of the localized adsorption sites.[31]

However, due to the vast range of nanoporous materials, molecular sieves, zeolites, and MCM-type materials, the results for different systems often give seemingly contradictory results. For instance, the diffusivity of methane may increase with loading in one nanoporous adsorbent, decrease in a second, and show a maximum in a third absorbent [91,92,93]. Such incongruent behavior is influenced by a variety of factors, which arise from the complex molecular physics within the adsorbate-adsorbent sphere of influence. A unifying theory that incorporates the differences in the nanoporous environment would be able to show that the seemingly contradictory results in the literature are in fact manifestations of the same underlying physical mechanisms. Furthermore, the computational efficiency provided by analytical theory would facilitate the extension of the body of knowledge from the basic molecular realm to the macroscopic realm. A predictive theory can be easily integrated into industry standard finite-element process simulators, which would demonstrate that the results indicated by molecular-level simulations do in fact have the suggested ramifications in a macroscopic chemical process.

3.1.2 Objective

In our previous work we developed an analytical theory to describe adsorption in nanoporous materials [94]. The objective of the proposed work is to develop a predictive theory of diffusion in nanoscopically confined pore spaces.

3.1.3 Theory

Our predictive theory of adsorption and diffusion in nanoscopically-confined pore spaces is a lattice model. In a recently published work, we developed the analytical model for adsorption of fluids in any arbitrary lattice [94]. In this work, we extend our knowledge to develop an analytical theory to predict lattice diffusion. The pore network of crystalline nanoporous materials is regular, and hence the materials can be described as a network of well-defined sites. A significant body of literature is dedicated to random-walk diffusion on regular lattices [95-99]. Molecules hop from one site to another depending on the nanoscale environment and the energetic interactions. Diffusion in the lattice sites is modeled as an activated process, with the jumping frequency of molecules determined by transition-state theory [85,86].

Mean-field approximations and the site-blocking model have been employed to describe the dependence of diffusion on concentration. Of note in this connection is the work done by Auerbach, and Saravanan et.al [85-88]. Our theory is similar to the one proposed by Saravanan et.al [85,86] in that both the theories include nearest neighbor interactions and site blocking in calculating diffusivity. However, we suggest that our theory is more easily generalizable to a variety of adsorbate-adsorbent interacting systems. Also, there are some notable differences in the two approaches. First of all, their analytical theory assumes a leading-order approximation, which limits adsorption to the sites that are more stable before filling the sites that are less stable. Our lattice theory does not make this assumption. Furthermore, they assume that the site occupancies can either be 0 or 1. Our theory allows for higher maximum occupancies (in other words, we assume that diffusion can occur through partially occupied sites). Also, our theory does not assume the instantaneous occupancies in different sites to be identical.

Our lattice theory is statistical mechanical in nature and assumes a lattice composed of adsorption sites. As we further demonstrate in Sections 2 and 3, the diffusion component of the theory incorporates no fitting parameters. The theory incorporates molecular level information about the nanoporous material, which is obtainable from an energy minimization and does not require molecular dynamics computer simulations. The theory yields a self-diffusion coefficient, which is a function of (i) temperature, (ii) adsorbate density, (iii) adsorbate size, (iv) adsorbate-adsorbate energetic interaction, and (v) adsorbate-pore energetic interaction. (Section 2 explains the theory in detail.)

Outline

The remainder of this paper is organized as follows. In Section II, we derive the lattice diffusion theory, and obtain analytical expressions for the factors required. In doing so, we refer to our lattice adsorption theory whenever needed. In Section III, we present the results of our diffusion model for different lattice geometries and also provide a discussion on the behavior predicted. The density and temperature dependencies of the self-diffusion coefficient are explained.

3.2 THEORY

3.2.1 Lattice Diffusion Theory

Consider a lattice model with $N_t = 2$ types of sites, Site 1 and Site 2. Of these sites there are m_1 sites of Type 1 and m_2 sites of Type 2. We have a total number of sites, m, where $m = m_1 + m_2$. Sites of Type 1 have a maximum occupancy of $m_{s,1}$ adsorbates. Sites of Type 2 have a maximum occupancy of $m_{s,2}$ adsorbates. Each type of site has an internal volume $V_{s,1}$ or $V_{s,2}$. The connectivity of the lattice is defined by an $N_t x N_t$ matrix, $\underline{\underline{c}}$, where c_{ij} is the number of sites of type j adjacent to a single site of

Type i. The separation between sites is defined by an $N_t x N_t$ matrix, $\underline{\underline{\ell}}$. See Figure 1 for an example of such a matrix with $\underline{\underline{c}} = \begin{bmatrix} 0 & 3 \\ 2 & 0 \end{bmatrix}$.

We know that lattice diffusion is an activated process with Arrhenius temperature dependence. Typically, the activated process is modeled by requiring motion from a site of Type 1 to an adjacent site of type 1 to pass through a site of Type 2. Sites of Type 2 are considered "the activated state" site. The activation energy is simply the difference in total energy for a single adsorbate in a site of Type 1 and Type 2. We assume a functional form of the diffusion coefficient as

$$D = D_o e^{\frac{-\Delta E_{21}}{kT}} \tag{1.a}$$

Where the prefactor, D_o, is defined as half the product of the frequency with which moves are attempted and the square of the displacement associated with the move.

$$D_o = \frac{\omega \ell^2}{2d} \tag{1.b}$$

where d is the dimensionality of the lattice. The factor of $\frac{1}{2d}$ appears in the prefactor in order to make the diffusion coefficient derived from atomic motions agree with the form of the diffusion coefficient derived from a macroscopic solution of Fick's equation.[93]

This formulation is valid if the site of Type 2 is always the activated state. However, in a more generalized lattice, the energy is a function of loading (site occupancy) and temperature. Thus the activated state is not universally defined. For example, a site of Type 2 may have a higher energy when the site of origin (Type 1) has occupancy of unity and the destination site (Type 2) is initially empty. However, a site of Type 2 may have a lower energy when the site of origin (Type 1) has occupancy of two and the destination site (Type 2) is initially empty. This effect is due to the functional dependence of energy on site occupancy. The temperature can also change which state is

the "activated" state. This can be seen by comparing the two temperature asymptotes. At low temperature, the total energy is dominated by energetic contributions. Thus, if a site of Type 1 is energetically favorable, then sites of Type 2 are activated states. However, at infinite temperature, the total energy is dominated by the entropic contribution. Therefore, the larger site is favored, which could very well be sites of Type 2, making sites of Type 1 the activated sites.

To account for the functional dependence of the total energy on occupancy and temperature, we must account for the various activation barriers as seen by molecules in different local situations. This accounting must take into effect the occupancy and type of the origin site and the occupancy and type of the destination site, as well as the temperature. For each situation, the change in total energy is calculated. If the change is positive, then it is to be considered an activation barrier. The various activation barriers are weighted according to the probability of seeing an opportunity for a hop from a site of Type i with occupancy x to a site of type j with occupancy y. Of course, this probability is a function of temperature.

In short, we pursue an average self-diffusivity that is weighted for all local environments in the system:

$$D(n,m,T) = \sum_{i=1}^{N_t} \sum_{x=0}^{m_{s,i}} w_i(x,n,m) D_i(x,T) \qquad (2)$$

where $D(n,m,T)$ is the self-diffusivity of the system, and in the canonical ensemble, is a function of the number of adsorbates, n, the number of sites, m, and the temperature, T. $D_i(x,T)$ is the diffusivity of an adsorbate sitting in a site of type i with occupancy x and $w_i(x,n,m)$ is the corresponding weighting function.

We have recently published an analytical theory of adsorption which can provide total energies and adsorbate distributions for the arbitrary lattice described above [94].

The theory delivers the number of sites of type i with occupancy x, $n_{s,i}(x)$. The $n_{s,i}(x)$ are related to the total number of sites, m, by the constraint

$$m = \sum_{i=1}^{N_t} \sum_{x=0}^{m_{s,i}} n_{s,i}(x) \tag{3}$$

The probability of observing a site of Type i with occupancy x, $p_{s,i}(x)$, is given by

$$p_{s,i}(x) = \frac{n_{s,i}(x)}{m} \tag{4}$$

The number of adsorbates in a site of Type i with occupancy x is related to the total number of adsorbates, n, by the constraint

$$n = \sum_{i=1}^{N_t} \sum_{x=0}^{m_{s,i}} x \cdot n_{s,i}(x) \tag{5}$$

The probability of observing an adsorbate in a site of Type i with occupancy x, $p_{a,i}(x)$, is given by

$$p_{a,i}(x) = \frac{x \cdot n_{s,i}(x)}{n} \tag{6}$$

Equation (6) is the weighting function required in the average diffusivity of Equation (2). Substitution yields

$$D(n,m,T) = \sum_{i=1}^{N_t} \sum_{x=0}^{m_{s,i}} p_{a,i}(x) D_i(x,T) = \sum_{i=1}^{N_t} \sum_{x=0}^{m_{s,i}} \frac{x \cdot n_{s,i}(x)}{n} D_i(x,T) \tag{7}$$

An adsorbate in a site of type i has $c_i = \sum_{i=1}^{N_t} c_{ij}$ adjacent sites through which diffusion can occur. The activation barrier for moving to one of these adjacent sites depends not only on characteristics of the site of origin (Type i with occupancy x) but also upon the characteristics of the destination site (Type j with occupancy y). Thus, the local diffusivity, $D_i(x,T)$, must be expressed as an average over all possible paths.

$$D_i(x,T) = \frac{1}{c_i} \sum_{j=1}^{N_t} c_{ij} \sum_{y=0}^{m_{s,j}} w_{ij}(x,y) D_{ij}(x,y,T) \tag{8}$$

where $D_{ij}(x,y,T)$ is a diffusivity along a path leading from a site of Type i with occupancy x to a site of type j with occupancy y. The new weighting function, $w_{ij}(x,y)$, provides the probability that such a pathway exists, given that the site of origin is Type i with occupancy x and given that the destination is Type j. This is a conditional probability, which is defined as

$$w_{ij}(x,y) = \frac{N_{ij}(x,y)}{\sum_{z=1}^{m_{s,j}} N_{ij}(x,z)} \tag{9}$$

where the number of adjacent sites where one site is of Type i with occupancy x and the second of Type j with occupancy y is defined as $N_{ij}(x,y)$. Our analytical theory of adsorption also delivers all values of $N_{ij}(x,y)$.

Substitution of Equations (8) and (9) into Equation (7) yields

$$D(n,m,T) = \sum_{i=1}^{N_t} \sum_{x=0}^{m_{s,i}} \frac{x \cdot n_{s,i}(x)}{n} \frac{1}{c_i} \sum_{j=1}^{N_t} c_{ij} \sum_{y=0}^{m_{s,j}} \frac{N_{ij}(x,y)}{\sum_{z=0}^{m_{s,j}} N_{ij}(x,z)} D_{ij}(x,y,T) \tag{10}$$

As a check that our weighting functions are appropriate, we can examine the case where the local diffusivities, $D_{ij}(x,y,T)$, are all the same. In that case the local diffusivity can be pulled from the quadruple summation and the summation must therefore total unity, which upon evaluation is shown to be true.

The only remaining factor required to obtain the average diffusivity is the local diffusivity, $D_{ij}(x,y,T)$. This function has the standard activated form

$$D_{ij}(x,y,T) = D_{o,ij}(x) e^{\frac{\Delta E^*_{ji}(y+1,x,T)}{kT}} h_{ij}(x,y) \tag{11}$$

where $\Delta E^*_{ji}(y+1,x,T)$ is an activation barrier to motion, which is defined as

$$\Delta E_{ij}(x,y,T) = \begin{cases} \Delta E_{ij}(x,y,T) & \text{if } \Delta E_{ij}(x,y,T) > 0 \\ 0 & \text{if } \Delta E_{ij}(x,y,T) \le 0 \end{cases} \tag{12}$$

This modified barrier allows activated motion to occur when the change in total energy is positive, and allows the move to occur freely when the change is zero or negative.

We have introduced an additional weighting function in Equation (11). The weighting function, $h_{ij}(x,y)$, eliminates impossible moves, such as a hop from an origin site which is empty, or a hop to a destination site which is already at maximum occupancy.

$$h_{ij}(x,y,T) = \begin{cases} 0 & \text{if } x = 0 \\ 0 & \text{if } y = m_{s,j} \\ 1 & \text{otherwise} \end{cases} \tag{13}$$

Our analytical theory of adsorption delivers $E_i(x,T)$. From this we can obtain the difference needed in Equation (12),

$$\Delta E_{ji}(y+1,x,T) = E_i(x,T) - E_j(y+1,T) \tag{14}$$

The only remaining undetermined factor in Equation (11) is the prefactor, $D_{o,ij}(x)$, to the diffusivity. The purpose of the prefactor is to provide the frequency with which moves are attempted and the mean square displacement of a successful move:

$$D_{o,ij}(x,y) = \frac{\omega_i(x)\ell_{ij}^2}{2} \tag{15}$$

The frequency of attempted hops of an adsorbate in a site of Type i with occupancy x, $\omega_i(x)$, is given by the average velocity over the characteristic dimension of the site

$$\omega_i(x) = \frac{v}{D_{s,eff,i}(x)} \tag{16}$$

where the velocity, v, is given by

$$v = \sqrt{\frac{3kT}{m_a}} \tag{17}$$

and m_a is the molecular mass of the adsorbate. The velocity is the same for all adsorbates regardless of the type of site in which they reside, or its occupancy. The effective diameter of the site, $D_{s,eff,i}(x)$, assumes spherical sites and adsorbates and is given by

$$D_{s,eff,i}(x) = \sqrt[3]{\frac{6}{\pi} V_{s,eff,i}(x)} = \sqrt[3]{\frac{6}{\pi}\left(V_{s,i} - xV_a\right)} \tag{18}$$

where $V_{s,eff,i}(x)$ is the effective volume of a site of Type i with occupancy x, $V_{s,i}$ is the empty volume, and V_a is the volume of the adsorbate.

Thus, we have defined the diffusivity in equation (2) with no adjustable parameters.

An Example Demonstrating Appropriate Asymptotical Behavior

The model proposed above replicates known behavior. To illustrate this, consider a 1-dimensional lattice of alternating sites of type 1 and 2. In this case, we have two types of sites, $N_t = 2$, and maximum occupancies in each site of 1, $m_{s,1} = 1$ and $m_{s,2} = 1$, with connectivity matrix $\underline{\underline{c}} = \begin{bmatrix} 0 & 2 \\ 2 & 0 \end{bmatrix}$.

If we examine the quadruple summation in Equation (10) we see that there will be 16 terms arising, since i and j can take on values of 1 and 2, and x and y can take on values of 0 and 1, for a total of 2^4=16 combinations. Eight of these sixteen terms involve i=j and therefore are identically zero, since there is no connectivity between these sites, i.e. $c_{11} = c_{22} = 0$. By the definition of $h_{ij}(x, y, T)$, Equation (13), six more of these terms are zero, since a move cannot originate in an empty site or terminate in an already full site. Thus, we are left with only two non-zero moves, $p_{12}(1,0)$ and $p_{21}(1,0)$.

For the purposes of the example, suppose that the move from a site of Type 1 to a site of Type 2 is activated, meaning $\Delta E_{ji}(y+1, x, T) < 0$. With these assumptions, Equation (10) becomes

$$D(n,m,T) = \frac{n_{s,1}(1)}{n}\frac{N_{12}(1,0)}{N_{12}(1,0)+N_{12}(1,1)}D_{o,12}(1,T)e^{\frac{\Delta E_{12}(1,1,T)}{kT}} + \frac{n_{s,2}(1)}{n}\frac{N_{21}(1,0)}{N_{21}(1,0)+N_{21}(1,1)}D_{o,21}(1,T) \tag{19}$$

The same difference in the total energy that forms the activation barrier also partitions the adsorbates between sites. Thus, it can be shown by using our analytical theory of adsorption and algebra that

$$\frac{c_{21}\frac{n_{s,2}(1)}{n}\frac{N_{21}(1,0)}{N_{21}(1,0)+N_{21}(1,1)}}{c_{12}\frac{n_{s,1}(1)}{n}\frac{N_{12}(1,0)}{N_{12}(1,0)+N_{12}(1,1)}} = e^{\frac{-\Delta E_{21}(1,1,T)}{kT}} \tag{20}$$

with the resulting simplification of Equation (19) to

$$D(n,m,T) = \frac{n_{s,1}(1)}{n}\frac{N_{12}(1,0)}{N_{12}(1,0)+N_{12}(1,1)}e^{\frac{-\Delta E_{21}(1,1,T)}{kT}}\left[D_{o,12}(1,T)+D_{o,21}(1,T)\right] \tag{21}$$

If we additionally assume that the two sites have the same volume then the prefactors are the same: $D_{o,12}(1,T) = D_{o,21}(1,T) = D_o(T)$, yielding

$$D(n,m,T) = 2\frac{n_{s,1}(1)}{n}\frac{N_{12}(1,0)}{N_{12}(1,0)+N_{12}(1,1)}D_o(T)e^{\frac{-\Delta E_{21}(1,1,T)}{kT}} \tag{22}$$

At this point we can compare Equation (22) with the standard form of activated diffusion in equation (1). We see three differences. The first difference is that we have a prefactor containing $n_{s,1}(1)$, $N_{12,10}$, and $N_{12,11}$. These factors do not appear in equation (1) because equation (1) assumes that there is negligible occupancy of the activated state. In this limit, $n_{s,2}(1) \to 0$ and $n_{s,1}(1) \to n$, i.e. all molecules are found in sites of Type 1. Furthermore, in this limit $N_{12,11} \to 0$. Therefore, both of the factors become unity and the first difference is resolved. As a reminder, this difference is due solely to the assumption in Equation (1) that the activated state has negligible occupancy. This is an unrealistic assumption, since the barrier to activation is also the drive toward partitioning between sites. If the barrier were so large that there is no occupancy of the activated state, then there would be no diffusion past it. Our theory doesn't make this assumption.

The second difference is the factor of two in Equation (22). Again, this difference is a result of the assumption of negligible occupancy of the activated state. This assumption implies that the time spent in site 2 is negligible. In this limit, the total time for the complete move from a site of Type 1 via a site of Type 2 to a site of Type1 is $t = t_1 + t_2 = 1/\omega + 0 = 1/\omega$. However, in Equation (22) where we have a finite residence time in the activated site, the total time for the same move is $t = t_1 + t_2 = 1/\omega + 1/\omega = 2/\omega$. This explanation accounts for the factor of two.

The third and final difference between Equation (1) and Equation (22) is that in equation (1.b) the jump distance was ℓ_{11}, but in Equation (22) the jump distance is ℓ_{12}, which, if the activated site is midway between the two ground sites, yields $\ell_{12} = \frac{\ell_{11}}{2}$. Thus Equation (1) and Equation (22) differ by a constant factor, which in this example is ¼. This difference is due to a different assumption made in Equation (1), namely that the second half of the move, from the activated site to another site of Type 1, *always* proceeds to a *different* site of Type 1. In this equation there is no instance of an adsorbate moving from a type of site 1 to a site of Type 2 then back to the original site.

The fact that the molecule can move back along this conjugated jump is taken into account in the ensemble average.

To see this we must begin with the derivation of Equation (1). Assuming an atom begins at the origin, the position of the atom after n steps, $\underline{R}_n$, is given by

$$\underline{R}_n = \sum_{i=1}^{n} \underline{r}_i \tag{23}$$

where $\underline{r}_i$ is the vector representing the i^{th} jump. The square of the displacement at the n^{th} step is

$$\underline{R}_n^2 = \sum_{i=1}^{n} \left|\underline{r}_i\right|^2 = \sum_{i=1}^{n} \left|\underline{r}_i\right|^2 + 2\sum_{j=1}^{n-1}\sum_{i=1}^{n-j} \left|\underline{r}_i\right| \left|\underline{r}_{i+j}\right| \cos\theta_{i,i+j} \tag{24}$$

In Equation (1) all jumps are of magnitude ℓ_{11} (because a jump is strictly from ground site to ground site) so Equation (24) becomes

$$\underline{R}_n^2 = n\ell_{11}^2\left(1 + \frac{2}{n}\sum_{j=1}^{n-1}\sum_{i=1}^{n-j}\cos\theta_{i,i+j}\right) \tag{25}$$

The ensemble average of the double summation of the cosine is zero, since forward and reverse hops are equally likely. Thus the mean square displacement is $\underline{R}_n^2 = n\ell_{11}^2$.

However, we now assume that moves are of length ℓ_{12} and that we have two types of hops, from 1 to 2 and from 2 to 1 (and thus moves from a site of Type 1 to an activated site then back to the original site are possible). We will examine equation (24) now for twice as many hops ($2n$) since we want to compare for the same number of possible 1→1 motions. Under these assumptions, we find

$$\underline{R}_n^2 = 2n\ell_{12}{}^2\left(1+\frac{2}{2n}\sum_{j=1}^{2n-1}\sum_{i=1}^{2n-j}\cos\theta_{i,i+j}\right) \tag{26}$$

If we examine the summation over cosines, we see that all moves are not weighted equally (since the 1→2 move is activated and the 2→1 move is barrier-free. Therefore, we must split up the summation into four components, noting that for all odd values of i, the hop was of type 1→2 and for all even values of i the hop was of type 2→1. All hops of the same type have equal weights, although different types of hops have different weights. We can call these normalized weights f_1 and f_2, respectively.

$$\begin{aligned}\sum_{j=1}^{2n-1}\sum_{i=1}^{2n-j}\cos\theta_{i,i+j} &= \sum_{\substack{j=1\\ \text{odd } j}}^{2n-1}\sum_{\substack{i=1\\ \text{odd } i}}^{2n-j} f_1 f_1\cos\theta_{i,i+j} + \sum_{\substack{j=1\\ \text{even } j}}^{2n-1}\sum_{\substack{i=1\\ \text{even } i}}^{2n-j} f_2 f_2\cos\theta_{i,i+j} \\ &\quad + \sum_{\substack{j=1\\ \text{odd } j}}^{2n-1}\sum_{\substack{i=1\\ \text{even } i}}^{2n-j} f_1 f_2\cos\theta_{i,i+j} + \sum_{\substack{j=1\\ \text{even } j}}^{2n-1}\sum_{\substack{i=1\\ \text{odd } i}}^{2n-j} f_1 f_2\cos\theta_{i,i+j}\end{aligned} \tag{27}$$

As was the case before, the odd-odd and even-even summations vanish, due to common probabilities. If and only if the probability of returning from the activated state to the original site is the same as moving to a new ground site, will the second two summations vanish. In other words f_1 and f_2 must be constants. In this case, $\underline{R}_n^2 = n\ell_{12}{}^2$, and in our example we are off by a factor of four.

However, if we make the same assumption as Equation (1), that an adsorbate moving into Site 2 *always* proceeds to a *different* ground site, then f_2 is not a constant. In fact, it is zero for returning to the same site. Therefore the cosines do not vanish. In fact for the 2-D lattice of this example, the cosines in the summation over odd i and $i+1$ (of which there are n) take on a value of unity, with an ensemble average of n. Therefore equation (26) becomes

$$\underline{R}_n^2 = 2n\ell_{12}{}^2\left(1+\frac{1}{n}n\right) = 4n\ell_{12}{}^2 = 4n\left(\frac{\ell_{11}}{2}\right)^2 = n\ell_{11}{}^2 \tag{28}$$

which is the same result as was obtained using Equation (1) as our starting point, but which can only be obtained from Equation (25) if we assume that all activated hops proceed to a different ground state.

We have provided this example to show our generalized theory can obtain the same results as the standard formulation of activated diffusion, under the same assumptions, namely (i) that the occupancy of the activated state is negligible and (ii) that all activated hops are successful. In practice, our generalized theory for diffusion does not make these assumptions.

The next logical question is, "Are the assumptions of the standard model of activated diffusion legitimate?" In the case of the localized adsorption sites of nanoporous materials, experiments and simulation have shown that the high-energy sites have appreciable occupancy [30]. Furthermore, the assumption that all activated motion is successful is generally false. This can be seen immediately by considering the case where the destination site is already fully occupied. The adsorbate makes it up to the activated state then has no choice but to return to the original site. In short, the fact that our model avoids these assumptions is an advantage, resulting from our consideration of the finite loading of the lattice.

3.3 RESULTS AND DISCUSSION

In this section, we report the self-diffusion coefficients predicted by our lattice diffusion theory. (Note that our lattice adsorption theory provides the interaction energies and the adsorbate distribution, which are used in the diffusion component of the theory. See Section 2 for details). The lattice diffusion theory yields a self-diffusion coefficient, which is a function of (i) temperature, (ii) adsorbate density, (iii) adsorbate size, (iv) adsorbate-adsorbate energetic interaction, and (v) adsorbate-pore energetic interaction.

This section presents four plots, which show the diffusivity for four different lattice configurations. Particularly, the adsorption lattices are distinct from each other in the maximum occupancy of the two types of sites. i.e.

1. Sites of type 1 with maximum occupancy of one and sites of type 2 with maximum occupancy of one (2-11 case).
2. Sites of type 1 with maximum occupancy of one and sites of type 2 with maximum occupancy of two (2-12 case).
3. Sites of type 1 with maximum occupancy of two and sites of type 2 with maximum occupancy of one (2-21 case).
4. Sites of type 1 with maximum occupancy of two and sites of type 2 with maximum occupancy of two (2-22 case).

The lattice parameters are listed in Table 1. The two types of sites are connected to each other by a connectivity of $c = \begin{bmatrix} 0 & 3 \\ 2 & 0 \end{bmatrix}$. In other words, 40% of the total sites are of Type 1 and 60% are Type 2. Furthermore, sites of Type 2 are assumed to be larger than sites of Type 1. The well depth, $\underline{\underline{U_{AP}}}$, is given as a matrix in Table 1 where rows indicate the type of site and columns indicate the occupancy of the site.

The four plots study the temperature and loading dependence of the diffusivity. It is worthwhile to mention here that the diffusion component of our lattice theory incorporates no fitting parameters.

Figure (2) plots the self-diffusion coefficients for the 2-11 case (two types of sites each with a maximum occupancy of one). We can clearly make out that the self-diffusion coefficient has a strong dependence on temperature. At all loadings, the diffusivity increases with temperature. Clearly, this is the behavior we expect from the Arrhenius temperature dependence of the diffusivity. Molecules acquire increased kinetic motion at higher temperatures, resulting in more successful 'jumps' from one site to another.

The second trend is the density dependence of the diffusivity. At high temperatures, we see that the diffusivity decreases with loading. We expect this behavior

due to the fact that the prefactor to the diffusivity term, D_0, decreases with loading due to the decrease in the number of sites open to motion – the entropic effect. However, we notice that the diffusivity displays a maximum at 100 K. To understand this behavior, we plot in Figure (3), the potential energy of the adsorbates in the two types of sites. The difference in these energies is the activation energy for diffusion, which is plotted in Figure (4). Figure (4) shows that the activation energy displays a minimum at 100 K. This minimum in the activation energy corresponds to a maximum in the diffusivity. The fact that we observe a minimum in the activation energy only at low temperatures is a consequence of the combined effects of the adsorbate-pore interactions, intersite adsorbate-adsorbate interactions, and the entropic contributions to the adsorbate distributions as predicted by our adsorption theory [94].

Figure (5) displays the self-diffusion coefficients for the 2-12 case. This case is different from the 2-11 case due to the increased maximum occupancy of the larger and energetically more shallow Type 2 sites (two adsorbates/site). An immediate observation on comparing with Figure (2), i.e., the 2-11 case, is that at infinite dilution, the self-diffusion coefficients in both the cases have equal values (in other words, both cases have the same intercept at all temperatures). This indicates that at infinite dilution, a negligible fraction of the sites are doubly occupied. Furthermore, we notice that the temperature and loading dependence of the diffusivity is qualitatively similar to the 2-11 case. The diffusivity decreases with loading at high temperatures, and displays a maximum at 100 K. Also, at all loadings, an increase in temperature increases the diffusivity.

However, we notice that the self-diffusion coefficients for the 2-12 case are quantitatively higher than the self-diffusion coefficients for the 2-11 case at high loadings. (For instance, compare the diffusivities for the 2-11 case and the 2-12 case at a loading of one adsorbate/site.) This is simply because the total adsorptive capacity of the 2-12 case is greater than the 2-11 case due to the higher maximum occupancy of Type 2 sites.

Figure (6) plots the self-diffusion coefficients for the 2-21 case. In this case, the energetically deeper sites of Type 1 have a higher maximum occupancy of two. On one hand, the temperature dependence is qualitatively similar to the previous two cases. At all loadings, an increase in the temperature increases the diffusivity. However, the loading dependence of the diffusivity is different from that seen in the previous two cases. The diffusivity decreases with loading at high temperatures. It is interesting to note that the decrease in the diffusivity observed in the 2-21 case is not as steep as seen in the previous two cases. The differences in the variations in the activation energies with loading cause this deviation of the 2-21 case from the previous two cases. At low temperatures (100 K, 200 K, and 300 K), the diffusivity displays a maximum near a loading of 1 adsorbate/site. This maximum in the diffusivity is an effect of the minimum in the activation energy seen at low temperatures. The minimum in the activation energy is a consequence of the fact that there is an energetic advantage in moving through a singly occupied site of Type 1 because the first molecule lowers the activation energy for the passage of another molecule. We did not observe this behavior in the 2-12 case because in that case, the energetically more shallow sites of Type 2 were the higher occupancy sites, resulting in a monotonic increase in the activation energy. Thus, we see a strong effect of multiple occupancies on the mean diffusivity and its strong correlation with the pore well depth.

Furthermore, given the pore well depth $\underline{\underline{U_{AP}}}$, we see that there are few doubly occupied sites at a loading of one adsorbate/site. In other words, most of the sites are filled with one molecule each, regardless of the type of the site. For the given $\underline{\underline{U_{AP}}}$, we would expect the diffusivity to approach zero at a loading of one adsorbate/site. (Other values of $\underline{\underline{U_{AP}}}$ would produce different results.) On the contrary, we see in Figure (6) that the diffusivity displays a maximum. We attribute this aphysical behavior to the fact that our mean diffusivity is calculated from the local diffusivities weighted by their respective distribution of adsorbates. This procedure produces a mean diffusivity that does not incorporate the global distribution of adsorbates. It is well known that the global

distribution of adsorbates in a diffusive system can result in a percolation threshold, namely that there no longer appear sample spanning clusters through which global motion can occur.[7,102,103] Typically, percolative behavior leads to zero diffusivity before complete loading. Since our "blocking" species are mobile, we do not expect an absolute percolative threshold. We would expect the diffusivities to approach zero. In the future, we intend to take the local diffusivities generated by our model, and use an effective medium approximation (EMA) [103,104] to incorporate the percolative effects of the lattice. We expect the inclusion of percolative behavior will most strongly affect the mean diffusivity, D, at high loadings. We expect the nonmonotonic trends shown here to persist, albeit weighted by the percolative effect of the lattice.

The self-diffusion coefficients for the 2-22 case are displayed in Figure (7). As seen in the previous three cases, we observe an increase in the diffusivity with temperature at all loading, which is a result of the Arrhenius temperature dependence of the diffusivity. The molecules acquire increased mobility at high temperatures, thus resulting in more successful jumps between sites.

The study of the density dependence of the diffusivity reveals some interesting patterns. The diffusivity displays a maximum near a loading of 1.4 adsorbates/site. It is interesting to note that unlike the 2-21 case, the diffusivity displays a minimum even at high temperatures. The maximum in the diffusivity is a consequence of the minimum in the activation energy, seen at all temperatures. It is important to note that in the 2-22 case, both the types of sites have a maximum occupancy of two. There is a high energetic advantage involved in moving the molecules from and through singly occupied sites of Type 1 and 2, which results in the decrease in the activation energy. Furthermore, at all temperatures, we observe a slight kink in the diffusivity near a loading of 0.75 adsorbates/site. This kink corresponds to the fact that some of the sites are doubly occupied and hence there is a slightly higher activation barrier for diffusion in the presence of these sites. At high loadings, as observed in the previous cases, the diffusivity decreases with loading at all temperatures. As discussed in the previous case,

the inclusion of the percolative effects would strongly affect the diffusivities at high loadings.

3.4 CONCLUSIONS

In this work, we have presented an analytical theory for lattice diffusion. The lattice diffusion theory predicts the behavior of fluids confined in zeolites, molecular sieves, and other nanoporous materials. The theory incorporates molecular level information about the nanoporous material, which is obtainable from an energy minimization and does not require molecular dynamics computer simulations. The theory yields a self-diffusion coefficient, which is a function of (i) temperature, (ii) adsorbate density, (iii) adsorbate size, (iv) adsorbate-adsorbate energetic interaction, and (v) adsorbate-pore energetic interaction.

The theory is beneficial because it incorporates no fitting parameters. The theory is self-contained and does not require computational effort beyond a few seconds on a standard personal computer, as opposed to hundreds of CPU hours of molecular dynamics simulations on a supercomputer or parallel cluster.

REFERENCES

1. Keffer, D., Davis, H.T., McCormick, A.V., "The effect of nanopore shape and loading on adsorption selectivity of a binary mixture" *J. Phys. Chem.* 1996 **100** p. 638-645.
2. Keffer, D., Davis, H.T., McCormick, A.V., "The effect of nanopore shape on the structure and isotherms of adsorbed fluids" *Adsorption* 1996 **2** p. 9-21.
3. Keffer, D., "Molecular Models of Adsorption and Diffusion in Nanoporous Materials", Ph.D. Thesis, University of Minnesota, July, 1996.
4. Keffer, D., McCormick, A.V., Davis, H.T., " Uni-directional and single-file diffusion in $AlPO_4$-5: a molecular dynamics study", *Mol. Phys.* 1996 **87** p. 367-387.
5. Keffer, D., McCormick, A.V., Davis, H.T., "Agreement between Theory and Simulation of Single-file diffusion in a molecular sieve", Proceedings from the XI International Workshop on Condensed Matter Theories, Caracas, Venezuela, June, 1995.
6. Hahn, K. Kärger, J., "Molecular Dynamics Simulations of Single-File Systems", *J. Phys. Chem.*, 1996 100 p. 316-326.
7. Keffer, D., McCormick, A.V., Davis, H.T., "Diffusion and Percolation on Zeolite Sorption Lattices", *J. Phys. Chem.* 1996 **100** p. 967-973.
8. Kono, H., Takasaka, A., "Statistical mechanics calculation of the sorption characteristics of Ar and N2 in dehydrated zeolite 4A by a Monte Carlo method for determining configuration integrals", *J. Phys. Chem.* 1987 **91** p. 4044-4055.
9. Razmus, D.M., Hall, C.K., "Prediction of gas adsorption in 5A zeolites using Monte Carlo simulations", *AIChE J.* 1991 **37** p. 769-779.
10. Van Tassel, P.R., Davis, H.T., McCormick, A.V., "Monte Carlo calculations of adsorbate placement and thermodynamics in a micropore: Xe in NaA", *Mol. Phys.* 1991 **73** p. 1107-1125.
11. Van Tassel, P.R., Davis, H.T., McCormick, A.V., "Monte Carlo calculations Xe arrangement and energetics in the NaA alpha cage", *Mol. Phys.* 1992 **76** p. 411-432.
12. Van Tassel, Phillips, J.C., P.R., Davis, H.T., McCormick, A.V., "Zeolite adsorption site location and shape shown by simulated isodensity surfaces", *J. Mol. Graphics* 1993 **11** p. 180-184,188.
13. Van Tassel, P.R., Davis, H.T., McCormick, A.V., "Open-system Monte Carlo simulations of Xe in NaA" *J. Chem. Phys.* 1993 **98** p. 8919-8928.
14. Van Tassel, P.R., Somers, S.A., Davis, H.T., McCormick, A.V., "Lattice model and simulation of dynamics of adsorbate motion in zeolites" *Chem. Eng. Sci.* 1994 **49** p. 2979-2989.
15. Van Tassel, P.R., Davis, H.T., McCormick, A.V., "New lattice model for adsorption of small molecules and their mixtures in a zeolite micropore", *AIChE J.* 1994 **40** p. 925-934.
16. Van Tassel, P.R., Davis, H.T., McCormick, A.V., "Adsorption simulations of small molecules and their mixtures in a zeolite micropore", *Langmuir* 1994 **10** p. 1257-1267.

17. Soto, J.L., Myers, A.L., "Monte Carlo studies of adsorption in molecular sieves", *Mol. Phys.* 1981 **42** p. 971-983.
18. Woods, G.B., Panagiotopolous, A.Z., Rowlinson, J.S., "Adsorption of Fluids in Model Zeolites" *Mol. Phys.* 1988 **63** p. 49-63.
19. Woods, G.B., Rowlinson, J.S., "Computer Simulations of fluids in zeolites X and Y" *J. Chem. Soc. Faraday Trans. 2* 1989 **85** p. 765-781.
20. Yashonath, S., Thomas, J.M., Novak, A.K., Cheetham, A.K., "The siting, energetics and mobility of saturated hydrocarbons inside zeolitic cages: methane in zeolite Y", *Nature* 1988 **331** p. 601-604.
21. Yashonath, S., Demontis, P., Klein, M.L., "A molecular dynamics study of methane in zeolite NaY", *Chem. Phys. Lett.* 1988 **153** p. 551-556.
22. Demontis, P. Yashonath, S., Klein, M.L., "Location and mobility of benzene in sodium-Y zeolite by molecular dynamics calculations", *J. Phys. Chem.* 1989 **93** p. 5016-5019.
23. Yashonath, S., "A molecular dynamics study of cage-to-cage migration in sodium Y zeolite: Role of surface-mediated diffusion", *J. Phys. Chem.* 1991 **95** p. 5877-5881.
24. Yashonath, S., Demontis, P., Klein, M.L., "Temperature and concentration dependence of adsorption properties of methane in NaY: A molecular dynamics study", *J. Phys. Chem.* 1991 **95** p. 5881-5889.
25. Santikary, P., Yashonath, S., Ananthakrishna, G., "A molecular dynamics study of xenon sorbed in sodium Y zeolite. 1. Temperature and concentration dependence", *J. Phys. Chem.* 1992 **96** p. 10469-10477.
26. Yashonath, S., Santikary, P., "Xenon in sodium Y zeolite 2. . Arrhenius relation, mechanism, and barrier height distribution for cage-to-cage diffusion", *J. Phys. Chem.* 1993 **97** p. 3849-3857.
27. Yashonath, S., Santikary, P., "Diffusion of sorbates in zeolites Y and A: Novel dependence on sorbate size and strength of sorbate-zeolite interaction", *J. Phys. Chem.* 1994 **98** p. 6368-6376.
28. Klein, H. Kirschhock, C., Fuess, H., "Adsorption and diffusion of aromatic hydrocarbons in zeolite Y by molecular mechanics calculation and x-ray powder diffraction", *J. Phys. Chem.* 1994 **98** p. 12345-12360.
29. Gupta, V., Davis, H.T., McCormick, A.V., "Comparison of the ^{129}Xe NMR chemical shift with simulation in zeolite Y", *J. Phys. Chem.* 1996 **100** p. 9824-9833.
30. Gupta, V., Davis, H.T., McCormick, A.V., "^{129}Xe NMR chemical shifts in zeolites: Effect of Loading studied by Monte Carlo simulations", *J. Phys. Chem.* 1997 **101** p. 129-137.
31. Keffer, D., Gupta, V., Kim, D., Lenz, E., Davis, H.T., McCormick, A.V., "A compendium of zeolite potential energy maps" *J. Mol. Graphics* 1996 **14** p. 108-116, 100-104.

32. Nivarthi, S.S., Van Tassel, P.R., Davis, H.T., McCormick, A.V., "Adsorption and energetics of xenon in mordenite: a Monte Carlo simulation study", *J. Chem. Phys.* 1995 **103** p. 3029-3037.
33. Vernov, A.V., Steele, W.A., "Sorption of xenon in zeolite Rho: A thermodynamics/simulation study", *J. Phys. Chem.* 1993 **97** p. 7660-7664.
34. Loriso, A., Bojan, M.J., Vernov, A., Steele, W.A., "Computer simulation studies of ordered structures formed by rare gases sorbed in zeolite Rho", *J. Phys. Chem.* 1993 **97** p. 7665-7671.
35. Snurr, R.Q., June, R.L., Bell, A.T., Theodorou, D.N., "Molecular simulations of methane adsorption in silicalite", *Mol. Sim.* 1991 **8** p. 73-92.
36. Snurr, R.Q., June, R.L., Bell, A.T., Theodorou, D.N., "A hierarchical atomistic/lattice simulation approach for the prediction of adsorption thermodynamics of benzene in silicalite", *J. Phys. Chem.* 1994 **98** p. 5111-5119.
37. Demontis, P., Fois, E.S., Suffriti, G.B., Quartieri, S., "Molecular dynamics studies on zeolites 4. Diffusion of methane in silicalite", *J. Phys. Chem.* 1990 **94** p. 4329-4334.
38. Demontis, P., Suffriti, G.B., Fois, E.S., Quartieri, S., "Molecular dynamics studies on zeolites 6. Temperature dependence of diffusion of methane in silicalite", *J. Phys. Chem.* 1992 **96** p. 1482-1490.
39. Nowak, A.K., Cheetham, A.K., Pickett, S.D., Ramdas, S., "A computer simulation of the adsorption and diffusion of benzene and toluene in the zeolites Theta-1 and silicalite", *Mol. Sim.* 1987 **1** p. 67-77.
40. Vigne-Maeder, F., Jobic H., "Adsorption sites and packing of benzene in silicalite", *Chem. Phys. Lett.* 1990 **169** p. 31-35.
41. Vigne-Maeder, F., Auroux, A., "Potential maps of methane, water, and methanol in silicalite", *J. Phys. Chem.* 1990 **94** p. 316-322.
42. June, R.L., Bell, A.T., Theodorou, D.N., "Molecular Dynamics studies of methane and xenon in silicalite", *J. Phys. Chem.* 1990 **94** p. 8232-8240.
43. June, R.L., Bell, A.T., Theodorou, D.N., "Transition-state studies of xenon and SF_6 diffusion in silicalite", *J. Phys. Chem.* 1991 **95** p. 8866-8878.
44. Goodbody, S.J., Watanabe, K. MacGowan, D., Walton, J.P.R.B., Quirke, N., "Molecular simulation of methane and butane in silicalite", *J. Chem. Soc. Faraday Trans.* 1991 **87** p. 1951-1958.
45. June, R.L., Bell, A.T., Theodorou, D.N., "Molecular Dynamics studies of butane and hexane in silicalite", *J. Phys. Chem.* 1992 **96** p. 1051-1060.
46. Snurr, R.Q., Bell, A.T., Theodorou, D.N., "Prediction of adsorption of aromatic hydrocarbons in silicalite from grand canonical Monte Carlo simulations with biased insertions", *J. Phys. Chem.* 1993 **97** p. 13472-13752.
47. Nicholas, J.B., Trouw, F.R., Mertz, J.E., Iton, L.E., Hopfinger, A.J., "Molecular Dynamics simulation of propane and methane in silicalite", *J. Phys. Chem.* 1993 **97** p. 4149-4163.
48. Vigne-Maeder, F., "Analysis of ^{129}Xe chemical shifts in zeolites from molecular dynamics calculations", *J. Phys. Chem.* 1994 **98** p. 4666-4672.

49. Smit, B. Siepmann, J.I., "Computer simulations of the energetics and siting of n-alkanes in zeolites", *J. Phys. Chem.* 1994 **98** p. 8442-8452.
50. Smit, B., Maesen, T.L.M., "Commensurate 'freezing' of alkanes in the channels of a zeolite" *Nature* 1995 **374** p. 42-44.
51. Bandopadhyay, S., Yashonath, S., "Diffusion anomaly in silicalite and VPI-5 from molecular dynamics simulations', *J. Phys. Chem.* 1995 **99** p. 4286-4292.
52. Yashonath, S., Bandopadhyay, S., "Surprising diffusion behavior in the restricted regions of silicalite", *Chem. Phys. Lett.* 1994 **228** p. 284-288.
53. Heffelfinger, G.S., Pohl, P.I., Frink, L.J.D., "Molecular Dynamics computer simulations of diffusion in porous silicates", *Mater. Res. Soc. Symp. Proc.* 1995 **366** p. 225-230.
54. Antonchenko, V.Y., Ilyin, V.V., Makovsky, N.N., Khryapa, V.M., "Short-range order in cylindrical liquid-filled micropores", *Mol. Phys.* 1988 **65** p. 1171-83.
55. Bratko, D., Blum, L., Wertheim, M.S., "Structure of hard sphere fluids in narrow cylindrical pores", *J. Chem. Phys.* 1989 **90** p. 2752-2757.
56. Carigan, Y.P., Vladimiroff, T., Macpherson, A.K., "Molecular Dynamics of hard spheres III. Hard spheres in an almost spherical container", *J. Chem. Phys.* 1988 **88** p. 4448-4450.
57. Demi, T., "Molecular Dynamics studies of adsorption and transport in micropores of different geometries", *J. Chem. Phys.* 1991 **95** p. 9242-9247.
58. Dunne, J., Myers, A.L., "Adsorption of gas mixtures in micropores: effect of difference in size of adsorbate molecules", *Chem. Eng. Sci.* 1994 **49** p. 2941-2951.
59. Glandt, E.D., "Density distribution of hard-spherical molecules inside small pores of various shapes", *J. Col. Inter. Sci.* 1980 **77** p. 512-524.
60. Groot, R.D., Faber, N.M., van der Eerden, "Hard sphere fluids near a hard wall and a hard cylinder", *Mol. Phys.* 1987 **62** p. 861-874.
61. Han, K.K., Cushman, J.H., Diestler, D.J., "Grand Canonical Monte Carlo simulations of a Stockmayer fluid in a slit micropore", *Mol. Phys.* 1993 **79** p. 537-545.
62. Heinbuch, U., Fischer, J., "Liquid argon in a cylindrical carbon pore: molecular dynamics and Born-Green-Yvon Results", *Chem. Phys. Lett.* 1987 **135** p. 587-590.
63. Jiang, S., Rhykerd, C.I., Gubbins, K.E., "Layering, freezing transitions, capillary condensation, and diffusion of methane in slit carbon pores", *Mol. Phys.* 1993 **79** p. 373-391.
64. Macelroy, J.M.D., Suh, S.H., "Computer simulation of moderately dense hard-sphere fluids and mixtures in microcapillaries", *Mol. Phys.* 1987 **60** p. 475-501.
65. Macelroy, J.M.D., Suh, S.H., "Simulation studies of a Lennard-Jones liquid in micropores", *Mol. Sim.* 1989 **2** p. 313-315.
66. Macpherson, A.K., Carignan, Vladimiroff, T., "Molecular dynamics of hard spheres II. Hard spheres in a spherical cavity", *J. Chem. Phys.* 1987 **87** 1768-1770.
67. Murad, S., Ravi, P., Powles, J.G., "A computer simulation study of fluids in model slit, tubular, and cubic micropores", *J. Chem. Phys.* 1993 **98** p. 9771-9781.

68. Peterson, B.K., Walton, J.P.R.B., Gubbins, K.E., “Fluid behaviour in narrow pores*”, J. Chem. Soc. Faraday Trans. 2* 1986 **82** p. 1789-1800.
69. Peterson, B.K., Gubbins, K.E., “Phase Transitions in a cylindrical pore: Grand canonical Monte Carlo, mean field theory, and the Kelvin equation”, *Mol. Phys.* 1987 **62** p. 215-226.
70. Saito, A., Foley, H.C., “Curvature and parametric sensitivity in models for adsorption in micropores”, *AIChE J.* 1990 **37** p. 429-436.
71. Sarman, S., “The influence of the fluid-wall interaction potential on the structure of a simple fluid in a narrow slit”, *J. Chem. Phys.* 1990 **92** p. 4447-4455.
72. Schoen, M., Rhykerd, C.L., Cushman, J.H., Diestler, D.J., “Slit-pore sorption isotherms by the grand-canonical Monte Carlo method: Manifestations of Hysteresis”, *Mol. Phys.* 1989 **66** p. 1171-1187.
73. Somers, S.A., Davis, H.T., “Microscopic dynamics of fluids confined between smooth and atomically structured solid surfaces”, *J. Chem. Phys.* 1992 **96** p. 5389-5407.
74. Somers, S.A., McCormick, A.V., Davis, H.T., “Superselectivity and solvation forces of a two component fluid adsorbed in nanopores”, J. Chem. Phys. 1993 99 p. 9890-9898.
75. Tan, Z., Gubbins, K.E., “Selective adsorption of simple mixtures in slit pores: A model of methane-ethane mixtures in carbon”, J. Phys. Chem. 1992 96 p. 845-854.
76. Walton, J.P.R.B., Quirke, N., “Capillary condensation: a molecular simulation study”, *Mol. Sim.* 1989 **2** p. 361-391.
77. Page, K.S., Monson, P.A., "Phase equilibrium in a molecular model of a fluid confined in a disordered porous material", *Phys. Rev. E* 1996 **54** p. R29-32.
78. Vuong, T., Monson, P.A., "Monte Carlo calculations of heats of adsorption in heterogeneous solids", *Langmuir* 1996 **12** p. 5425-5432.
79. Fan, Y., Finn, J.E., Monson, P.A., "A Monte Carlo simulation study of adsorption from a liquid mixture at states near liquid-liquid coexistence", *J. Chem. Phys.* 1993 **99** p. 8238-8243.
80. Peterson, B.K., Heffelfinger, G.S., Gubbins, K.E., Van Swol, F., “Layering transitions in cylindrical nanopores”, *J. Chem. Phys.* 1990 **93** p. 679-685.
81. Heffelfinger, G.S., Van Swol, F., Gubbins, K.E., “Liquid-Vapor coexistence in a cylindrical pore”, *Mol. Phys.* 1987 **61** p. 1381-1390.
82. Demontis, P., Suffritti, G.B., “Molecular Dynamics Investigations of the Diffusion of Methane in a Cubic Symmetry Zeolite of Type ZK4”, *Chem. Phys. Lett.* 1994 **223** p. 355.
83. Beezus, A.G., Kiselev, A.V., Lopatkin, A.A., Pham Quang Du, “Molecular statistical calculation of the thermodynamic adsorption characteristics of zeolites using the atom-atom approximation. Adsorption of methane by zeolite NaX”, *J. Chem. Soc. Faraday Trans.* 1978 **74** p. 367-379.
84. Coppens, M-O., Bell, A.T., Chakraborty, A.K., “Effect of topology and molecular occupancy on self-diffusion in lattice models of zeolites-Monte-Carlo simulations”, *Chem. Engg. Sci.* 1998 **53** p. 2053-2061.

85. Auerbach, S.M., "Analytical theory of benzene diffusion in Na-Y zeolite", *J. Chem. Phys.* 1997 **106** p. 7810-7815.
86. Saravanan, C., Auerbach, S.M., "Modeling the concentration dependence of diffusion in zeolites. I. Analytical theory of benzene in Na-Y", *J. Chem. Phys.* 1997 **107** p. 8120-8131.
87. Saravanan, C., Auerbach, S.M., "Modeling the concentration dependence of diffusion in zeolites. II. Kinetic Monte Carlo simulations of benzene in Na-Y", *J. Chem. Phys.* 1997 **107** p. 8132-8137.
88. Saravanan, C., Jousse, F., Auerbach, S.M., "Modeling the concentration dependence of diffusion in zeolites. III. Testing Mean Field Theory for benzene in Na-Y with simulation", *J. Chem. Phys.* 1998 **108** p. 2162-2169.
89. Weitkamp, J., in "Catalysis and adsorption by zeolites", edited by Olhmann, G., Vendrine, J.C., Jacobs, P.A., Elsevier, Amsterdam, 1991.
90. Newsam, J.M., "Zeolites, in solid state chemistry: Compounds", edited by Cheetham, A.K., Day, P., Oxford University Press, Oxford, 1992, p. 234-280.
91. Sanborn, M.J., Snurr, R.Q., "Diffusion of binary mixtures of CF sub 4 and n-alkanes in faujasite", *Sep. Pur. Tech.* 2000 **20** p. 1-13.
92. Eagen, J.A., Anderson, R.B., "Kinetics and equilibrium of adsorption on 4A zeolite", *J. Coll. Interface. Sci*. 1975 **50** p. 419.
93. Karger, J., Ruthven, D. M., "Diffusion in zeolites and other microporous solids", Wiley-Interscience, New York, 1992.
94. Kamat, M.K., Keffer, D., "An analytical theory for adsorption of fluids in nanoporous materials", submitted to Molecular Physics.
95. Barber, M.N., Ninham, B.W., "Random and restricted walks", Gordon and Breach, New York, 1970.
96. Hughes, B.D., "Random walks and random environment", Oxford University Press, New York, 1995.
97. Montroll, E.W., Weiss, G.H., "Random walks on lattices. II.", *J. Math. Phys.* 1965 **6,** p. 167-181.
98. Schesinger, M.F., Weiss, G.H. (ed.), "The wonderful world of stochastics. A tribute to Elliott W. Montroll", Norht-Holland, Amsterdam, 1985.
99. Weiss, G.H., "Aspects and applications of the random walk", North-Holland, Amsterdam, 1994.
100. Hirschfelder, J.O., Curtiss, C.F., Bird, R.B., "Molecular theory of gases and liquids", Wiley, New York, 1964.
101. Hill, T.L., " Introduction to statistical thermodynamics", Addison Wesley Pub. Co., Mass., 1960.
102. Kirkpatrick, S., "Percolation and conduction", *Reviews of Modern Physics*, 1973, **45**, p. 574-588.
103. Davis, H.T., Valencourt, L.R., Johnson, C.E., "Transport processes in composite media", *J. Am. Cer. Soc.*, 1975, **58** (9-10), p. 446-452.

104. Kirkpatrick, S., “Classical transport in disordered media-scaling and effective medium theories”, *Phys. Rev. Let*. 1971, **27**, p. 1722-&.

APPENDICES

Nomenclature

SYMBOL	DESCRIPTION	UNITS
A	Helmholtz free energy	{K/molecule}
$\underline{\underline{c}}$	Connectivity matrix	-
c_{ij}	Number of sites of type j connected to a site of type i	-
d	Dimensionality of the lattice	-
$D(N,M,T)$	Diffusivity as a function of N, M, and T	$\{m^2/s\}$
$D_{0,ij}(x)$	Prefactor to diffusivity	$\{m^2/s\}$
$D_{s,eff,i}(x)$	Effective diameter of a site as a function of x	{A}
E	Total energy	{K/molecule}
$E_i(x,T)$	Total energy contributed by site of type I as a function of occupancy x and temperature	{K/molecule}
$g(N,M)$	Configurational degeneracy of the lattice	-
$h_{ij}(x,y,T)$	Weighting factor to diffusivity	-
k	Boltzmann constant	{J/mole/K}
$\underline{\underline{\ell}}$	Matrix of distances between sites	{A}
m_a	Mass of an adsorbate	{}
$m_{s,i}$	Maximum occupancy of sites of type i	-
m_i	Number of sites of types i	-
$n_{s,i}(x)$	Number of sites of type i with an occupancy of x	-
$n\mu$	Label of unknowns	-
N	Number of adsorbates	-
$N_{ij,xy}$	Number of neighbors between sites of type i with occupancy x and sites of type j with occupancy y	-
N_t	Number of types of sites	
$p_{a,i}(x)$	Probability of observing an adsorbate in a site of	-

	type i with occupancy x	
$p_{s,i}(x)$	Probability of observing a site of type i with occupancy x	-
$q_i(x,T)$	Intrasite partition function of sites of type i	-
$Q(N,M,T)$	Partition function of a function of N, M, and T	-
r	Lennard- Jones distance between molecules	{A}
r_{min}	Distance of well minimum	{A}
$\underline{R_n}$	Position of an atom after n steps	{m}
S	Entropy	{/molecule}
T	Temperature	{K}
$U_{AP,i}(x)$	Well-depth of a site of type i having an occupancy of x	{K}
v	Velocity of a molecule	{m/s}
V_A	Volume of adsorbate	$\{A^3\}$
$V_{S,i}$	Volume of sites of type i	$\{A^3\}$
$\underline{\underline{w_x}}$	Matrix of adsorbate-adsorbate potential energy due to adsorbates in neighboring sites	{K}
x	Occupancy of a site of type i	-
$\Delta E^*_{ij}(x,y,T)$	Difference in total energy between site of type I with site of type j, as a function of occupancies x, y, and T	{K}
θ	Fractional occupancy	-
δ_{xy}	Kronecker delta function	-
μ	Chemical potential	{K/molecule}
ω	Angular velocity	{rad/s}

Table 1. Lattice Parameters

Case	N_T	$\underline{m_s}$	$\underline{\underline{c}}$	$\underline{\underline{\ell}}$ (Å)	$\underline{V_S}$ (Å^3)	$\underline{\underline{U_{AP}}}$ (K)
1	2	[1,1]	$\begin{bmatrix} 0 & 3 \\ 2 & 0 \end{bmatrix}$	$\begin{bmatrix} - & 4.304 \\ 4.304 & - \end{bmatrix}$	[78.1, 142]	$\begin{bmatrix} -1000 \\ -500 \end{bmatrix}$
2	2	[1,2]	$\begin{bmatrix} 0 & 3 \\ 2 & 0 \end{bmatrix}$	$\begin{bmatrix} - & 4.304 \\ 4.304 & - \end{bmatrix}$	[78.1, 142]	$\begin{bmatrix} -1000 & - \\ -500 & -350 \end{bmatrix}$
3	2	[2,1]	$\begin{bmatrix} 0 & 3 \\ 2 & 0 \end{bmatrix}$	$\begin{bmatrix} - & 4.304 \\ 4.304 & - \end{bmatrix}$	[78.1, 142]	$\begin{bmatrix} -1000 & -350 \\ -500 & - \end{bmatrix}$
4	2	[2,2]	$\begin{bmatrix} 0 & 3 \\ 2 & 0 \end{bmatrix}$	$\begin{bmatrix} - & 4.304 \\ 4.304 & - \end{bmatrix}$	[78.1, 142]	$\begin{bmatrix} -1000 & -350 \\ -500 & -350 \end{bmatrix}$

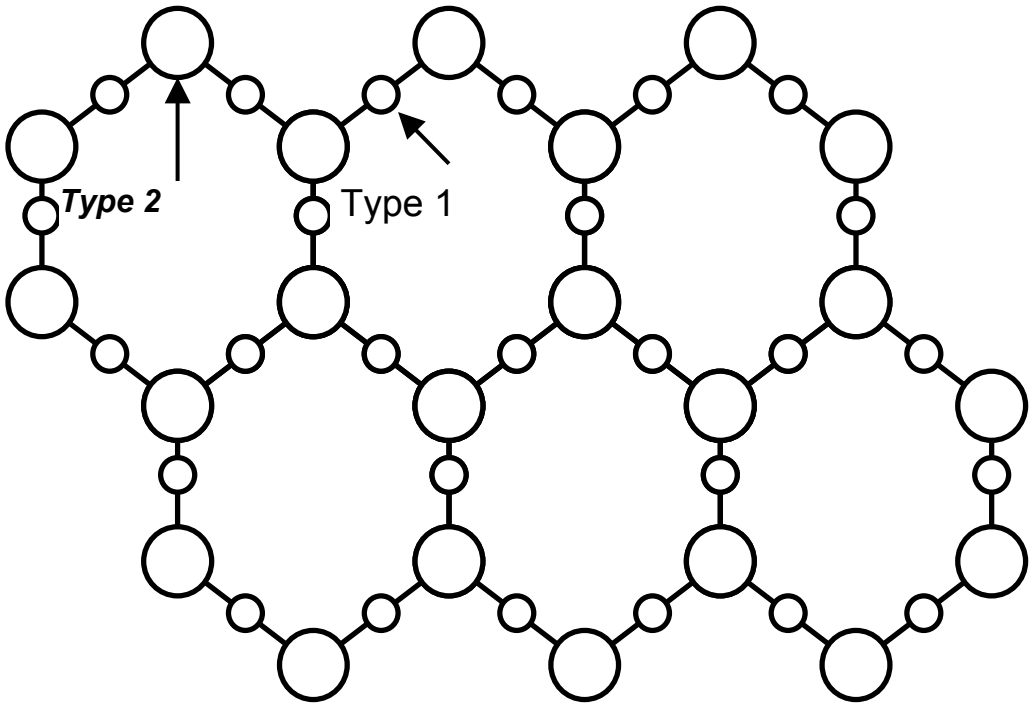

Figure 1: Lattice structure with two types of sites and connectivity matrix $\underline{\underline{c}} = \begin{bmatrix} 0 & 3 \\ 2 & 0 \end{bmatrix}$

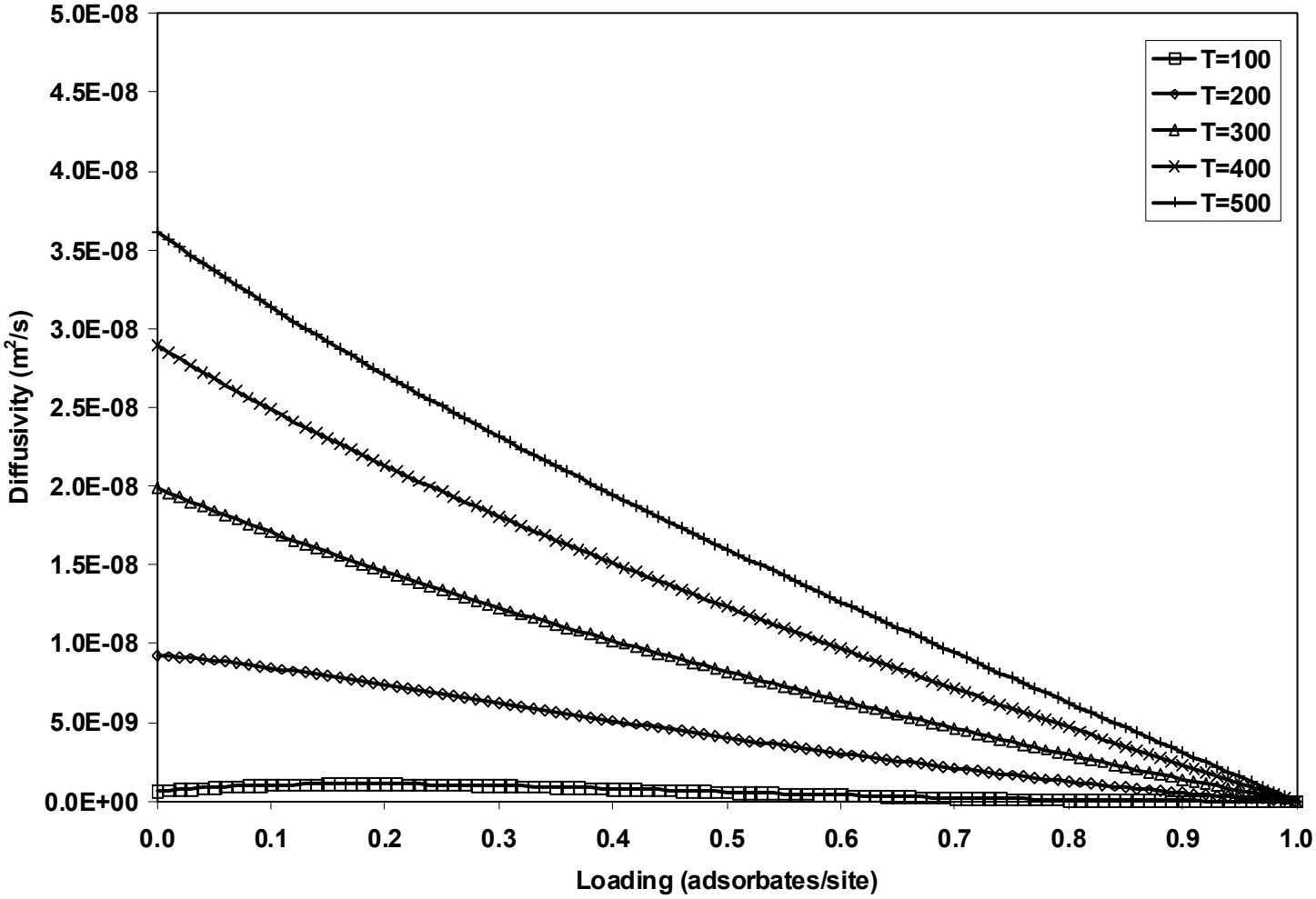

Figure 2: Self-diffusion coefficient as a function of loading for the 2-11 case where $N_T = 2$, $\underline{m_s} = (1,1)$.

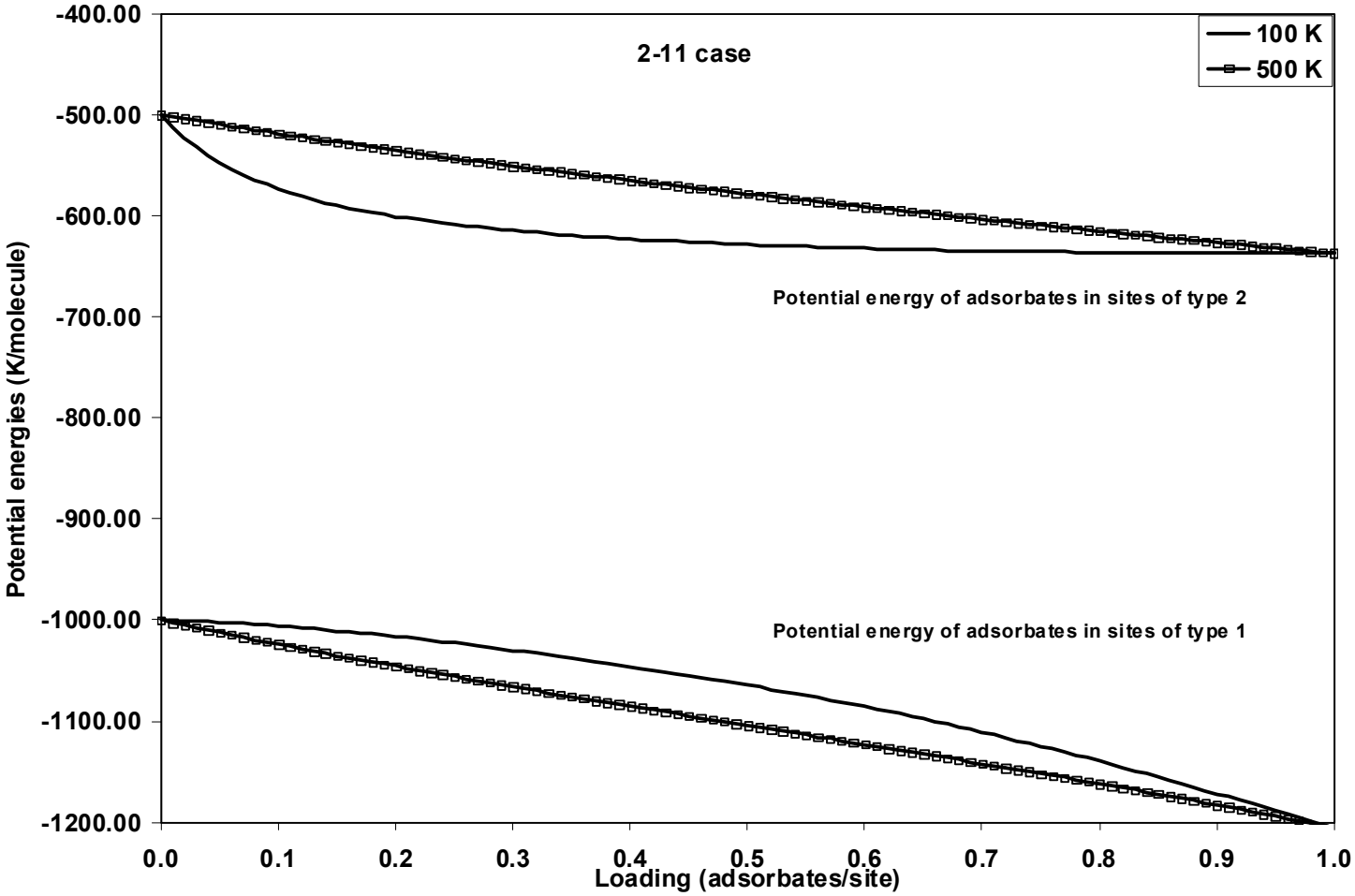

Figure 3: Potential energy for the adsorbates in the two types of sites as a function of loading for the 2-11 case where $N_T = 2$, $\underline{m_s} = (1,2)$.

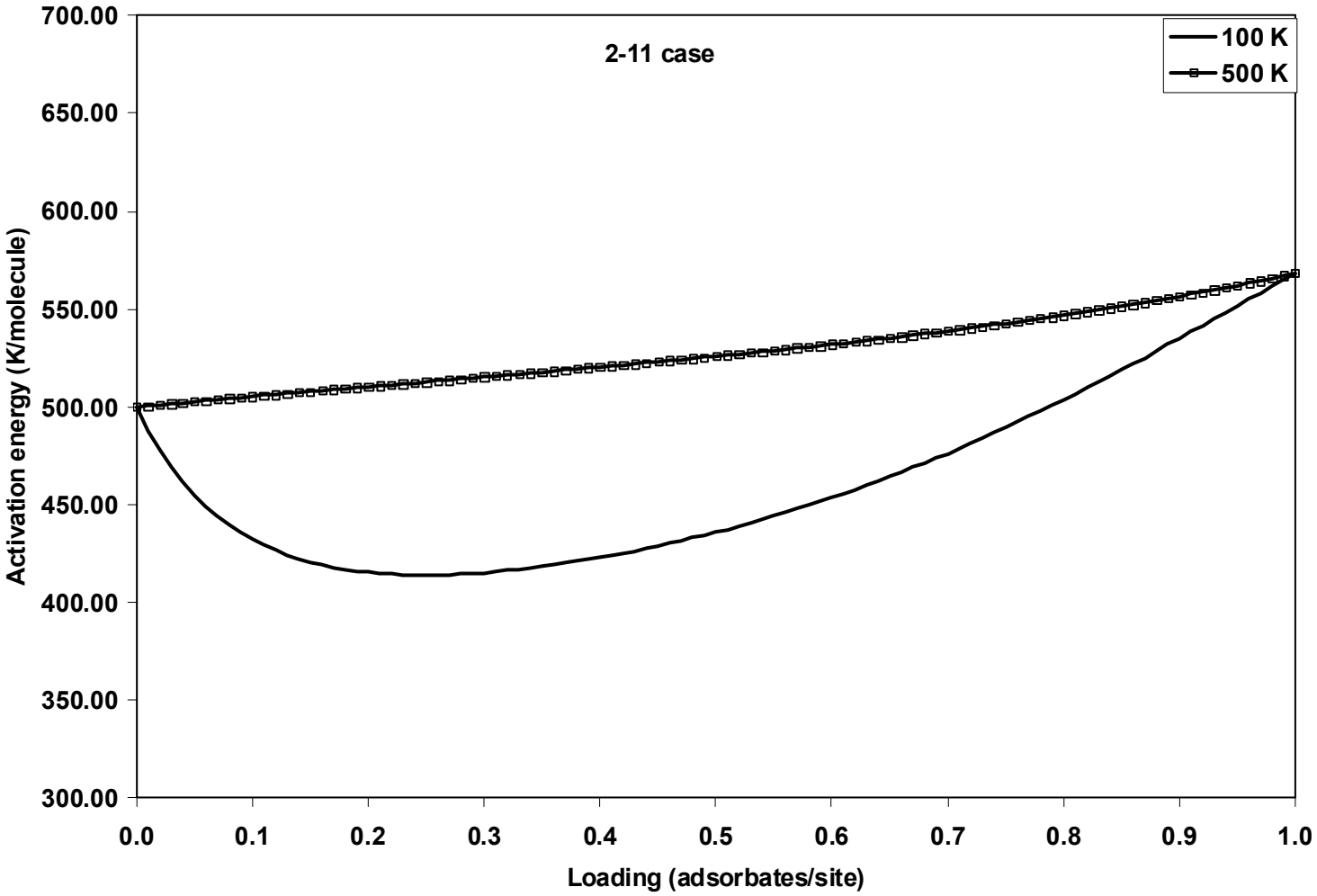

Figure 4: Activation energy as a function of loading for the 2-11 case where $N_T = 2$, $\underline{m_s} = (1,2)$.

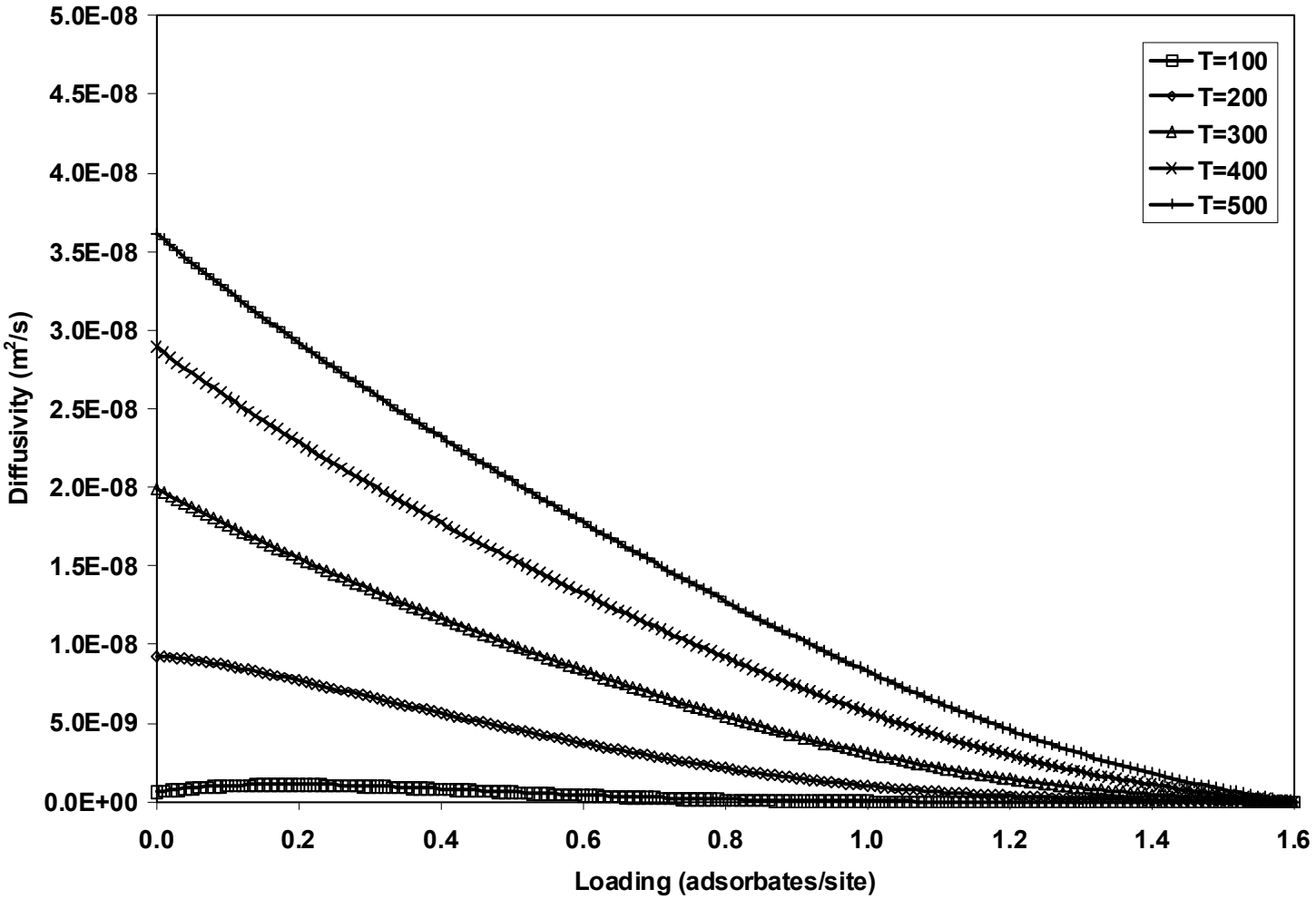

Figure 5: Self-diffusion coefficient as a function of loading for the 2-12 case where $N_T = 2$, $\underline{m_s} = (1,2)$.

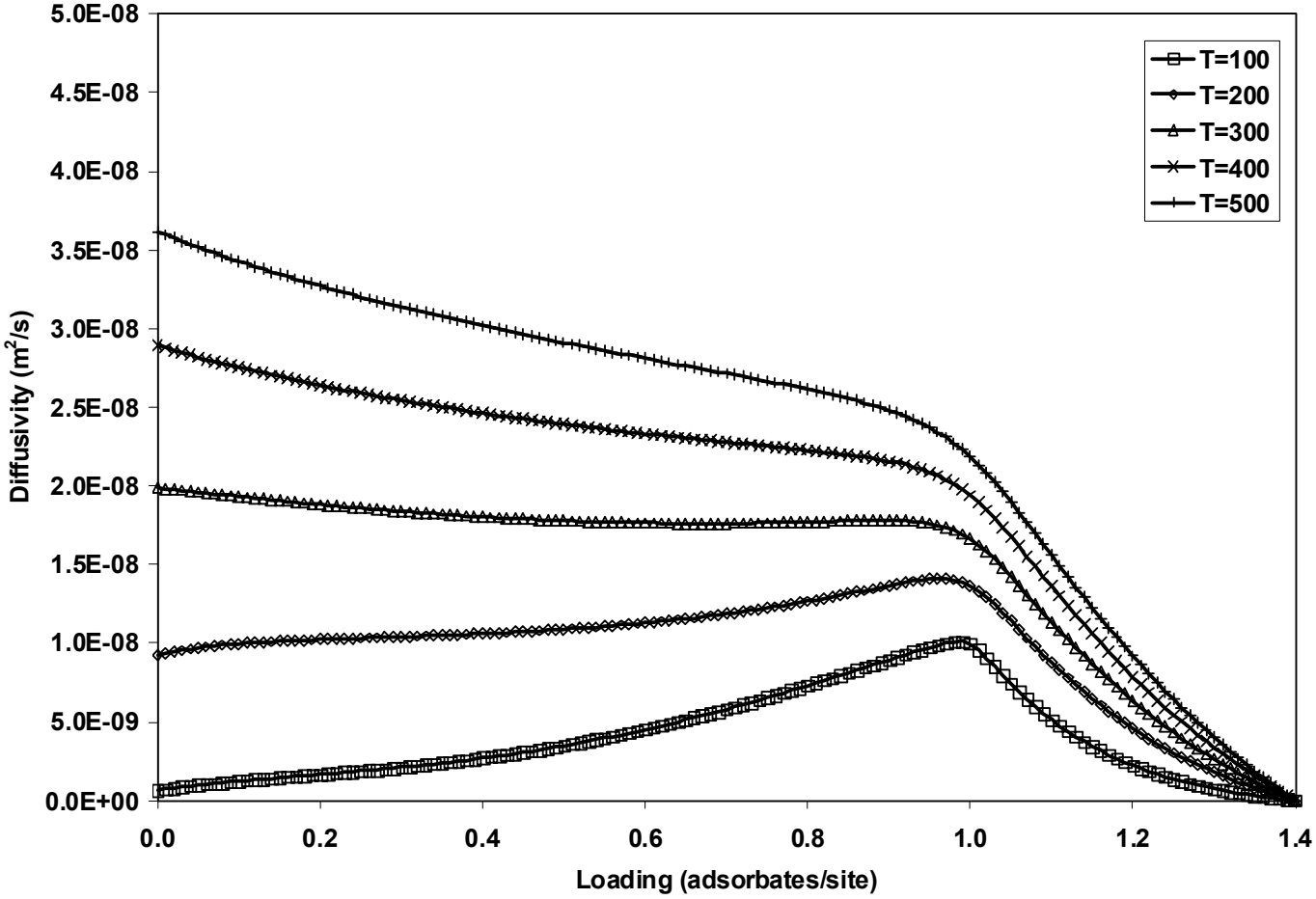

Figure 6: Self-diffusion coefficient as a function of loading for the 2-21 case where $N_T = 2$, $\underline{m_s} = (2,1)$.

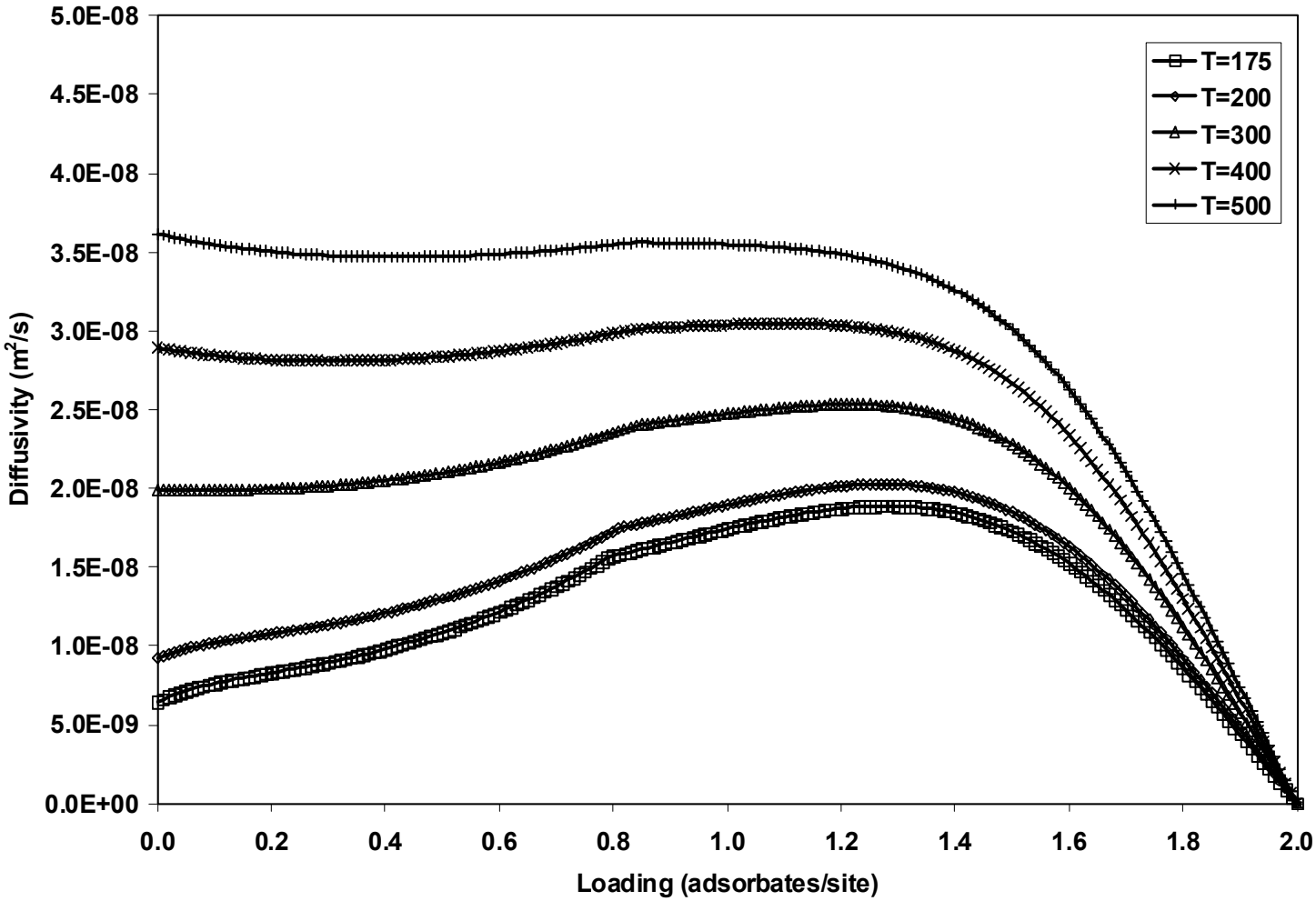

Figure 7: Self-diffusion coefficient as a function of loading for the 2-22 case where $N_T = 2$, $\underline{m_s} = (2,2)$.

Part 4

Agreement Between the Analytical Theory and Molecular Dynamics Simulations for Adsorption and Diffusion in Crystalline Nanoporous Materials

ABSTRACT

Analytical theories for lattice adsorption and diffusion recently published are tested with Molecular Dynamics (MD) simulations. Our analytical theories are generalized and can be applied to various small molecules in different nanoporous structures such as zeolites and molecular sieves. In this work, we validate our theory by comparing the results with those predicted by simulations. We study the behavior of methane in zeolite Na-Y. Specifically, the MD simulations are conducted to obtain the interaction energies and self-diffusion coefficients at five different temperatures and loadings. While the lattice adsorption theory incorporates minimum parameters to obtain the thermodynamic properties, the diffusion component of the theory incorporates no adjustable parameters.

Our theory is in very good qualitative agreement with the simulations. Overall, reasonably good quantitative agreement is found between the theory and simulations. Our theory studies the effect of temperature and density on the adsorption and diffusion of methane in Na-Y. Our theory requires approximately only a minute to obtain the results, as compared with the tens of CPU hours required for simulations.

4.1 INTRODUCTION

4.1.1 Background

A significant body of literature has been devoted to investigate the phenomenon of adsorption and diffusion in nanoporous materials [1-92]. These phenomenon are of great scientific interest due to their increasing wide range applicability in separation and catalysis processes [91,92]. Molecular level simulations have established that competing entropic and energetic effects play an important role in the placement of adsorbates within the nanoporous materials. It has been determined that the ongoing adsorbate-adsorbate and adsorbate-pore interactions within the nanoporous material dictate the extent of adsorption. However, some of the problems still persist. For instance, literature suggests that different systems evolving from the vast range of nanoporous materials such as molecular sieves, zeolites, and MCM-type materials, often give contradictory results for different fluids. E.g. the diffusivity of methane varies differently for different adsorbents as a function of loading and temperature [93-95]. Also, the industry is constantly exploring the applicability of new nanoporous materials as effective adsorbents. The problem is that the computationally expensive simulations are often seen as inefficient platforms to produce quick results. These problems can be overcome by the development of a quick, predictive theory, which would successfully replace the simulations and increase the understanding of the behavior of fluids in nanoporous materials. The theory would provide a unified approach to highlight the physical mechanisms occurring at the molecular level, which would elucidate such seemingly contradictory results.

There have been previous worthwhile attempts to develop analytical theories of adsorption and diffusion based on lattice models. Of note in this connection is the work of Saravanan et.al. who developed an analytical theory of diffusion for benzene in Na-Y [87-90]. Van Tassel et. al. introduced a lattice model for the adsorption of small molecules in zeolite NaA. Snurr et al. presented a lattice model for adsorption of benzene in silicalite [16,38]. In our previous work, we presented unifying analytical

theories for adsorption and diffusion of fluids in nanoporous materials such as molecular sieves and zeolites [1,2]. We suggested that our analytical theory is more easily generalizable to various solid-fluid interacting systems than the previously attempted models. Also, our theory incorporates minimum parameters, which makes it easily accessible for broader usage. Having said that, our second step is to validate these theories with the simulations.

4.1.2 Objective

This paper intends to compare the results of our analytical theories for adsorption and diffusion with Molecular Dynamics simulations for specific solid-fluid contacting system, namely- methane in Na-Y.

Zeolite Na-Y has a three-dimensional channel system consisting of cavities separated by 12-membered oxygen rings. It has nearly 50% of the volume of the crystal available for adsorption with a Si/Al ratio of 1.3. We have mentioned previously how the diffusivity of methane shows different trends for different adsorbents. It is seen that the diffusivity increases with loading for one adsorbent, decreases with loading for a second, and shows a minimum for a third adsorbent [93-95]. Though simulations reveal these trends and explain them to a reasonable extent, our theory investigates the fundamental molecular level mechanisms to understand the underlying physical mechanisms.

4.1.3 Outline

The remainder of this paper is organized as follows. Section 2 provides a brief review of our analytical theories of adsorption and diffusion. Also included is a discussion on the functional form of the external potential. Section 3 discusses the MD simulation methodology and convergence criteria. Also, the numerical optimization routine for convergence parameters is discussed. Section 4 presents the results from theory and simulation for methane in Na-Y and the comparison between the two. Finally, Section 5 presents the conclusions and findings from this work.

4.2 THEORY

4.2.1 Review of the lattice adsorption theory

Our predictive theory of adsorption in nanoscopically-confined pore spaces is a lattice model [1]. We use standard statistical mechanics to develop the partition functions for the adsorbate molecules. The partition functions are used to obtain the desired thermodynamic and transport properties. There are four factors that determine the nanoporous environment, viz. (i) adsorption site volume, (ii) adsorption site energetic well depth, (iii) lattice connectivity, and (iv) lattice spacing. In other words, these four parameters characterize the lattice.

The lattice model uses a generalization of the standard quasi-chemical approximation to account for the adsorbate-adsorbate interactions. The quasi-chemical approximation is the simplest approximation that still allows for adsorbate clustering within the pore [96]. The standard quasi-chemical theory is limited to a lattice consisting of just one type of site. But most of the zeolites and molecular sieves are found to have more than one type of site. The standard quasi-chemical approximation cannot model these complex lattices. However, we expand upon the quasi-chemical theory and use it to describe these lattices because the lattice sites are still localized.

Let's assume an arbitrary lattice with two types of sites, $N_T = 2$. This lattice is described by a connectivity matrix, $\underline{\underline{c}}$, where

$$\underline{\underline{c}} = \begin{bmatrix} c_{11} & c_{12} \\ c_{21} & c_{22} \end{bmatrix} \tag{1}$$

where each of these elements, c_{ij}, describes the number of sites of Type j connected to a site of Type i. Specifying the connectivity in this way specifies the relative number of sites of Types 1 and 2, M_1 and M_2.

As an example consider the lattice schematic in Figure (1). In this case, $\underline{\underline{c}} = \begin{bmatrix} 0 & 3 \\ 2 & 0 \end{bmatrix}$.

The number of sites of Type 1 and 2 must obey the relations:

$$\sum_{i=1}^{N_T} M_i = M \tag{2.1}$$

and a neighbor balance

$$c_{12} M_1 = c_{21} M_2 \tag{2.2}$$

which determines M_1 and M_2 to be

$$M_1 = \frac{c_{21}}{c_{12} + c_{21}} M \qquad \text{and} \qquad M_2 = \frac{c_{12}}{c_{12} + c_{21}} M \tag{3}$$

The separation between nearest neighbor sites is given by a matrix of distances, $\underline{\underline{\ell}}$. The sites have a well-depth of $U_{AP,i}(x)$, which is the potential energy due to adsorbate-pore interactions. $U_{AP,i}(x)$ is a function of x, the occupancy of the site, and of site Type i. The sites have volume, $V_{S,i}$. The four parameters—$\underline{\underline{c}}$, $\underline{\underline{\ell}}$, $\underline{U_{AP}}(x)$, and $\underline{V_S}$—completely characterize the lattice.

We use an arbitrary pairwise potential to model the adsorbate-adsorbate interactions, evaluating it at $\underline{\underline{\ell}}$ to obtain $\underline{\underline{\underline{w_x}}}$.

The partition function has three factors, a configurational degeneracy, intrasite partition function, and intersite interaction energy:

$$Q(N,M,T) = \sum_{\text{configurations}} g(N,\underline{M}) \prod_{i=1}^{N_T} \left[\prod_{x=1}^{m_{s,i}} q_i(x,T)^{x \cdot n_{s,i}(x)} \right] e^{-\sum_{i=1}^{N_T} \sum_{j \geq i}^{N_T} \sum_{x=1}^{m_{s,i}} \sum_{y^*}^{m_{s,i}} N_{ij,xy} \frac{w_x}{kT} \frac{w_x}{kT}} \tag{4}$$

There are two points to be noted here. First, the summation includes only combinations of i and j which have nearest neighbors (i.e. $c_{ij} \neq 0$). Second, the index y^* varies. If $i = j$, $y^* \geq x$. If $i \neq j$, $y^* \geq 1$. This way we avoid double counting. Also, the maximum occupancy of a site of Type i is $m_{s,i}$, the intrasite partition function is $q_i(x,T)$, and the number of sites with occupancy x, $n_{s,i}(x)$ is defined for each site of Type i. The number

of neighbors, $N_{ij,xy}$, designates the number of neighbors between sites of Type i with occupancy x and sites of Type j with occupancy y.

We extend the quasi-chemical approximation to determine the general configurational degeneracy as

$$g(N,M) = \left[\prod_{\substack{i=1 \\ j \neq i}}^{N_T} \left(\frac{M_i!}{\prod_{x=0}^{m_{s,i}} n_s(x)!} \right)^{1-c_{ij}} \right] \left[\frac{(c_{12}M_1)!}{\prod_{x=0}^{m_{s,i}} \prod_{y=0}^{m_{s,j}} N_{ij,xy}!} \right] \tag{5}$$

This general form would be altered to meet particular forms of the connectivity matrix. We consider the case of the connectivity matrix given in Equation (1).

Determining the partition function would be a case of solving a set of equations for the various unknowns. These equations can be generated from the following relations.

- Site balances
- Adsorbate balances
- Symmetry relations for the number of neighbors, and
- A balance on the number of neighbors.

We minimize the partition function with respect to these unknowns to obtain the remaining equations. Thus, we have a system of non-linear algebraic equations with an equal set of unknowns. It was shown in our previous paper on lattice adsorption theory [1] that an analytical solution was obtained only for the single case, $N_T = 2$, $m_{s,1} = 1$, $m_{s,2} = 1$, and $w = 0$. For all other cases, we employed a numerical solution.

Once the variables are known, we can formulate the partition function and solve for any thermodynamic variables of interest.

For example the Helmholtz Free Energy, A, given by

$$A = -kT \ln Q \tag{8}$$

can be obtained by solving for numerical values of the unknowns and substituting them into the partition function. Similarly, we can obtain analytical expressions for the total energy , E, (kinetic and potential) and the entropy, S, from

$$E = kT^2 \left(\frac{\partial \ln Q}{\partial T} \right)_{N,\underline{M},\{unknowns\}} \tag{9}$$

and

$$S = \frac{-A + E}{T} \tag{10}$$

4.2.2 Review of the lattice diffusion theory

The diffusion component of our lattice theory is based on the assumption that lattice diffusion is an activated process with Arrhenius temperature dependence [2]. For instance, an activated process requires motion from a site of Type 1 to an adjacent site of Type 1 to pass through a site of Type 2. Sites of Type 2 are considered "the activated state" sites. Similarly, sites of Type 1 are the activated sites when allowing motion between two adjacent sites of Type 2. The activation energy is simply the difference in the potential energy for an adsorbate in a site of Type 1 and Type 2. It is important to bear in mind the fact that the activation energy has a strong dependence on the site occupancy and the pore well depth. We assume a functional form of the diffusion coefficient as:

$$D(n,m,T) = \sum_{i=1}^{N_t} \sum_{x=0}^{m_{s,i}} \frac{x \cdot n_{s,i}(x)}{n} \frac{1}{c_i} \sum_{j=1}^{N_t} c_{ij} \sum_{y=0}^{m_{s,j}} \frac{N_{ij}(x,y)}{\sum_{z=0}^{m_{s,j}} N_{ij}(x,z)} D_{ij}(x,y,T) \tag{13}$$

Some of the unknowns in Equation (13) can be obtained from our lattice adsorption theory. Also, the above equation includes weighting functions to account for the various factors such as site occupancy and lattice connectivity, affecting a jump of an adsorbate molecule from site of Type 1 to site of Type 2. The only factor required to obtain the average diffusivity then, is the local diffusivity, $D_{ij}(x,y,T)$. This function has the standard activated form:

$$D_{ij}(x,y,T) = D_{o,ij}(x) e^{\frac{\Delta E_{ji}^{*}(y+1,x,T)}{kT}} h_{ij}(x,y) \tag{14}$$

where $\Delta E^{*}_{ji}(y+1,x,T)$ is an activation barrier to motion, which is defined as

$$\Delta E_{ij}(x,y,T) = \begin{matrix} \Delta E_{ij}(x,y,T) & \text{if } \Delta E_{ij}(x,y,T) > 0 \\ 0 & \text{if } \Delta E_{ij}(x,y,T) \le 0 \end{matrix} \tag{15}$$

This modified barrier allows activated motion to occur, when the change in total energy is positive, and allows the move to occur freely, when the change is zero or negative.

The weighting function, $h_{ij}(x,y)$, eliminates impossible moves, such as a hop from an origin site which is empty, or a hop to a destination site which is already at maximum occupancy.

$$h_{ij}(x,y,T) = \begin{cases} 0 & \text{if } x = 0 \\ 0 & \text{if } y = m_{s,j} \\ 1 & \text{otherwise} \end{cases} \tag{16}$$

Our analytical theory of adsorption delivers $E_i(x,T)$ from which we can obtain the difference needed in Equation (12).

$$\Delta E_{ji}(y+1,x,T) = E_i(x,T) - E_j(y+1,T) \tag{17}$$

Furthermore, the prefactor $D_{o,ij}(x)$ in Equation (11) provides the frequency with which moves are attempted and the mean square displacement of a successful move.

$$D_{o,ij}(x,y) = \frac{\omega_i(x)\ell_{ij}^2}{2} \tag{18}$$

The frequency of attempted hops of an adsorbate in a site of Type i with occupancy x, $\omega_i(x)$, is given by

$$\omega_i(x) = \frac{v}{D_{s,eff,i}(x)} \tag{19}$$

The frequency is the average velocity over the characteristic dimension of the site. The velocity, v, is given by

$$v = \sqrt{\frac{3kT}{m_a}} \tag{20}$$

where m_a is the molecular mass of the adsorbate. The velocity is the same for all adsorbates regardless of the type of site in which they reside, or its occupancy. The effective diameter of the site, $D_{s,eff,i}(x)$, assumes that the sites and the adsorbate are spherical, and is given by

$$D_{s,eff,i}(x) = \sqrt[3]{\frac{6}{\pi}V_{s,eff,i}(x)} = \sqrt[3]{\frac{6}{\pi}\left(V_{s,i} - xV_a\right)} \tag{21}$$

where $V_{s,eff,i}(x)$ is the effective volume of a site of Type i with occupancy x, $V_{s,i}$ is the empty volume, and V_a is the volume of the adsorbate.

4.2.3 Functional form of the external potential

Our lattice theory can be generalized to any arbitrary functional form of the external potential, $\underline{\underline{U}}_{AP}$ - the adsorbate-pore interaction energy. Here, we select a slightly different functional form. Unlike assumed previously, the adsorbate-pore (ap) interaction energy could have a strong dependence on temperature in addition to the site occupancy. In other words, the ap interaction energy, $\underline{\underline{U}}_{AP}$, is now a function of site occupancy and temperature.

The functional form of the local ap interaction energy assumes spherical sites and adsorbates, and is a parabolic function of the site radius, r. Let's designate the local ap interaction energy as $U_{AP,i}(r,x)$. Thus, the interaction energy between the adsorbate and the walls of the pore is a function of (i) energetic well depth, (ii) site occupancy, and (iii) pore radius, given by

$$U_{AP,i}(r,x) = U_{AP,i}(x) + U_{APc,i} \times r_i^2 \tag{22}$$

The pore radius, r_i, can be evaluated from the site volume:

$$V_{s,i} = \frac{4}{3}\pi r_i^3 \tag{23}$$

$U_{AP,i}(x)$ is the pore well depth, which is a function of the site occupancy. We use a Boltzmann distribution to calculate the average ap interaction energy for a given temperature T, given by

$$U_{AP,i}(r,x,T) = \frac{\int_{r=0}^{r=r_{max}} U_{AP,i}(r,x)\, e^{\left(\frac{-U_{AP,i}(r,x)}{k_b T}\right)} r_i^2}{\int_{r=0}^{r=r_{max}} e^{\left(\frac{-U_{AP,i}(r,x)}{k_b T}\right)} r_i^2} \tag{24}$$

where $e^{\left(\frac{-U_{AP,i}(r,x)}{k_b T}\right)}$ is Boltzmann weighting distribution. Solving the integral, we obtain

$$U_{AP,i}(r,x,T) = U_{AP,i}(r,x) + \frac{3}{2} k_b T + \frac{U_{APc,i}\, r_{max}^2}{1 - \frac{1}{2}\sqrt{\pi}\, \frac{\operatorname{erf}\left[r_{max}\sqrt{\frac{U_{APc,i}}{k_b T}}\right]}{r_{max}\sqrt{\frac{U_{APc,i}}{k_b T}}\, e^{\left[\frac{r_{max}^2 U_{APc,i}}{k_b T}\right]}}} \tag{25}$$

Notice in Equation (23), we use a constant term $U_{APc,i}$, for each type of site. Overall, the net result of including the temperature dependence of the ap interaction energy is that we have one additional fitting parameter, $U_{APc,i}$, for each type of lattice site.

4.3 SIMULATIONS AND NUMERICAL METHODS

4.3.1 Simulation Methodology

We perform Molecular Dynamics (MD) simulations in the microcanonical ensemble, i.e. keeping the number of adsorbates, N, volume, V, and the total energy, E, fixed.[97,98] We use the Lennard-Jones 6-12 potential to model the adsorbate-adsorbate interactions:

$$U_{AA} = \sum_{i=1}^{N-1} \sum_{j-i+1}^{N} U_{ij} = \sum_{i=1}^{N-1} \sum_{j=1+1}^{N} 4\,\varepsilon_{ij} \left[\left(\frac{\sigma_{ij}}{r_{ij}} \right)^{12} - \left(\frac{\sigma_{ij}}{r_{ij}} \right)^{6} \right] \tag{26}$$

where the potential parameters ε and σ for methane are obtained from [99] and are given in Table 1. For the adsorbate-pore interactions we use atomic positions for the oxygen atoms in zeolite Na-Y. Only oxygen atoms contribute significantly to the external potential [85], permitting us to ignore the Si and Al. We ignore the charge on the oxygen. We use the Lennard Jones 6-12 potential to model the adsorbate-pore interactions. The parameters are listed in Table 1.

We simulate 128-512 atoms per unit cell, depending upon the density. For low density, we use 128 atoms, and increase the number for higher densities. A cut-off distance, r_{cut}, of 15 Å and a neighbor distance, r_{nbr}, of 18 Å is employed. We use a time step of 2 fs, and carry out 10,000 equilibration steps and 100,000 data production steps. The numerical solution technique used is the 5th order gear predictor-corrector [100,101]. Periodic boundary conditions and the standard minimum image convention are employed along the boundaries of the unit cell of Na-Y.

The self-diffusivities are calculated using the Einstein relation [97], which relates the self-diffusion coefficient to the mean square displacement of a particle as a function of observation time, given by

$$D = \frac{1}{2d} \lim_{\Delta t \to \infty} \frac{\left\langle \left[\underline{r}\,(t_0 + \Delta t) - \underline{r}\,(t_0) \right]^2 \right\rangle}{\Delta t} \tag{27}$$

where D is the self-diffusion coefficient, and d is the dimensionality of the system. The numerator of equation (27) is the mean square displacement.

4.3.2 Numerical Methods

This section describes the numerical optimization routine employed to conduct the parameter fitting for the lattice. We optimize the parameters - $\underline{\underline{U_{AP}}}$, $\underline{U_{APc}}$ and $\underline{V_s}$. $\underline{\underline{U_{AP}}}$ is the pore well depth, $\underline{V_s}$ is the site volume, and $\underline{U_{APc}}$ is a vector of two constants that are included due to the modification of our lattice theory as discussed in the previous section. The lattice parameters— $\underline{\underline{c}}$, $\underline{\underline{\ell}}$ are not fitted because they are easily available from the information about the lattice dimensions.

The objective function is the error between the results predicted by our theory and simulation for the adsorbate-pore (ap) interaction energy. We optimized the ap interaction energy because we suspect that it is physically the most significant property of interest.

The objective function is given by,

$$f = \sum_{i=1}^{n} \frac{X_i^{simulation} - X_i^{theory}}{X_i^{simulation}} \tag{25}$$

where X denotes the ap interaction energy, and the summation encompasses all the data points available from simulations. We employ Nelder and Mead's Downhill Simplex Method to minimize the objective function.[102] The Downhill Simplex Method is chosen because of its simplicity and robustness. However, the method suffers from a drawback that it depends heavily on the goodness of the initial guesses. A poor initial guess would result in the code converging to a local minimum. We run the code with numerous initial guesses to overcome this limitation and thus ensure that it searches the entire domain of convergence values to locate decisively the global minimum. It is worth mentioning here that the entire optimization routine takes only a few minutes on a desktop PC to converge to the solution. The optimized lattice parameters are listed in Table 2.

4.4 RESULTS AND DISCUSSION

The molecular dynamics (MD) simulations were employed to determine the adsorbate-pore (ap) interaction energy, adsorbate-adsorbate (aa) interaction energy, total energy, and diffusivity. Simulations were conducted at five temperatures and loadings. The simulations took approximately 200 hours on the 16-node super computing facility at The University of Tennessee. The simulation results are reported in Table 2. In this section, we present plots to test the results predicted by our theory against these simulations. The theory generated the results in approximately a minute on a standard desktop PC. Both theory and the simulation methodology have been discussed in previous sections.

We study the behavior of single-component methane in Na-Y. Na-Y has roughly spherical nanopores tetrahedrally connected by 12-ring windows See Figure (1). There are ten adsorption sites in a cage of Na-Y. Six of them are located octahedrally, one in front of each of the central 4-rings and the other four are located tetrahedrally, one in front of each 6-rings. Simulations have previously shown that the adsorption lattice of Na-Y is comprised of two types of localized adsorption sites [31]. The sites differ in the relative accessible pore volume (site volume and occupancy), and the energetic well depth. The numerical values of the lattice parameters are obtained by conducting an optimization See Section 3. The values are reported in Table 3. It is seen that the sites of Type 2 are larger and energetically shallower than the sites of Type 1. We mentioned earlier that simulations have shown that the two types of sites have different maximum occupancies. We found that the 2-12 lattice configuration (lattice of two types of sites with sites of Type 1 having a maximum occupancy of one and sites of Type 2 having a maximum occupancy of two) provided a better fit than the 2-21 case. We hence model the Na-Y sorption lattice as a 2-12 case in our lattice adsorption theory. Also, the sites are connected to each other by a connectivity of $\mathrm{c} = \begin{bmatrix} 0 & 3 \\ 2 & 0 \end{bmatrix}$ i.e. a site of Type 1 is

connected to 3 sites of Type 2 and a site of Type 2 is connected to two sites of Type 1.[31] Thus 40% of the total sites are of Type 1 and 60% are of Type 2.

Figure (2) plots the adsorbate-pore (ap) interaction energy as a function of adsorbate loading for five different temperatures. The ap interaction energy, U_{AP}, is the energetic contribution of the CH_4-O interactions to the total energy. Although Gupta et.al [31] experimentally achieved a maximum adsorbate loading of 18 adsorbates/cage under high-pressure conditions, they report an average density of 10 adsorbates/cage of Na-Y. Correspondingly, we conduct simulations only up through a maximum loading of 0.8 adsorbates/site or 8 adsorbates/cage. Theoretically, however, the 2-12 lattice has 40% of Type 1 sites with a maximum occupancy of one and 60% of Type 2 sites with a maximum occupancy of 2. In other words, the maximum adsorbate loading is $0.4 \times 1 + 0.6 \times 2 = 1.6$ adsorbates/site or 16 adsorbates/cage. Although not shown, our theory can report the interaction energies up through the maximum possible loading of 1.6 adsorbates/site, corresponding to 16 adsorbates/cage.

Figure (2) reveals a very good agreement between the theory and simulations for the ap interaction energy. Our theory and simulation results lie within an average error of 2.3%, which is indicative of the good quantitative agreement between the two. At all loadings, the ap interaction energy increases with an increase in temperature for both theory and simulation. We discussed in Section 2 that the ap interaction energy is a function of the site occupancy and temperature. As temperature increases, an adsorbed molecule explores less energetically favorable positions within the site, which increases the ap interaction energy.

The loading dependence of the ap interaction energy is different at different temperatures. At low temperatures, the ap interaction energy monotonically increases with loading. At higher temperatures, the ap interaction energy generally decreases with loading. (Anomalous behavior at infinite dilution will be addressed) Both theory and simulations predict the non-monotonic behavior of the ap interaction energy with density and temperature. To understand this behavior, we plot in Figure (3) the adsorbate distribution as a function of loading at three different temperatures. An immediate

observation here is that the number of sites of Type 2 with two adsorbates, $n_{s,2}(2)$, is negligible at all loadings considered. In other words, none of the sites of Type 2 are doubly occupied. We see that at higher temperatures, $n_{s,2}(1)$ assumes higher values than $n_{s,1}(1)$ at all loadings up to 0.8 adsorbates/site. In other words, at higher temperatures, a higher number of adsorbates are filled in the sites of Type 2 than in the Type 1 sites. There is an entropic advantage to placing the molecules in the larger (but energetically more shallow) sites of Type 2. The combined entropic and energetic effects cause an increase in the number of ap interactions with increasing loading, which results in a decrease of the ap interaction energy. Hence, we see in Figure (2) that the ap interaction energy decreases with loading at higher temperatures. In contrast, at low temperatures, a high number of molecules are adsorbed in the smaller (but energetically deeper) sites of Type 1, which results in a decrease in the ap interactions with loading. Correspondingly, we see in Figure (2) that the ap interaction energy increases with loading at low temperatures.

We notice that the theory and simulations do not agree at infinite dilution. At higher temperatures, the simulations show a steep increase in the ap interaction energy at infinite dilution. Our theory does not predict this behavior. We suspect that there is a subtle cross-correlation between the placement of the adsorbate within the sites and the transition from infinite dilution (no neighbors) to low density (few neighbors), which our model does not capture.

Figure (4) plots the adsorbate-adsorbate (aa) interaction energy as a function of loading for five temperatures. The aa interaction energy, U_{AA}, is the energetic contribution of the CH_4-CH_4 interactions to the total energy. It is important to note that the aa interactions occur between the molecules adsorbed in neighboring sites as well as within sites (2-12 case has doubly occupied sites of Type 2). We notice that the theory is qualitatively in agreement with the simulations. Both theory and simulations show that at all temperatures, the aa interaction energy decreases with loading. At all temperatures, the adsorbate-adsorbate interactions increase as loading increases. The density dependence of the aa interactions and correspondingly the aa interaction energy, arises

from the fact that both the intra-site and the inter-site partition functions have a high loading functionality.

Our theory and simulations also observe the same temperature dependence of the aa interaction energy. Both show that the aa interaction energy increases with temperature at all loadings. The number of neighbor aa interactions decrease with rising temperature, which is energetically less favorable. Hence we see an increase in the ap interaction energy with increasing temperature. It should be noted that the aa interaction energy curves for all temperatures have the same intercept – zero. We expect this trend because there are no aa interactions at infinite dilution.

The qualitative agreement of the aa interaction energy established by our theory with the simulations is welcome since it has provided a much needed platform to understand the adsorbate-adsorbate clustering within sites and between neighboring sites using intra-site and inter-site partition functions.

We report an overall error of 47% for the aa interaction energy. The error between the theory and simulations is more pronounced at high loadings. We suspect that the confined geometry of our lattice model, as against the continuum space assumed by simulation, is the prime cause for the inaccurate predictions at high loadings. Fluid crowding forces the adsorbates to sit slightly outside of the lattice sites, which violates our strict lattice assumption. However, one needs to realize that the aa interaction energy contributes only a small fraction of the total energy. The major contributor to the total energy, i.e. the ap interaction energy has been modeled with relatively high accuracy.

Figure (5) plots the total interaction energy as a function of loading and temperature. It should be noted that the total energy, U_{TOT}, is merely a sum of the ap interaction energy, U_{AP}, the aa interaction energy, U_{AA}, and the kinetic energy of motion. The plot reveals that the theory is in good overall agreement with the simulations. We observe the correct density and temperature dependence of the total energy. Both theory and simulations show that at all temperatures, the total energy decreases as loading increases. Also, the total energy increases with temperature at all loadings. Both the density and temperature behavior of the total energy were expected,

as similar trends were observed in general for U_{AP} and U_{AA}. Quantitatively, the results predicted by the theory are off within an average error of 4.5%. It should be noted that the two errors that were discussed in the plots for U_{AP} and U_{AA} are reflected in the present plot too. For one, our lattice adsorption theory does not predict the maximum in the total energy as shown by simulations, at infinite dilution for higher temperatures. This maximum corresponds to the maximum seen in Figure (2) for U_{AP}. Also, as discussed for U_{AA}, the theory does not follow the simulations at high loadings. The fluid crowding observed by simulations at high loadings is not captured by the theory. However, it should be noted that the fact that U_{AA} constitutes only a fraction of the total energy makes the error less profound than was seen in Figure (4).

From the discussion of Figures (2, 4, & 5), we demonstrated the capabilities of our lattice adsorption theory in successfully capturing the trends shown by simulations. The CH_4-CH_4 interactions and CH_4-O interactions, in other words, the aa interactions and the ap interactions at different temperatures and loadings, are elucidated by exploring the domain of intra-site and inter-site partition functions. We noticed that there were two issues that were not handled well by the lattice adsorption theory; (1) infinite dilution adsorbate-pore interaction energy, and (2) high density adsorbate-adsorbate interaction energy. However, we believe that the simplicity and the fundamental basis of this lattice model definitely provide the impetus to carry out further explorations in this area in the near future.

In Figure (6), we compare the self-diffusion coefficients predicted by our lattice diffusion theory and simulations for methane in Na-Y. It is worthwhile to mention here that the diffusion component of our lattice theory makes use of the results of the lattice adsorption theory. The diffusion component of our lattice theory is explained in Section 2, and in [2]. Unlike the lattice adsorption theory, which incorporated adjustable fitting parameters, our lattice diffusion theory contains absolutely no fitting parameters.

We plot the diffusivity as a function of loading for five temperatures. The lattice diffusivity versus loading profile shares features predicted by the MD simulations. The

theory and simulations are in good agreement. We observe the correct temperature and density dependence. Both theory and simulation predict that at all temperatures, the diffusion coefficient decreases with increase in loading. As the loading increases, there are less vacant sites to facilitate diffusive motion through the lattice – the entropic effect, which decreases the diffusivity.

Furthermore, the diffusivity increases with temperature at all loadings. This is expected from the Arrhenius temperature dependence of the diffusivity. At higher temperatures, the molecules make more successful 'jumps' between sites, which increases the diffusivity.

We notice that the diffusivity predicted by the theory is much higher than the simulations at high loadings. In our recently published paper on the lattice diffusion theory, we mentioned that the theory needs to incorporate the percolative effects of the lattice, which would lower the mean diffusivity, D, at high loadings [2]. We intend to include the percolative behavior in the near future. We expect the trends shown here to persist, albeit weighted by the percolative effect of the lattice.

The theory is in poor quantitative agreement with the simulations. The theory is off with an average error of 62.9%. Incorporating fitting parameters into the diffusion component of our theory could mask this error. While the inclusion of the adjustable parameters in our lattice diffusion model may enable better quantitative agreement with the simulations, the power of the modeling approach presented here lies in its conceptual simplicity and its ability to compare *reasonably* well with the simulation data on a wide variety of zeolites, which for one, is demonstrated here with Na-Y.

4.5 CONCLUSIONS

In this work, we have presented a validation analysis of our previously published analytical theories for adsorption and diffusion in nanoporous materials. The results predicted by our theory are tested with MD simulations for the system Methane in Na-Y.

A very good agreement is found between the theory and simulations. The theory incorporates the atomistic structure of the adsorbent and also incorporates the fundamental physical mechanisms that dictate the behavior of methane molecules in zeolite Na-Y.

While the lattice adsorption theory required five fitting parameters, the diffusion component of the theory incorporated no fitting parameters. The theory was found to be computationally efficient, as it took approximately only a minute to generate the results against 200 hours of CPU time required by simulations.

We are currently in the midst of addressing some issues that were left unresolved by the theory; namely percolative effects at high loadings, and infinite dilution behavior of the adsorbate-pore interactions. Also, we are extending our theory for multicomponent fluids.

REFERENCES

1. Kamat, M.R., Keffer, D., “An analytical theory for adsorption of fluids in nanoporous materials”, *Molecular Physics* 2002 **100** (16) 2689-2701.
2. Kamat, M.R., Keffer, D., “An analytical theory for diffusion of fluids in nanoporous materials”, submitted to Molecular Physics.
3. Keffer, D., Davis, H.T., McCormick, A.V., "The effect of nanopore shape and loading on adsorption selectivity of a binary mixture" *J. Phys. Chem.* 1996 **100** p. 638-645.
4. Keffer, D., Davis, H.T., McCormick, A.V., "The effect of nanopore shape on the structure and isotherms of adsorbed fluids" *Adsorption* 1996 **2** p. 9-21.
5. Keffer, D., “Molecular Models of Adsorption and Diffusion in Nanoporous Materials”, Ph.D. Thesis, University of Minnesota, July, 1996.
6. Keffer, D., McCormick, A.V., Davis, H.T., " Uni-directional and single-file diffusion in $AlPO_4$-5: a molecular dynamics study", *Mol. Phys.* 1996 **87** p. 367-387.
7. Keffer, D., McCormick, A.V., Davis, H.T., "Agreement between Theory and Simulation of Single-file diffusion in a molecular sieve", Proceedings from the XI International Workshop on Condensed Matter Theories, Caracas, Venezuela, June, 1995.
8. Hahn, K. Kärger, J., “Molecular Dynamics Simulations of Single-File Systems”, *J. Phys. Chem.*, 1996 100 p. 316-326.
9. Keffer, D., McCormick, A.V., Davis, H.T., "Diffusion and Percolation on Zeolite Sorption Lattices", *J. Phys. Chem.* 1996 **100** p. 967-973.
10. Kono, H., Takasaka, A., “Statistical mechanics calculation of the sorption characteristics of Ar and N2 in dehydrated zeolite 4A by a Monte Carlo method for determining configuration integrals”, *J. Phys. Chem.* 1987 **91** p. 4044-4055.
11. Razmus, D.M., Hall, C.K., “Prediction of gas adsorption in 5A zeolites using Monte Carlo simulations”, *AIChE J.* 1991 **37** p. 769-779.

12. Van Tassel, P.R., Davis, H.T., McCormick, A.V., "Monte Carlo calculations of adsorbate placement and thermodynamics in a micropore: Xe in NaA", *Mol. Phys.* 1991 **73** p. 1107-1125.
13. Van Tassel, P.R., Davis, H.T., McCormick, A.V., "Monte Carlo calculations Xe arrangement and energetics in the NaA alpha cage", *Mol. Phys.* 1992 **76** p. 411-432.
14. Van Tassel, Phillips, J.C., P.R., Davis, H.T., McCormick, A.V., "Zeolite adsorption site location and shape shown by simulated isodensity surfaces", *J. Mol. Graphics* 1993 **11** p. 180-184,188.
15. Van Tassel, P.R., Davis, H.T., McCormick, A.V., "Open-system Monte Carlo simulations of Xe in NaA" *J. Chem. Phys.* 1993 **98** p. 8919-8928.
16. Van Tassel, P.R., Somers, S.A., Davis, H.T., McCormick, A.V., "Lattice model and simulation of dynamics of adsorbate motion in zeolites" *Chem. Eng. Sci.* 1994 **49** p. 2979-2989.
17. Van Tassel, P.R., Davis, H.T., McCormick, A.V., "New lattice model for adsorption of small molecules and their mixtures in a zeolite micropore", *AIChE J.* 1994 **40** p. 925-934.
18. Van Tassel, P.R., Davis, H.T., McCormick, A.V., "Adsorption simulations of small molecules and their mixtures in a zeolite micropore", *Langmuir* 1994 **10** p. 1257-1267.
19. Soto, J.L., Myers, A.L., "Monte Carlo studies of adsorption in molecular sieves", *Mol. Phys.* 1981 **42** p. 971-983.
20. Woods, G.B., Panagiotopolous, A.Z., Rowlinson, J.S., "Adsorption of Fluids in Model Zeolites" *Mol. Phys.* 1988 **63** p. 49-63.
21. Woods, G.B., Rowlinson, J.S., "Computer Simulations of fluids in zeolites X and Y" *J. Chem. Soc. Faraday Trans. 2* 1989 **85** p. 765-781.
22. Yashonath, S., Thomas, J.M., Novak, A.K., Cheetham, A.K., "The siting, energetics and mobility of saturated hydrocarbons inside zeolitic cages: methane in zeolite Y", *Nature* 1988 **331** p. 601-604.

23. Yashonath, S., Demontis, P., Klein, M.L., "A molecular dynamics study of methane in zeolite NaY", *Chem. Phys. Lett.* 1988 **153** p. 551-556.
24. Demontis, P. Yashonath, S., Klein, M.L., "Location and mobility of benzene in sodium-Y zeolite by molecular dynamics calculations", *J. Phys. Chem.* 1989 **93** p. 5016-5019.
25. Yashonath, S., "A molecular dynamics study of cage-to-cage migration in sodium Y zeolite: Role of surface-mediated diffusion", *J. Phys. Chem.* 1991 **95** p. 5877-5881.
26. Yashonath, S., Demontis, P., Klein, M.L., "Temperature and concentration dependence of adsorption properties of methane in NaY: A molecular dynamics study", *J. Phys. Chem.* 1991 **95** p. 5881-5889.
27. Santikary, P., Yashonath, S., Ananthakrishna, G., "A molecular dynamics study of xenon sorbed in sodium Y zeolite. 1. Temperature and concentration dependence", *J. Phys. Chem.* 1992 **96** p. 10469-10477.
28. Yashonath, S., Santikary, P., "Xenon in sodium Y zeolite 2. . Arrhenius relation, mechanism, and barrier height distribution for cage-to-cage diffusion", *J. Phys. Chem.* 1993 **97** p. 3849-3857.
29. Yashonath, S., Santikary, P., "Diffusion of sorbates in zeolites Y and A: Novel dependence on sorbate size and strength of sorbate-zeolite interaction", *J. Phys. Chem.* 1994 **98** p. 6368-6376.
30. Klein, H. Kirschhock, C., Fuess, H., "Adsorption and diffusion of aromatic hydrocarbons in zeolite Y by molecular mechanics calculation and x-ray powder diffraction", *J. Phys. Chem.* 1994 **98** p. 12345-12360.
31. Gupta, V., Davis, H.T., McCormick, A.V., "Comparison of the ^{129}Xe NMR chemical shift with simulation in zeolite Y", *J. Phys. Chem.* 1996 **100** p. 9824-9833.
32. Gupta, V., Davis, H.T., McCormick, A.V., "^{129}Xe NMR chemical shifts in zeolites: Effect of Loading studied by Monte Carlo simulations", *J. Phys. Chem.* 1997 **101** p. 129-137.

33. Keffer, D., Gupta, V., Kim, D., Lenz, E., Davis, H.T., McCormick, A.V., "A compendium of zeolite potential energy maps" *J. Mol. Graphics* 1996 **14** p. 108-116, 100-104.
34. Nivarthi, S.S., Van Tassel, P.R., Davis, H.T., McCormick, A.V., "Adsorption and energetics of xenon in mordenite: a Monte Carlo simulation study", *J. Chem. Phys.* 1995 **103** p. 3029-3037.
35. Vernov, A.V., Steele, W.A., "Sorption of xenon in zeolite Rho: A thermodynamics/simulation study", *J. Phys. Chem.* 1993 **97** p. 7660-7664.
36. Loriso, A., Bojan, M.J., Vernov, A., Steele, W.A., "Computer simulation studies of ordered structures formed by rare gases sorbed in zeolite Rho", *J. Phys. Chem.* 1993 **97** p. 7665-7671.
37. Snurr, R.Q., June, R.L., Bell, A.T., Theodorou, D.N., "Molecular simulations of methane adsorption in silicalite", *Mol. Sim.* 1991 **8** p. 73-92.
38. Snurr, R.Q., June, R.L., Bell, A.T., Theodorou, D.N., "A hierarchical atomistic/lattice simulation approach for the prediction of adsorption thermodynamics of benzene in silicalite", *J. Phys. Chem.* 1994 **98** p. 5111-5119.
39. Demontis, P., Fois, E.S., Suffriti, G.B., Quartieri, S., "Molecular dynamics studies on zeolites 4. Diffusion of methane in silicalite", *J. Phys. Chem.* 1990 **94** p. 4329-4334.
40. Demontis, P., Suffriti, G.B., Fois, E.S., Quartieri, S., "Molecular dynamics studies on zeolites 6. Temperature dependence of diffusion of methane in silicalite", *J. Phys. Chem.* 1992 **96** p. 1482-1490.
41. Nowak, A.K., Cheetham, A.K., Pickett, S.D., Ramdas, S., "A computer simulation of the adsorption and diffusion of benzene and toluene in the zeolites Theta-1 and silicalite", *Mol. Sim.* 1987 **1** p. 67-77.
42. Vigne-Maeder, F., Jobic H., "Adsorption sites and packing of benzene in silicalite", *Chem. Phys. Lett.* 1990 **169** p. 31-35.
43. Vigne-Maeder, F., Auroux, A., "Potential maps of methane, water, and methanol in silicalite", *J. Phys. Chem.* 1990 **94** p. 316-322.

44. June, R.L., Bell, A.T., Theodorou, D.N., "Molecular Dynamics studies of methane and xenon in silicalite", *J. Phys. Chem.* 1990 **94** p. 8232-8240.
45. June, R.L., Bell, A.T., Theodorou, D.N., "Transition-state studies of xenon and SF_6 diffusion in silicalite", *J. Phys. Chem.* 1991 **95** p. 8866-8878.
46. Goodbody, S.J., Watanabe, K. MacGowan, D., Walton, J.P.R.B., Quirke, N., "Molecular simulation of methane and butane in silicalite", *J. Chem. Soc. Faraday Trans.* 1991 **87** p. 1951-1958.
47. June, R.L., Bell, A.T., Theodorou, D.N., "Molecular Dynamics studies of butane and hexane in silicalite", *J. Phys. Chem.* 1992 **96** p. 1051-1060.
48. Snurr, R.Q., Bell, A.T., Theodorou, D.N., "Prediction of adsorption of aromatic hydrocarbons in silicalite from grand canonical Monte Carlo simulations with biased insertions", *J. Phys. Chem.* 1993 **97** p. 13472-13752.
49. Nicholas, J.B., Trouw, F.R., Mertz, J.E., Iton, L.E., Hopfinger, A.J., "Molecular Dynamics simulation of propane and methane in silicalite", *J. Phys. Chem.* 1993 **97** p. 4149-4163.
50. Vigne-Maeder, F., "Analysis of ^{129}Xe chemical shifts in zeolites from molecular dynamics calculations", *J. Phys. Chem.* 1994 **98** p. 4666-4672.
51. Smit, B. Siepmann, J.I., "Computer simulations of the energetics and siting of n-alkanes in zeolites", *J. Phys. Chem.* 1994 **98** p. 8442-8452.
52. Smit, B., Maesen, T.L.M., "Commensurate 'freezing' of alkanes in the channels of a zeolite" *Nature* 1995 **374** p. 42-44.
53. Bandopadhyay, S., Yashonath, S., "Diffusion anomaly in silicalite and VPI-5 from molecular dynamics simulations', *J. Phys. Chem.* 1995 **99** p. 4286-4292.
54. Yashonath, S., Bandopadhyay, S., "Surprising diffusion behavior in the restricted regions of silicalite", *Chem. Phys. Lett.* 1994 **228** p. 284-288.
55. Heffelfinger, G.S., Pohl, P.I., Frink, L.J.D., "Molecular Dynamics computer simulations of diffusion in porous silicates", *Mater. Res. Soc. Symp. Proc.* 1995 **366** p. 225-230.

56. Antonchenko, V.Y., Ilyin, V.V., Makovsky, N.N., Khryapa, V.M., "Short-range order in cylindrical liquid-filled micropores", *Mol. Phys.* 1988 **65** p. 1171-83.
57. Bratko, D., Blum, L., Wertheim, M.S., "Structure of hard sphere fluids in narrow cylindrical pores", *J. Chem. Phys.* 1989 **90** p. 2752-2757.
58. Carigan, Y.P., Vladimiroff, T., Macpherson, A.K., "Molecular Dynamics of hard spheres III. Hard spheres in an almost spherical container", *J. Chem. Phys.* 1988 **88** p. 4448-4450.
59. Demi, T., "Molecular Dynamics studies of adsorption and transport in micropores of different geometries", *J. Chem. Phys.* 1991 **95** p. 9242-9247.
60. Dunne, J., Myers, A.L., "Adsorption of gas mixtures in micropores: effect of difference in size of adsorbate molecules", *Chem. Eng. Sci.* 1994 **49** p. 2941-2951.
61. Glandt, E.D., "Density distribution of hard-spherical molecules inside small pores of various shapes", *J. Col. Inter. Sci.* 1980 **77** p. 512-524.
62. Groot, R.D., Faber, N.M., van der Eerden, "Hard sphere fluids near a hard wall and a hard cylinder", *Mol. Phys.* 1987 **62** p. 861-874.
63. Han, K.K., Cushman, J.H., Diestler, D.J., "Grand Canonical Monte Carlo simulations of a Stockmayer fluid in a slit micropore", *Mol. Phys.* 1993 **79** p. 537-545.
64. Heinbuch, U., Fischer, J., "Liquid argon in a cylindrical carbon pore: molecular dynamics and Born-Green-Yvon Results", *Chem. Phys. Lett.* 1987 **135** p. 587-590.
65. Jiang, S., Rhykerd, C.I., Gubbins, K.E., "Layering, freezing transitions, capillary condensation, and diffusion of methane in slit carbon pores", *Mol. Phys.* 1993 **79** p. 373-391.
66. Macelroy, J.M.D., Suh, S.H., "Computer simulation of moderately dense hard-sphere fluids and mixtures in microcapillaries", *Mol. Phys.* 1987 **60** p. 475-501.
67. Macelroy, J.M.D., Suh, S.H., "Simulation studies of a Lennard-Jones liquid in micropores", *Mol. Sim.* 1989 **2** p. 313-315.

68. Macpherson, A.K., Carignan, Vladimiroff, T., "Molecular dynamics of hard spheres II. Hard spheres in a spherical cavity", *J. Chem. Phys.* 1987 **87** 1768-1770.

69. Murad, S., Ravi, P., Powles, J.G., "A computer simulation study of fluids in model slit, tubular, and cubic micropores", *J. Chem. Phys.* 1993 **98** p. 9771-9781.

70. Peterson, B.K., Walton, J.P.R.B., Gubbins, K.E., "Fluid behaviour in narrow pores*", J. Chem. Soc. Faraday Trans. 2* 1986 **82** p. 1789-1800.

71. Peterson, B.K., Gubbins, K.E., "Phase Transitions in a cylindrical pore: Grand canonical Monte Carlo, mean field theory, and the Kelvin equation", *Mol. Phys.* 1987 **62** p. 215-226.

72. Saito, A., Foley, H.C., "Curvature and parametric sensitivity in models for adsorption in micropores", *AIChE J.* 1990 **37** p. 429-436.

73. Sarman, S., "The influence of the fluid-wall interaction potential on the structure of a simple fluid in a narrow slit", *J. Chem. Phys.* 1990 **92** p. 4447-4455.

74. Schoen, M., Rhykerd, C.L., Cushman, J.H., Diestler, D.J., "Slit-pore sorption isotherms by the grand-canonical Monte Carlo method: Manifestations of Hysteresis", *Mol. Phys.* 1989 **66** p. 1171-1187.

75. Somers, S.A., Davis, H.T., "Microscopic dynamics of fluids confined between smooth and atomically structured solid surfaces", *J. Chem. Phys.* 1992 **96** p. 5389-5407.

76. Somers, S.A., McCormick, A.V., Davis, H.T., "Superselectivity and solvation forces of a two component fluid adsorbed in nanopores", J. Chem. Phys. 1993 99 p. 9890-9898.

77. Tan, Z., Gubbins, K.E., "Selective adsorption of simple mixtures in slit pores: A model of methane-ethane mixtures in carbon", J. Phys. Chem. 1992 96 p. 845-854.

78. Walton, J.P.R.B., Quirke, N., "Capillary condensation: a molecular simulation study", *Mol. Sim.* 1989 **2** p. 361-391.

79. Page, K.S., Monson, P.A., "Phase equilibrium in a molecular model of a fluid confined in a disordered porous material", *Phys. Rev. E* 1996 **54** p. R29-32.
80. Vuong, T., Monson, P.A., "Monte Carlo calculations of heats of adsorption in heterogeneous solids", *Langmuir* 1996 **12** p. 5425-5432.
81. Fan, Y., Finn, J.E., Monson, P.A., "A Monte Carlo simulation study of adsorption from a liquid mixture at states near liquid-liquid coexistence", *J. Chem. Phys.* 1993 **99** p. 8238-8243.
82. Peterson, B.K., Heffelfinger, G.S., Gubbins, K.E., Van Swol, F., "Layering transitions in cylindrical nanopores", *J. Chem. Phys.* 1990 **93** p. 679-685.
83. Heffelfinger, G.S., Van Swol, F., Gubbins, K.E., "Liquid-Vapor coexistence in a cylindrical pore", *Mol. Phys.* 1987 **61** p. 1381-1390.
84. Demontis, P., Suffritti, G.B., "Molecular Dynamics Investigations of the Diffusion of Methane in a Cubic Symmetry Zeolite of Type ZK4", *Chem. Phys. Lett.* 1994 **223** p. 355.
85. Beezus, A.G., Kiselev, A.V., Lopatkin, A.A., Pham Quang Du, "Molecular statistical calculation of the thermodynamic adsorption characteristics of zeolites using the atom-atom approximation. Adsorption of methane by zeolite NaX", *J. Chem. Soc. Faraday Trans.* 1978 **74** p. 367-379.
86. Coppens, M-O., Bell, A.T., Chakraborty, A.K., "Effect of topology and molecular occupancy on self-diffusion in lattice models of zeolites-Monte-Carlo simulations", *Chem. Engg. Sci.* 1998 **53** p. 2053-2061.
87. Auerbach, S.M., "Analytical theory of benzene diffusion in Na-Y zeolite", *J. Chem. Phys.* 1997 **106** p. 7810-7815.
88. Saravanan, C., Auerbach, S.M., "Modeling the concentration dependence of diffusion in zeolites. I. Analytical theory of benzene in Na-Y", *J. Chem. Phys.* 1997 **107** p. 8120-8131.
89. Saravanan, C., Auerbach, S.M., "Modeling the concentration dependence of diffusion in zeolites. II. Kinetic Monte Carlo simulations of benzene in Na-Y", *J. Chem. Phys.* 1997 **107** p. 8132-8137.

90. Saravanan, C., Jousse, F., Auerbach, S.M., "Modeling the concentration dependence of diffusion in zeolites. III. Testing Mean Field Theory for benzene in Na-Y with simulation", *J. Chem. Phys.* 1998 **108** p. 2162-2169.
91. Weitkamp, J., in "Catalysis and adsorption by zeolites", edited by Olhmann, G., Vendrine, J.C., Jacobs, P.A., Elsevier, Amsterdam, 1991.
92. Newsam, J.M., "Zeolites, in solid state chemistry: Compounds", edited by Cheetham, A.K., Day, P., Oxford University Press, Oxford, 1992, p. 234-280.
93. Sanborn, M.J., Snurr, R.Q., "Diffusion of binary mixtures of CF sub 4 and n-alkanes in faujasite", *Sep. Pur. Tech.* 2000 **20** p. 1-13.
94. Eagen, J.A., Anderson, R.B., "Kinetics and equilibrium of adsorption on 4A zeolite", *J. Coll. Interface. Sci*. 1975 **50** p. 419.
95. Karger, J., Ruthven, D. M., "Diffusion in zeolites and other microporous solids", Wiley-Interscience, New York, 1992.
96. Hill, T.L., " Introduction to statistical thermodynamics", Addison Wesley Pub. Co., Mass., 1960.
97. Allen, M.P., Tildesely, D.J., "Computer simulation of liquids", Clarendon Press, Oxford, 1987.
98. Haile, J.M., "Molecular dynamics simulation", John Wiley & Sons, Inc., New York, 1992.
99. Hirschfelder, J.O., Curtiss, C.F., Bird, R.B., "Molecular theory of gases and liquids", Wiley, New York, 1964.
100. Gear, C.W., "The Numerical Integration of Ordinary Differential Equations of Various Orders", Argonne National Laboratory, ANL-7126, 1966.
101. Gear, C.W., "Numerical Initial Value Problems in Ordinary Differential Equations", Prentice Hall, Inc., Englewood Cliffs, New Jersey, 1971.
102. The Universal Library, "Numerical recipes online", http://www.ulib.org/webRoot/Books/Numerical_Recipes.

APPENDICES

Nomenclature

SYMBOL	DESCRIPTION	UNITS
A	Helmholtz free energy	{K/molecule}
c_{ij}	Number of sites of type j connected to a site of type i	-
$D(N,M,T)$	Diffusivity as a function of N, M, and T	{m^2/s}
$D_{0,ij}(x)$	Prefactor to diffusivity	{m^2/s}
$D_{s,eff,i}(x)$	Effective diameter of a site as a function of x	{Å}
E	Total energy	{K/molecule}
$g(N,M)$	Configurational degeneracy of the lattice	-
$h_{ij}(x,y,T)$	Weighting factor to diffusivity	
k	Boltzmann constant	{J/mole/K}
$\underline{\underline{\ell}}$	Matrix of distances between sites	{A}
m_a	Mass of an adsorbate	{kg}
$m_{s,i}$	Maximum occupancy of sites of type i	-
M_i	Number of sites of types 1	-
$n_{s,i}(x)$	Number of sites of type i with an occupancy of x	-
$n\mu$	Label of unknowns	-
N	Number of adsorbates	-
$N_{ij,xy}$	Number of neighbors between sites of type i with occupancy x and sites of type j with occupancy y	-
$q_i(x,T)$	Intrasite partition function of sites of type i	-
$Q(N,M,T)$	Partition function of a function of N, M, and T	-
r	Lennard- Jones distance between molecules	{A}

r_{min}	Distance of well minimum	{A}
S	Entropy	{K/molecule}
T	Temperature	{K}
$U_{AP,i}(r,x,T)$	Potential energy of a site of type I as a function of radius, occupancy, and temperature	{K/molecule}
U_{AA}	Adsorbate-adsorbate interaction energy	{K/molecule}
U_{TOT}	Total energy	{K/molecule}
v	Velocity of a molecule	{m/s}
V_A	Volume of adsorbate	{A^3}
$V_{S,i}$	Volume of sites of type i	{A^3}
$\underline{\underline{w_x}}$	Matrix of adsorbate-adsorbate potential energy due to adsorbates in neighboring sites	{K}
x	Occupancy of a site of type i	-
y	Occupancy of a site of type j	-
$\Delta E^*_{ij}(x,y,T)$	Difference in total energy between site of type i with site of type j, as a function of occupancies x, y, and T	{K}
θ	Fractional occupancy	-
δ_{xy}	Kronecker delta function	-
μ	Chemical potential	{K/molecule}
ω	Angular velocity	{rad/s}

TABLE 1. Potential parameters

	ε_{ij} / k {K}	σ_{ij} {Å}
Methane – methane	137	3.882
Methane – oxygen	141	3.08
Oxygen – oxygen	-	3.04

TABLE 2: Simulation Results: Methane in Zeolite Na-Y

Density adsorbate/site	*EAA {K}*	*EAP {K}*	*ETOT {K}*	*Diffusivity {m^2/s}*	*Temperature {K}*
0.0	0.00E+00	-8.62E+02	-7.12E+02	7.80E-09	***100***
0.05	-3.43E+01	-8.55E+02	-7.41E+02	6.36E-09	
0.2	-1.30E+02	-8.40E+02	-8.21E+02	6.29E-09	
0.4	-2.49E+02	-8.26E+02	-9.29E+02	3.75E-09	
0.8	-4.66E+02	-8.04E+02	-1.12E+03	2.27E-09	
0.0	0.00E+00	-7.61E+02	-4.61E+02	2.28E-08	***200***
0.05	-2.82E+01	-6.79E+02	-4.07E+02	2.50E-08	
0.2	-1.08E+02	-6.79E+02	-4.90E+02	1.87E-08	
0.4	-2.12E+02	-6.82E+02	-5.91E+02	1.25E-08	
0.8	-4.29E+02	-6.92E+02	-8.23E+02	6.06E-09	
0.0	0.00E+00	-6.97E+02	-2.50E+02	3.20E-08	***298***
0.05	-2.51E+01	-6.06E+02	-1.84E+02	3.70E-08	
0.2	-1.01E+02	-6.13E+02	-2.66E+02	3.06E-08	
0.4	-1.98E+02	-6.22E+02	-3.71E+02	1.85E-08	
0.8	-4.02E+02	-6.45E+02	-5.96E+02	8.73E-09	
0.00	0.00E+00	-6.34E+02	-3.38E+01	4.26E-08	***400***
0.05	-2.35E+01	-5.64E+02	1.19E+01	5.12E-08	
0.2	-9.27E+01	-5.76E+02	-6.85E+01	3.86E-08	
0.4	-1.87E+02	-5.87E+02	-1.75E+02	2.56E-08	
0.8	-3.70E+02	-6.13E+02	-3.85E+02	1.22E-08	
0.00	0.00E+00	-5.83E+02	1.67E+02	6.01E-08	***500***
0.05	-2.19E+01	-5.42E+02	1.86E+02	6.14E-08	
0.2	-8.69E+01	-5.50E+02	1.13E+02	4.39E-08	
0.4	-1.75E+02	-5.64E+02	1.12E+01	3.12E-08	
0.8	-3.37E+02	-5.90E+02	-1.77E+02	1.36E-08	

TABLE 3: Lattice Parameters

$N_T = 2$, $\underline{m_s} = [1 \quad 2]$

$\underline{\underline{c}}$	$\underline{\underline{\ell}}$ (Å)	$\underline{V_S}$ (Å^3)	$\underline{\underline{U_{AP}}}$ (K)	$\underline{U_{APc}}$ (K)
$\begin{bmatrix} 0 & 3 \\ 2 & 0 \end{bmatrix}$	$\begin{bmatrix} - & 4.304 \\ 4.304 & - \end{bmatrix}$	[35.82,61.87]	$\begin{bmatrix} -1114.826 & -1104.026 \\ -817.515 & -806.715 \end{bmatrix}$	$[689.1 \quad 635.4]$

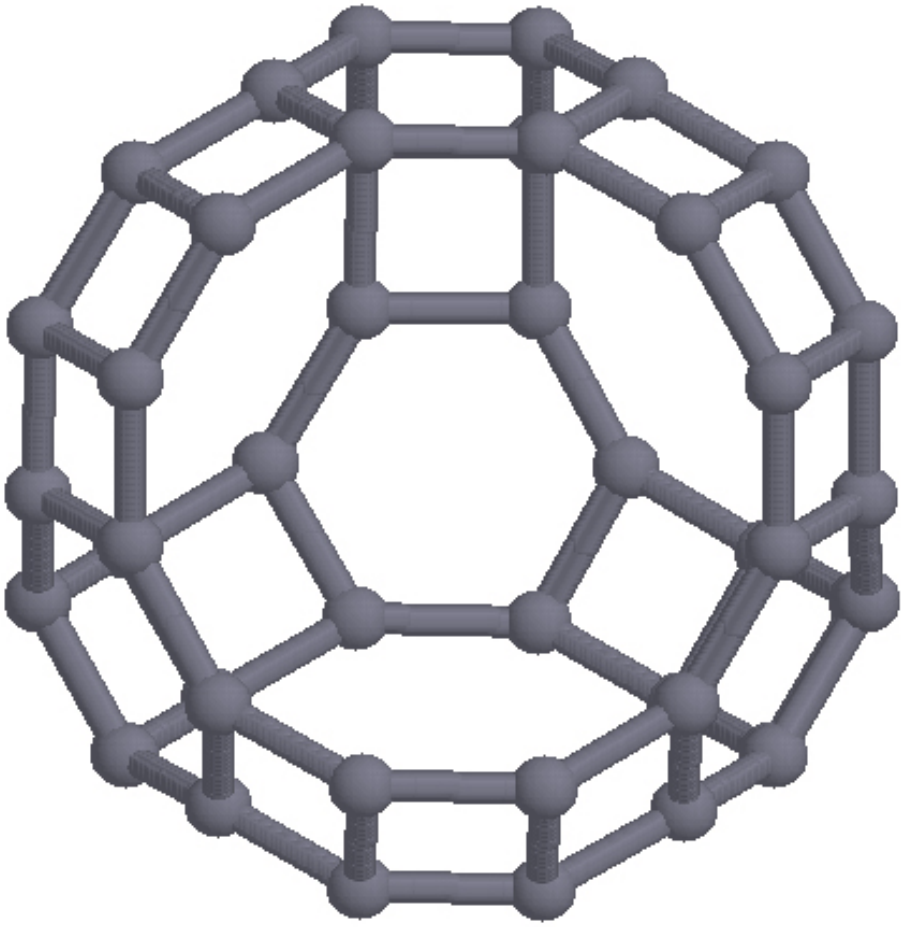

Figure 1: Schematic of the zeolite Na-Y cage structure

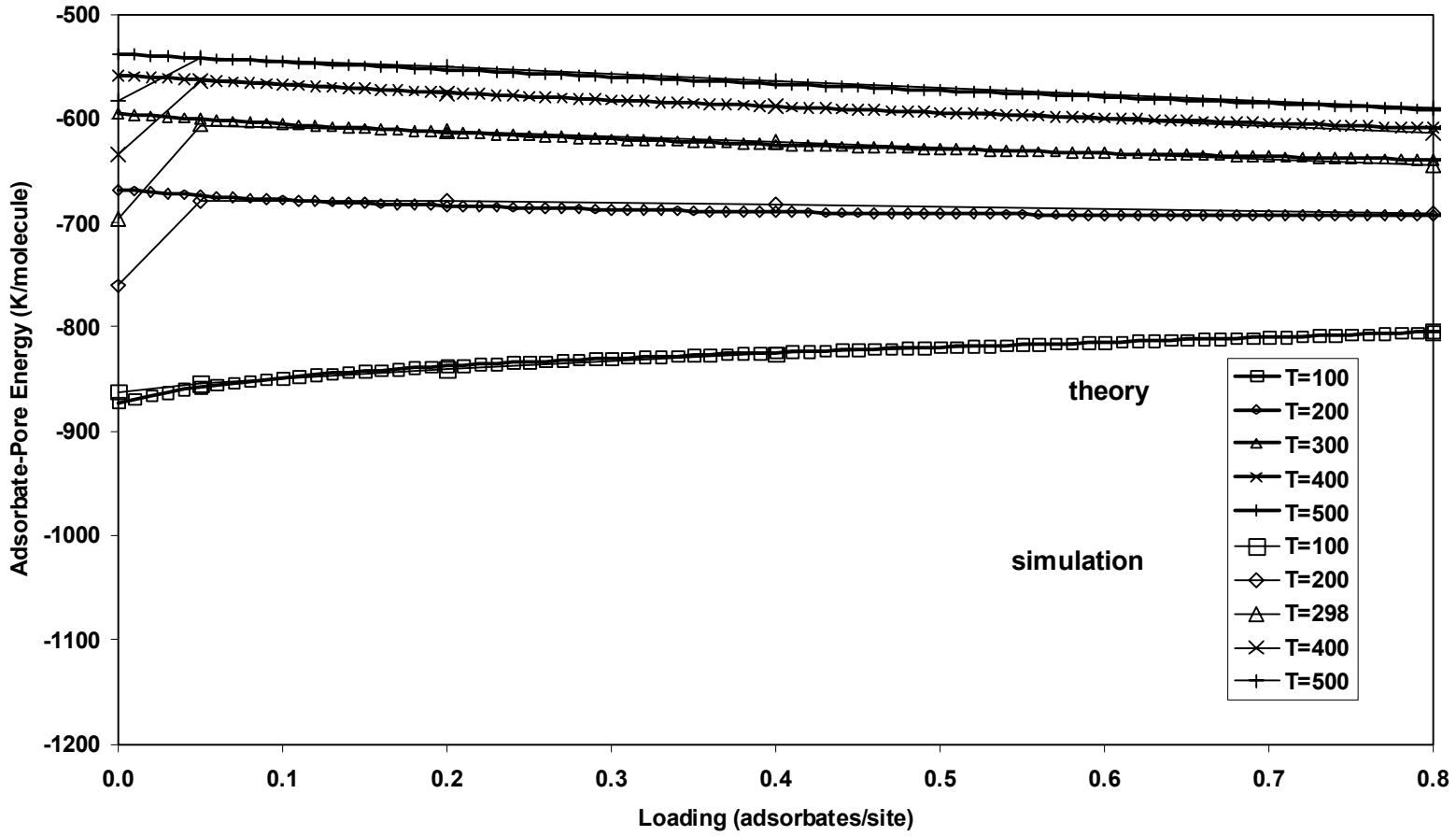

Figure 2: Adsorbate-pore interaction energy as a function of fractional occupancy.

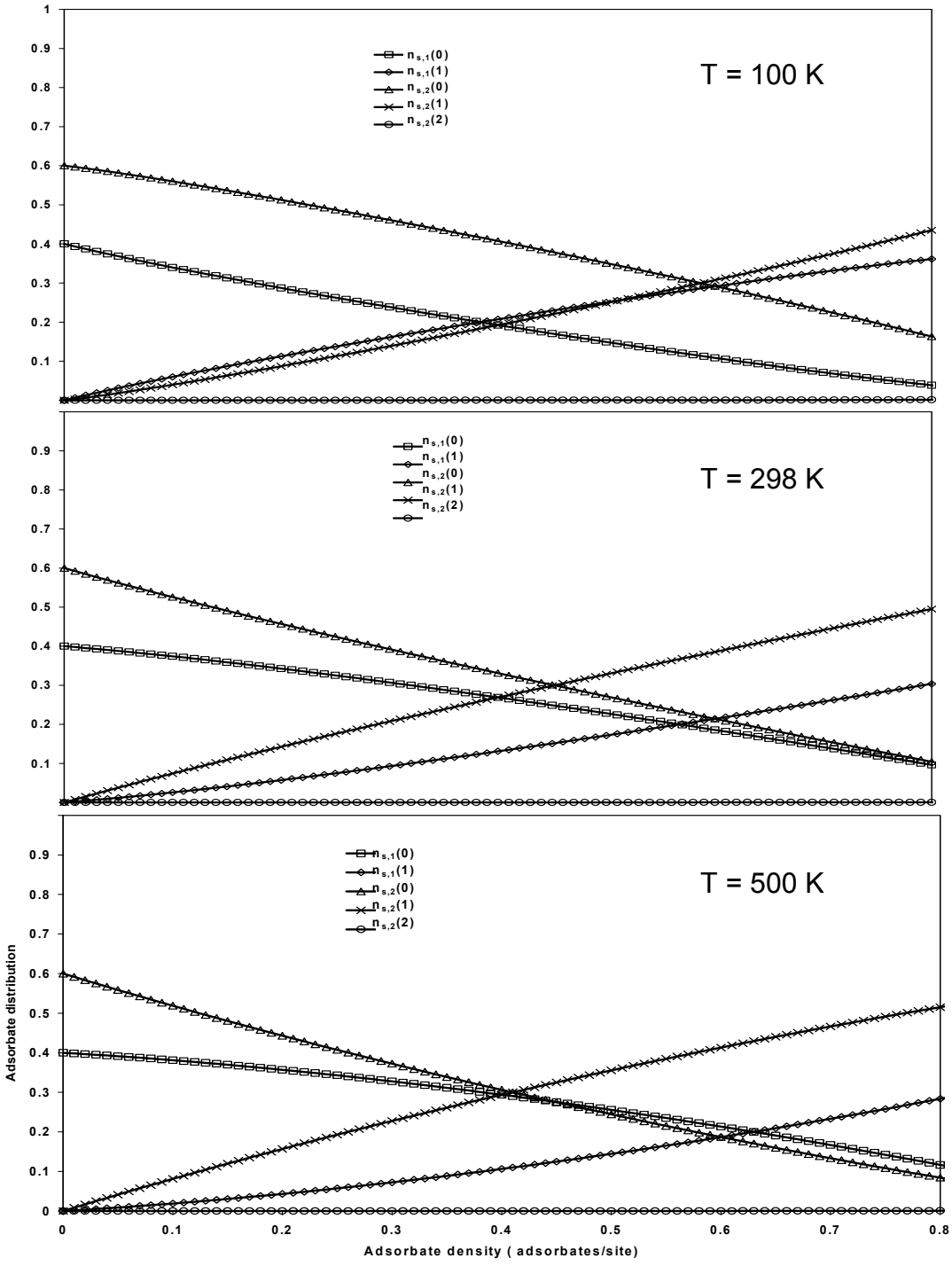

Figure 3: Adsorbate distribution versus adsorbate density

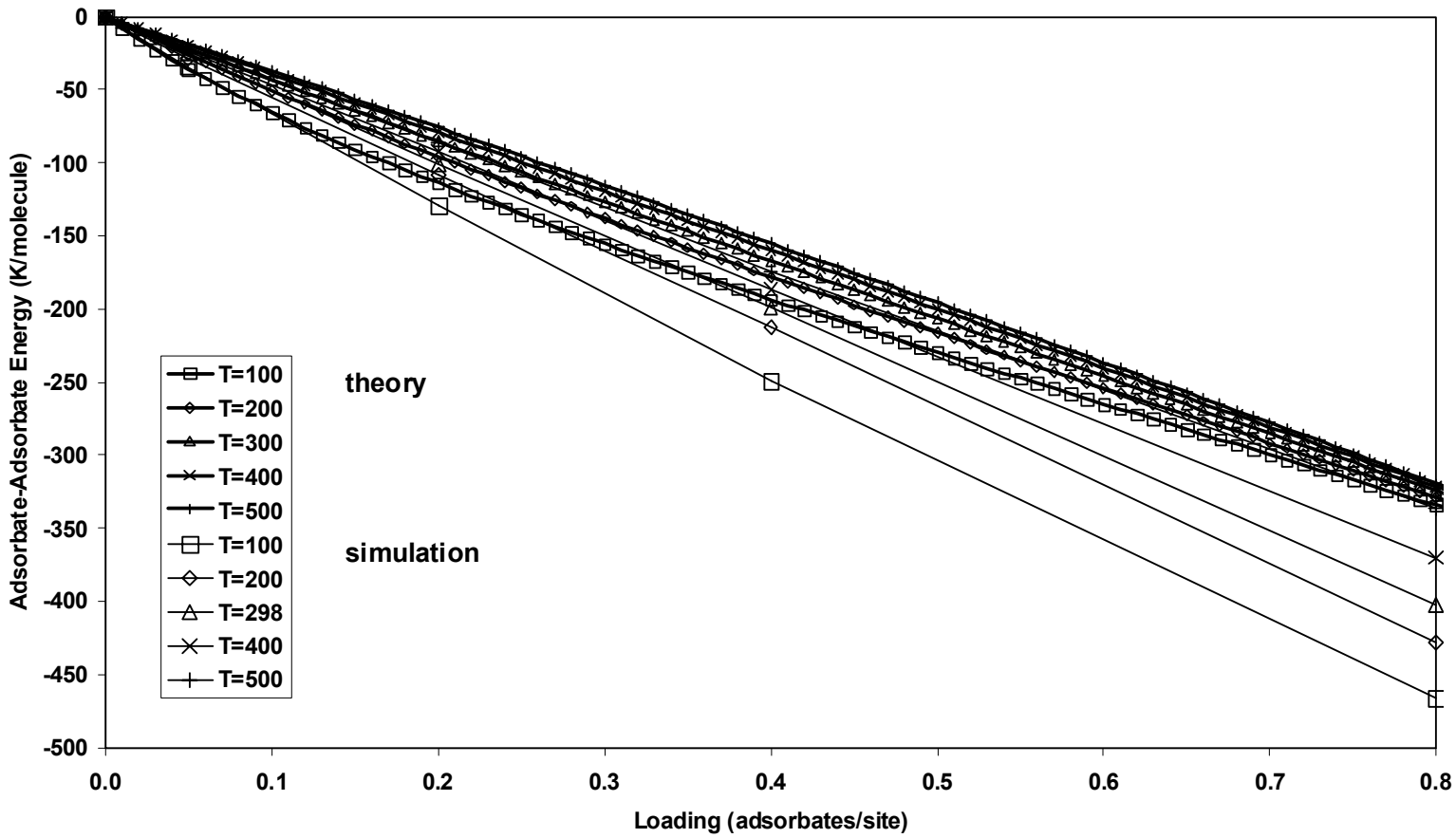

Figure 4: Adsorbate-adsorbate interaction energy as a function of fractional occupancy

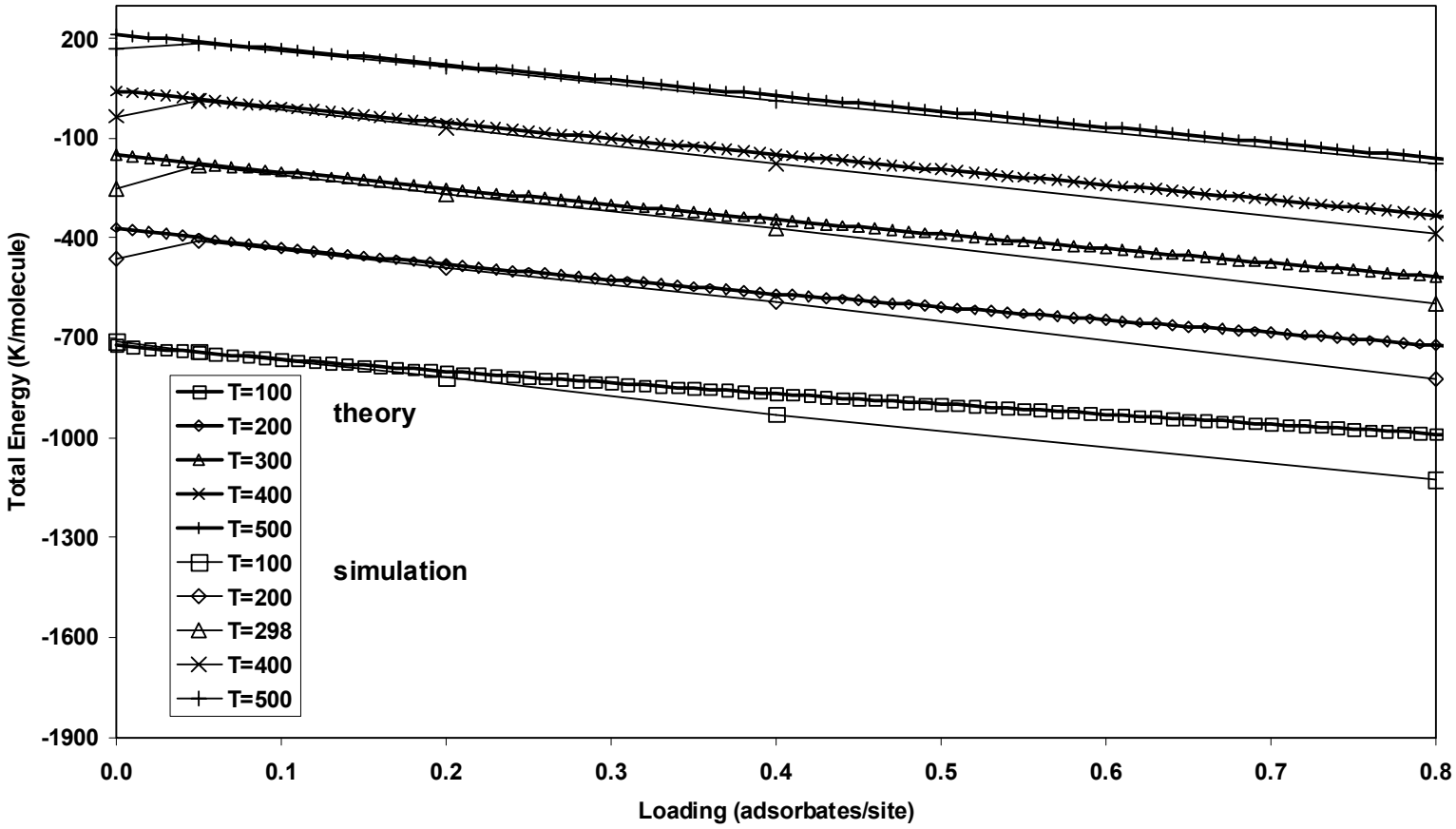

Figure 5: Total energy as a function of fractional occupancy.

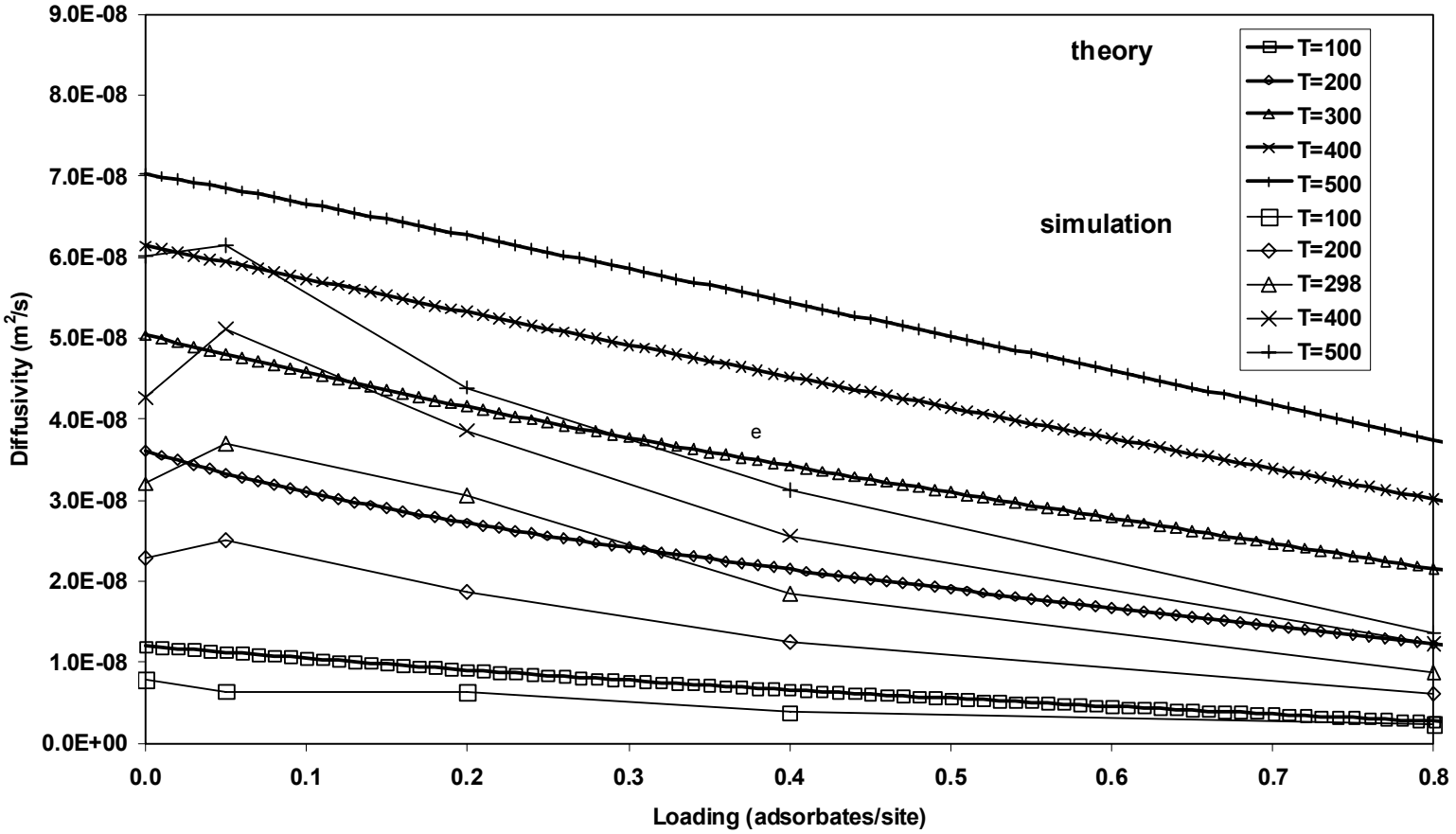

Figure 6: Diffusion coefficient as a function of fractional occupancy.

Part 5

A Predictive Model of Adsorption and Diffusion in Nanoporous Materials: Extension to Binary Mixtures

ABSTRACT

The analytical theories for lattice adsorption and diffusion, presented in Parts 2-4, are extended for binary fluids. The lattice theory is generalized and can be used to model different adsorbent-adsorbate systems.

We use statistical mechanical tools to develop a partition function, which is used to generate thermodynamic as well as transport properties. The theory can be generalized to different mixtures, and geometries. The lattice parameters can be obtained from a potential energy map of the adsorbent. In a previous paper, we optimized our theory with simulation data for single component methane in Zeolite Na-Y. In this work, we use the optimized lattice parameters, together with a few other randomly chosen ones, to generate the results for a binary system. The theory yields the chemical potential, the adsorbate-adsorbate energies, adsorbate-pore energies, and the diffusivity of the individual species in the mixture. Each of these properties is a function of temperature, pressure, and composition in the adsorbed phase. We also discuss the adsorbate distribution within the lattice, which provides useful insight into the molecular level mechanisms governing the behavior of binary fluids in zeolites and other nanoporous materials.

The theory requires very few parameters to characterize the lattice. The theory is computationally very efficient and requires only a minute to generate all the properties. The impact of this theory is that it can be easily integrated into process simulators to provide a molecular-level understanding of the macroscopic industrial processes.

5.1 INTRODUCTION

5.1.1 Background

Nanoporous materials find increasing use in the chemical industry due to their wide range of applications. A significant amount of research has been conducted to study the process of adsorption and diffusion of various fluids within nanoporous materials [1-23]. Historically, molecular level simulations have been employed to investigate these phenomena. The simulations have identified localized adsorption sites within the adsorbent lattice where the molecules sit depending upon the lattice parameters. Based on these findings, several researchers have concentrated on developing lattice theory to predict adsorption and diffusion in different adsorbate-adsorbent systems. The theoretical approach has a few advantages over the simulations: (1) The simulations are computationally very expensive – for instance, they require hours of supercomputing time to generate a few data points along the adsorption isotherm. (2) A predictive model can better describe the fundamental physical behavior of fluids adsorbed within the nanoporous materials.

In our recently published works [1, 2], we presented an analytical model to describe adsorption and diffusion of fluids in the nanoporous materials. The model extends the Quasi-Chemical Approximation Theory taking advantage of localized adsorption sites within the adsorbent lattice. The lattice model is generalized and can be used to describe any fluid within an arbitrary zeolite. We demonstrated the applicability of our model in [3] by comparing the results with Molecular Dynamics Simulations for the system - single component Methane in Zeolite Na-Y.

5.1.2 Objective

In this work, we extend our lattice theory of adsorption and diffusion to describe the behavior of binary fluids confined in nanoporous materials.

5.1.3 Outline

In the following Section 2, we provide a brief summary of our lattice adsorption theory. Specifically, we develop the partition function for binary fluids. The rest of the theory is analogous to our previously published work, and hence, for a detailed description of the theory, the reader is referred to [1]. Section 3 presents the results of our theory for randomly chosen lattice parameters.

5.2 THEORY

Our predictive analytical theory for lattice adsorption and diffusion [1, 2] uses standard statistical mechanics to develop the partition functions. The partition function provides the desired thermodynamic and transport properties. As described in our previous work, our lattice theory accounts for the adsorbate clustering within the pores as well as inter-site and intra-site adsorbate-adsorbate interactions. These phenomenon are critical to obtaining the correct isotherms, transport properties, and so on. The high degree of non-ideality provides a complex functional form to the partition function, which results in a system of non-linear algebraic equations to be solved simultaneously. The solution to this problem is non-trivial because many of the variables span several orders of magnitude. We use a similar scaling technique as the one presented in [1]. Hence, we avoid further discussion of the same. The interested reader is referred to [1].

As mentioned previously, this work extends our already published lattice theory to describe adsorption and diffusion of *binary* mixtures confined in nanoporous materials. Hence, we do not present the theory in this section. Instead, we only highlight certain variables and functions that we feel deserve special mention in the binary case. Many of the lattice parameters now assume more complex dimensionality due to the increased number of combinations of the two components. We notice that the adsorbent lattice can still be completely characterized by the same lattice parameters, namely – (i) lattice connectivity, (ii) lattice spacing, (iii) site well depth, (iv) site volume, and (v) adsorbate-pore energy constant. Some of these parameters are discussed in the Results and Discussion section. These parameters are distinct for each combination of adsorbate and

adsorbent and can be determined either by (1) using infinite dilution potential energy maps of the adsorbent or (2) fitting the parameters with simulation data. However, it is important to note that approach (1) eliminates the need to conduct molecular level simulations to obtain these parameters.

5.2.1 The Partition function

In this section, we develop the partition function since it assumes a complex form for the binary system. Our model assumes a static lattice structure composed of two different types of sites since we know from the literature that most zeolites and molecular sieves have more than one type of site (however, note that the theory is generalizable to one or three types of sites too). In this current example, we consider a lattice composed of two types of sites $N_T = 2$. This lattice is described by a connectivity matrix, $\underline{\underline{c}}$,

$$\underline{\underline{c}} = \begin{bmatrix} c_{11} & c_{12} \\ c_{21} & c_{22} \end{bmatrix} \tag{1}$$

where each of these elements, c_{ij}, describe the number of sites of Type j connected to a site of Type i.

The partition function has the same functional dependency as before. In other words, the partition function again has three factors, a configurational degeneracy, intrasite partition functions, and intersite interaction energy.

$$Q(N_1,N_2,M,T) = \sum_{\text{configurations}} g(N_1,N_2,M) * \text{qterm} * \text{eterm} \tag{2}$$

We notice that the functional form of the overall partition function is similar to the one observed for the single component case. However, the individual terms now assume more complex form.

The intrasite partition functions term, qterm say, is now given by,

$$qterm = \prod_{i}^{N_T} \prod_{x=0}^{x=m_{s,i1max}} \prod_{y=0}^{y=m_{s,i2max}} \left[q_{i,1}(x,y,T)^x \; q_{i,2}(x,y,T)^y \right]^{n_{s,i}(x,y)} \tag{3}$$

where N_T is the number of sites, N_C is the number of components, x and y are the occupancy of component one and two respectively, $m_{s,i,1max}$ is the maximum occupancy of component one in a site of Type i, and $m_{s,i,2max}$ is the maximum occupancy of component two in a site of Type i. Furthermore, $n_{s,i}(x,y)$ indicates the number of sites of Type i with occupancy x of component one and occupancy y of component two. $q_{i,j}(x,y,T)$ is the intra-site partition function for a site of Type i for component j, with an occupancy x for component one and y of component two. Note that in Equation (3), the intra-site partition function is subject to the following constraint.

$$q_{i,j}(x,y,T) = \begin{cases} 1 & \text{if } xV_a(1) + yV_a(2) > V_{s,i} \\ 1 & \text{if } j = 1 \,\&\, x = 0 \\ 1 & \text{if } j = 2 \,\&\, y = 0 \\ q_{i,j}(x,y,T) & \text{if otherwise} \end{cases} \tag{4}$$

The constraint, $xV_a(1) + yV_a(2) > V_{s,i}$, indicates that the total volume of adsorbates in a site cannot be greater than the site volume itself.

The intra-site partition function itself is given by,

$$q_{i,1}(x,y,T) = \left(\frac{V_{s,i} - (xV_a(1) + yV_a(2))}{(x\Lambda_1^3 + y\Lambda_2^3)} \right) e^{\frac{-\left(\frac{x(x-1)}{2} w_i(1,1) + \frac{xy}{2} w_i(1,2) \right)}{kT}} \tag{5.a}$$

$$q_{i,2}(x,y,T)=\left(\frac{V_{s,i}\text{ - }(xV_a(1)+yV_a(2))}{(x\Lambda_1^3+y\Lambda_2^3)}\right)e^{\frac{-\left(\frac{y(y-1)}{2}w_i(2,2)+\frac{xy}{2}w_i(1,2)\right)}{kT}} \tag{5.b}$$

Both of the above equations again are subject to Constraint (4).

The configuration degeneracy term is given by

$$g(N_1,N_2,M)=\left[\prod_{\substack{i=1\\ j\neq i}}^{N_T}\left(\frac{M_i!}{\prod_{x=0}^{m_{s,i}}\prod_{y=0}^{m_{s,i}}n_{s,i}(x,y)!}\right)^{1-c_{ij}}\right]\left[\frac{(c_{12}M_1)!}{\prod_{x=0}^{m_{s,i}}\prod_{y=0}^{m_{s,i}^*}\prod_{w=0}^{m_{s,j}}\prod_{z=0}^{m_{s,j}^*}N_{i,j}(x,y,w,z)!}\right] \tag{6}$$

where M_i indicates sites of Type i, $N_{i,j}(x,y,w,z)$ indicates number of neighbors of a site of Type i having occupancy x of component one and y of component two, with a site of Type j having occupancy w of component one and z of component two. The asterisks indicate that the summation is subject to the constraint,

$$xV_a(1)+yV_a(2)>V_{s,i} \tag{7}$$

Finally, the energetic term of the partition function is given by

$$\text{eterm}=e^{-\sum_{i=1}^{N_T}\sum_{j\geq i}^{N_T}\sum_{x=0}^{m_{s,i}}\sum_{y=0}^{m_{s,i}^*}\sum_{w=0}^{m_{s,j}}\sum_{z=0}^{m_{s,j}^*}N_{i,j}(x,y,w,z)\frac{[(xw)w_{11}+(xz+yw)w_{12}+(yz)w_{22}]}{kT}} \tag{8}$$

where asterisks indicate that the summation is subject to Constraint (7). Note that the adsorbate-adsorbate (aa) potential energy, w_{cd}, is the interaction energy between a molecule of component c and a molecule of component d sitting in the neighboring site. In Equation (8), we see three possible combinations of w (arising from the two

components), namely, w_{11}, which is the interaction energy for two molecules of component one occupying neighboring sites, w_{12}, which is the aa interaction energy between a molecule of component one and a molecule of component two, and w_{22}, which is the interaction potential energy for two molecules of component two occupying neighboring sites.

5.3 RESULTS AND DISCUSSION

In this section, we present plots that demonstrate the capability of our theory to predict the correct qualitative behavior for binary fluids in a particular lattice geometry that we have used in previous studies. As mentioned previously, our binary adsorption and diffusion models work for different fluids confined within any arbitrary lattice. Table 1 shows the lattice parameters that are used in these plots. There are a few points that need to be highlighted here before we discuss the plots. The results presented in this section assume a lattice composed of two types of site with sites of Type 1 having maximum occupancy of one and sites of Type 2 with a maximum occupancy of two. Simulations have shown that many zeolites and molecular sieves are composed of two types of sites. To supplement this work, we are also preparing a comparison study of our theory against Molecular Dynamics Simulations for binary adsorption of methane and ethane in Zeolite Na-Y. Zeolite Na-Y consists of two types of sites with sites of Type 1 having a maximum occupancy of one and sites of Type 2 with a maximum occupancy of two. Hence, we chose the same lattice structure in this example. Furthermore, the two components selected in this example bear the properties of Lennard-Jones single-center methane and ethane. In our earlier work, we optimized the lattice parameters for single component methane in Zeolite Na-Y by comparing with simulation data. We use the same lattice parameters for component one (which bears methane properties). The lattice parameters for ethane (i.e. component two) are randomly chosen and so are some of the parameters that arise from the binary combination. Our comparison study, as mentioned earlier, would optimize those parameters against the simulation data; however, presently

our aim is to illustrate the general advantages of the binary theory and the current assumptions provide a reasonable set of parameters to illustrate the qualitative behavior.

In this lattice structure, sites of Type 2 are assumed to be larger than sites of Type 1. Additionally, sites of Type 1 are assumed to be energetically deeper than sites of Type 2 at the single occupancy level. Table 1 also shows that the sites of Type 2 are energetically more shallow at double occupancy. Also note that the sites of Type 2 are energetically more shallow at a double occupancy of component one than at a double occupancy of component two. In other words, we assume that it is energetically favorable to place two molecules of component two in sites of Type 2 than two molecules of component one. The connectivity matrix is given by $\underline{\underline{c}} = \begin{bmatrix} 0 & 3 \\ 2 & 0 \end{bmatrix}$. This means that forty percent of the sites are Type 1 and sixty percent of the sites are Type 2. The well depth U_{AP} is divided into two parts, U_{AP_1} which shows the well depth of sites of Type 1 for different occupancies and U_{AP_2} which shows the well depth for sites of Type 2. The rows indicate the occupancy of component one and the columns indicate the occupancy of component two. Since, sites of Type 1 can hold a maximum of one molecule, U_{AP_1} is a 2x2 matrix of the respective combinations of the two components. On the other hand, sites of Type 2 are assumed to have a maximum occupancy of two. Hence, the occupancy of each component in site of Type 2 can vary between zero and two. Hence U_{AP_2} is a 3x3 matrix of the different possible occupancy levels. A similar logic is applied to the adsorbate-pore energetic constant, U_{APc} in Table 1. Also, the 2-12 lattice has 40% of Type 1 sites with a maximum occupancy of one and 60% of Type 2 sites with a maximum occupancy of two. In other words, the maximum adsorbate loading is $0.4 \times 1 + 0.6 \times 2 = 1.6$ adsorbates/site

Figure (1) shows the adsorbate distribution as a function of loading. As a reminder, $n_{s,i}(x,y)$ indicates the number of sites of type i with occupancy x of component one and occupancy y of component two. It should be noted that the summation of these sites variables at any given loading would always be unity, which is

the total number of sites, m. Initially, when no molecules are present, all the sites of Types 1 and 2 have zero occupancy. Hence we see that $n_{s,1}(0,0)$ and $n_{s,2}(0,0)$ attain maximum values whereas all the other site variables are zero. As the loading increases, $n_{s,1}(0,0)$ and $n_{s,2}(0,0)$ approach zero. On the other hand, $n_{s,1}(1,0)$, $n_{s,1}(0,1)$, $n_{s,2}(1,0)$, and $n_{s,2}(0,1)$ simultaneously increase as all sites are filled with one molecule each. There are two interesting observations here. First, we see that only the site variables with single occupancy are increasing while all the sites variables with double occupancy are still zero. In other words, we see a preference in both sites for occupancies of one. This is due to the fact that, despite an energetic attraction, there is an entropic barrier in the intra-site partition function to double occupancy. Second, we see that at low loadings, $n_{s,2}(1,0)$, and $n_{s,2}(0,1)$ always assume higher values than $n_{s,1}(1,0)$ and $n_{s,1}(0,1)$. This is at least partially because sites of Type 2 are more numerous than sites of Type 1.

As we continue to fill the sites, $n_{s,2}(2,0)$, $n_{s,2}(0,2)$, and $n_{s,2}(1,1)$ increase while $n_{s,2}(1,0)$ and $n_{s,2}(0,1)$ decrease. Interestingly, $n_{s,1}(1,0)$ and $n_{s,1}(0,1)$ increase with loading even at high loadings. This fact is easily understood because the sites of Type 1 have a maximum occupancy of one, unlike sites of Type 2, which are filled with two molecules. Table 1 shows that it is energetically most favorable to place one molecule of component two in sites of Type 1. Hence, we notice that at high loadings, $n_{s,1}(0,1)$ attains the maximum value.

Figure (1) showed that the theory could provide a reliable physical understanding of the adsorption behavior of fluids in the lattice geometry. Having thus demonstrated the capabilities of our theory in describing the molecular level mechanisms governing the adsorption of binary fluids confined in nanopores, we now present plots of the thermodynamic and transport properties as a function of loading.

Figure (2) plots the chemical potential of the individual components as a function of adsorbate loading at a temperature of 300 K. The mole fractions of both the components are 0.5. Hence, it is immaterial whether we plot the properties of the individual components as a function of the respective loading, or just as a function of the

total loading. All the plots henceforth show the properties as a function of total loading (adsorbates/site). Overall, we see that Figure (2) shows the correct qualitative behavior of the adsorption isotherms. Furthermore, we see that at low loadings, the adsorption isotherms show less favorable adsorption of component one than component two. We expected this behavior because it is more energetically favorable to place molecules of component two in both the types of sites at low loading. As the loading increases, at around a loading of 1.1 adsorbates/site, the isotherms show a preference for adsorption of molecules of component one. Again, we expected this behavior because at around a loading of 1 adsorbate/site (when the sites of Type 2 are placed with the second molecule), there is an entropic advantage to placing two molecules of component one in sites of Type 2, which dominates the overall placement of molecules.

Figure (3) plots the adsorbate-pore (ap) interaction energy as a function of adsorbate loading for three different temperatures. The ap interaction energy, U_{AP}, is the energetic contribution of the adsorbate-pore interactions to the total energy. (Please note that the ap interaction energy plotted here receives contributions from the ap interactions for components one and two.) We see that at low temperatures, the ap interaction energy increases with loading, whereas at higher temperatures, the ap interaction energy shows a minimum with loading.

Let us first consider the higher temperature plots. At low and intermediate loadings, more adsorbates (Components one and two) are filled in the sites of Type 2 than in the Type 1 sites. Apart from the fact that the sites of Type 2 are more numerous than the Type 1 sites, there is an entropic advantage to placing the molecules in the larger (but energetically more shallow) sites of Type 2. The combined entropic and energetic effects cause an increase in the number of ap interactions with increasing loading, which results in a decrease of the ap interaction energy. On the other hand, at low temperatures, we believe that a high number of molecules are adsorbed in the smaller (but energetically deeper) sites of Type 1, which results in a decrease in the ap interactions with loading. The decrease in the ap interactions causes an increase in the ap interaction energy at low temperatures.

At high loadings, the sites of Type 2 are filled with the second molecule. Immaterial of the type of component, the double occupancy involves an energetic as well as entropic penalty because of the smaller sites and more shallow depths. This explains the increase in the ap interaction energy observed at high loadings for all temperatures.

Figure (4) plots the adsorbate-adsorbate (aa) interaction energy as a function of loading for three temperatures. The aa interaction energy, U_{AA}, is the energetic contribution of the adsorbate-adsorbate interactions to the total energy. It is important to note that the aa interactions occur between the molecules adsorbed in neighboring sites as well as within sites. (The within sites aa interactions are observed only in sites of Type 2.)

We notice that at low and intermediate loadings, the aa interaction energy decreases in magnitude with temperature. As the temperature increases, the entropic factor becomes more important at the expense of the energetic interactions. However, at higher loadings, we see a slight positive concavity at lower temperatures. This trend is explained later.

The density dependence of the aa interaction energy arises from the fact that both the intra-site as well as inter-site partition functions have a high loading functionality. We see that at high temperatures, the aa interaction energy decreases with loading in an approximately linear pattern. At low temperatures too, we see that the aa interaction energy decreases with loading. However, at low temperatures, the slope of the decrease in the aa interaction energy decreases at higher loadings. In other words, we see a plateau at around a loading of 0.8 adsorbates/site in the aa interaction energy. To explain this trend, we plot in Figure (5), the adsorbate distribution of the site variables as a function of loading at 175 K. On comparing Figure (5) with Figure (1), we clearly see that at 175 K, the number of sites with double occupancy, $n_{s,2}(0,2)$, and the variable $n_{s,1}(0,1)$ attain higher values than at 300 K at around a loading of 0.8 adsorbates/site. This means that there are more numerous interactions between molecules of component two singly occupying sites of Type 1 and the molecules in the neighboring sites with double occupancy. These neighbor aa interactions are repulsive, and hence diminish the

inter-site contribution to the aa interaction energy. Correspondingly, we observe the decrease in slope of the aa interaction energy at low temperatures in Figure (4). Also, we notice that the aa interaction energy curves for all temperatures have the same intercept – zero. We expect this trend because there are no aa interactions at infinite dilution.

Figure (6) plots the total energy as a function of the adsorbate loading for three temperatures. It should be noted that the total energy is merely an addition of the adsorbate-pore interaction energy, adsorbate-adsorbate interaction energy, and the kinetic energy. The trends in Figure (6) arise from the competing effects of the ap interaction energy and the aa interaction energy. For instance, at low loadings, the aa interaction energy is very low. Hence, the trends in total energy are similar to those observed in the ap interaction energy plots. Whereas at higher loadings, the aa interaction energy decreases rapidly, which is reflected in the total energy. Also, we notice that at low temperatures, the total energy displays a local minimum at a loading of 0.8 adsorbates/site. This is an artifact of the trends observed in the aa interaction energy at similar conditions.

Figure (7) plots the diffusivities of the two components as a function of adsorbate loading. The diffusivity is plotted at only one temperature (T = 300 K). We notice that at infinite loading, the diffusivity of component one is higher than the diffusivity of the component two. This is due to the fact that component one has a lesser mass than component two, which makes component one easier to diffuse in the bulk phase. As expected, we see that the diffusivities of both the components decrease with loading. As the loading increases, there are less vacant sites to facilitate diffusive motion through the lattice. However, in addition to the number of free sites, the distribution of activation energies for motion is changing with the distribution of occupancies. Hence, we notice a crossover in the diffusivity for the two components at around a loading of 0.8 adsorbates/site. At very high loadings, most of the sites are occupied and hence the diffusivities of both the components approach zero.

5.4 CONCLUSIONS

In this work, we demonstrated the capabilities of our lattice theory in predicting the behavior of binary fluids within any arbitrary lattice. The theory required very few lattice parameters to describe the adsorbent. The theory is generalized and could be used to describe the behavior for different binary mixtures in nanoporous materials.

Competing energetic and entropic effects governed the placement of the molecules of the two components within the lattice. The theory provided various thermodynamic and transport properties as a function of adsorbate loading. The theory provided sound qualitative understanding of the trends observed in these plots.

We are currently comparing the results predicted by our theory against simulation data for adsorption of a binary mixture of methane and ethane in Zeolite Na-Y.

REFERENCES

1. Kamat, M.R., Keffer, D., “An analytical theory for adsorption of fluids in nanoporous materials”, *Molecular Physics* 2002 **100** (16) 2689-2701.
2. Kamat, M.R., Keffer, D., “An analytical theory for diffusion of fluids in nanoporous materials”, submitted to Molecular Physics.
3. Kamat, M.R., Dang, W., Keffer, D., “Agreement between analytical theory and Molecular Dynamics simulations for adsorption and diffusion in crystalline nanoporous materials”, submitted to Molecular Physics.
4. Keffer, D., Davis, H.T., McCormick, A.V., "The effect of nanopore shape and loading on adsorption selectivity of a binary mixture" *J. Phys. Chem.* 1996 **100** p. 638-645.
5. Keffer, D., Davis, H.T., McCormick, A.V., "The effect of nanopore shape on the structure and isotherms of adsorbed fluids" *Adsorption* 1996 **2** p. 9-21.
6. Keffer, D., “Molecular Models of Adsorption and Diffusion in Nanoporous Materials”, Ph.D. Thesis, University of Minnesota, July, 1996.
7. Keffer, D., McCormick, A.V., Davis, H.T., " Uni-directional and single-file diffusion in $AlPO_4$-5: a molecular dynamics study", *Mol. Phys.* 1996 **87** p. 367-387.
8. Keffer, D., McCormick, A.V., Davis, H.T., "Agreement between Theory and Simulation of Single-file diffusion in a molecular sieve", Proceedings from the XI International Workshop on Condensed Matter Theories, Caracas, Venezuela, June, 1995.
9. Hahn, K. Kärger, J., “Molecular Dynamics Simulations of Single-File Systems”, *J. Phys. Chem.*, 1996 100 p. 316-326.
10. Keffer, D., McCormick, A.V., Davis, H.T., "Diffusion and Percolation on Zeolite Sorption Lattices", *J. Phys. Chem.* 1996 **100** p. 967-973.
11. Van Tassel, P.R., Davis, H.T., McCormick, A.V., “Monte Carlo calculations of adsorbate placement and thermodynamics in a micropore: Xe in NaA”, *Mol. Phys.* 1991 **73** p. 1107-1125.
12. Van Tassel, P.R., Davis, H.T., McCormick, A.V., “Monte Carlo calculations Xe arrangement and energetics in the NaA alpha cage”, *Mol. Phys.* 1992 **76** p. 411-432.
13. Van Tassel, Phillips, J.C., P.R., Davis, H.T., McCormick, A.V., “Zeolite adsorption site location and shape shown by simulated isodensity surfaces”, *J. Mol. Graphics* 1993 **11** p. 180-184,188.
14. Van Tassel, P.R., Davis, H.T., McCormick, A.V., “Open-system Monte Carlo simulations of Xe in NaA” *J. Chem. Phys.* 1993 **98** p. 8919-8928.
15. Van Tassel, P.R., Somers, S.A., Davis, H.T., McCormick, A.V., “Lattice model and simulation of dynamics of adsorbate motion in zeolites” *Chem. Eng. Sci.* 1994 **49** p. 2979-2989.

16. Van Tassel, P.R., Davis, H.T., McCormick, A.V., "New lattice model for adsorption of small molecules and their mixtures in a zeolite micropore", *AIChE J.* 1994 **40** p. 925-934.
17. Van Tassel, P.R., Davis, H.T., McCormick, A.V., "Adsorption simulations of small molecules and their mixtures in a zeolite micropore", *Langmuir* 1994 **10** p. 1257-1267.
18. Gupta, V., Davis, H.T., McCormick, A.V., "Comparison of the ^{129}Xe NMR chemical shift with simulation in zeolite Y", *J. Phys. Chem.* 1996 **100** p. 9824-9833.
19. Gupta, V., Davis, H.T., McCormick, A.V., "^{129}Xe NMR chemical shifts in zeolites: Effect of Loading studied by Monte Carlo simulations", *J. Phys. Chem.* 1997 **101** p. 129-137.
20. Keffer, D., Gupta, V., Kim, D., Lenz, E., Davis, H.T., McCormick, A.V., "A compendium of zeolite potential energy maps" *J. Mol. Graphics* 1996 **14** p. 108-116, 100-104.
21. Nivarthi, S.S., Van Tassel, P.R., Davis, H.T., McCormick, A.V., "Adsorption and energetics of xenon in mordenite: a Monte Carlo simulation study", *J. Chem. Phys.* 1995 **103** p. 3029-3037.
22. Snurr, R.Q., June, R.L., Bell, A.T., Theodorou, D.N., "Molecular simulations of methane adsorption in silicalite", *Mol. Sim.* 1991 **8** p. 73-92.
23. Snurr, R.Q., June, R.L., Bell, A.T., Theodorou, D.N., "A hierarchical atomistic/lattice simulation approach for the prediction of adsorption thermodynamics of benzene in silicalite", *J. Phys. Chem.* 1994 **98** p. 5111-5119.

APPENDICES

Nomenclature

SYMBOL	DESCRIPTION	UNITS
c_{ij}	Number of sites of type j connected to a site of type i	-
E	Total energy	{K/molecule}
$m_{s,i}$	Maximum occupancy of a site of type i	
$m_{s,i,j}$	Maximum occupancy of sites of type i for component j.	-
M_i	Number of sites of types 1	-
$n_{s,i}(x,y)$	Number of sites of type i with an occupancy of x	-
N	Total number of adsorbates	-
N_1	Number of molecules of component one	
N_2	Number of molecules of component two	
$N_{i,j}(x,y,w,z)$	Number of neighbors of a site of type i having occupancy x of component one and y of component two, with a site of type j having occupancy w of component one and z of component two.	-
$q_{i,j}(x,y,T)$	Intrasite partition function of sites of type i for component j, having an occupancy x of component one and y of component two.	-
$Q(N_1,N_2,M,T)$	Partition function of a function of N_1, N_2, M, and T	-
r	Lennard- Jones distance between molecules	{A}
r_{min}	Distance of well minimum	{A}
T	Temperature	{K}

$U_{AP,i}(r,x,y,T)$	Potential energy of a site of type i as a function of radius, occupancy x of component one, occupancy y of component two, and temperature	{K/molecule}
$V_{A,i}$	Volume of adsorbate of component i	$\{A^3\}$
$V_{S,i}$	Volume of sites of type i	$\{A^3\}$
$\underline{\underline{w}}_x$	Matrix of adsorbate-adsorbate potential energy due to adsorbates in neighboring sites	{K}
x	Occupancy of a site of type i	-
y	Occupancy of a site of type j	-

Table 1: Lattice Parameters

$\underline{\underline{c}}$	$\underline{\underline{\ell}}$ (Å)	$\underline{V_S}$ (Å^3)	$\underline{\underline{U_{AP_1}}}$ (K)	$\underline{\underline{U_{AP_2}}}$ (K)
$\begin{bmatrix} 0 & 3 \\ 2 & 0 \end{bmatrix}$	$\begin{bmatrix} - & 4.304 \\ 4.304 & - \end{bmatrix}$	$\begin{bmatrix} 47 & 94 \end{bmatrix}$	$\begin{bmatrix} - & -1444 \\ -1115 & - \end{bmatrix}$	$\begin{bmatrix} - & -1060 & -1045 \\ -817.5 & -926 & - \\ -807 & - & - \end{bmatrix}$

$\underline{\underline{U_{AP_{c_1}}}}$ (K)	$\underline{\underline{U_{AP_{c_2}}}}$ (K)
$\begin{bmatrix} - & 892.7 \\ 689.1 & - \end{bmatrix}$	$\begin{bmatrix} - & 823.2 & 832.2 \\ 635.4 & 729.3 & - \\ 635.4 & - & - \end{bmatrix}$

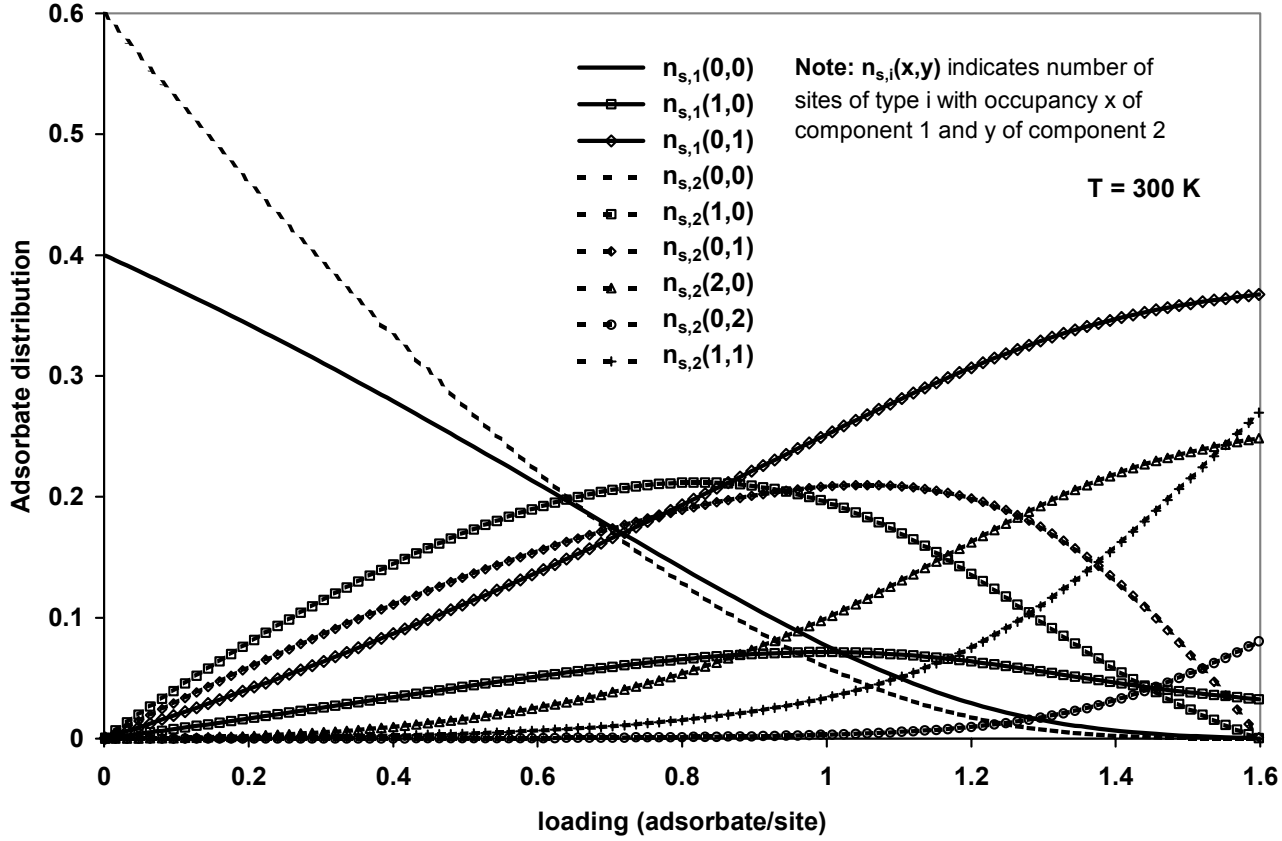

Figure 1: Adsorbate distribution as a function of loading

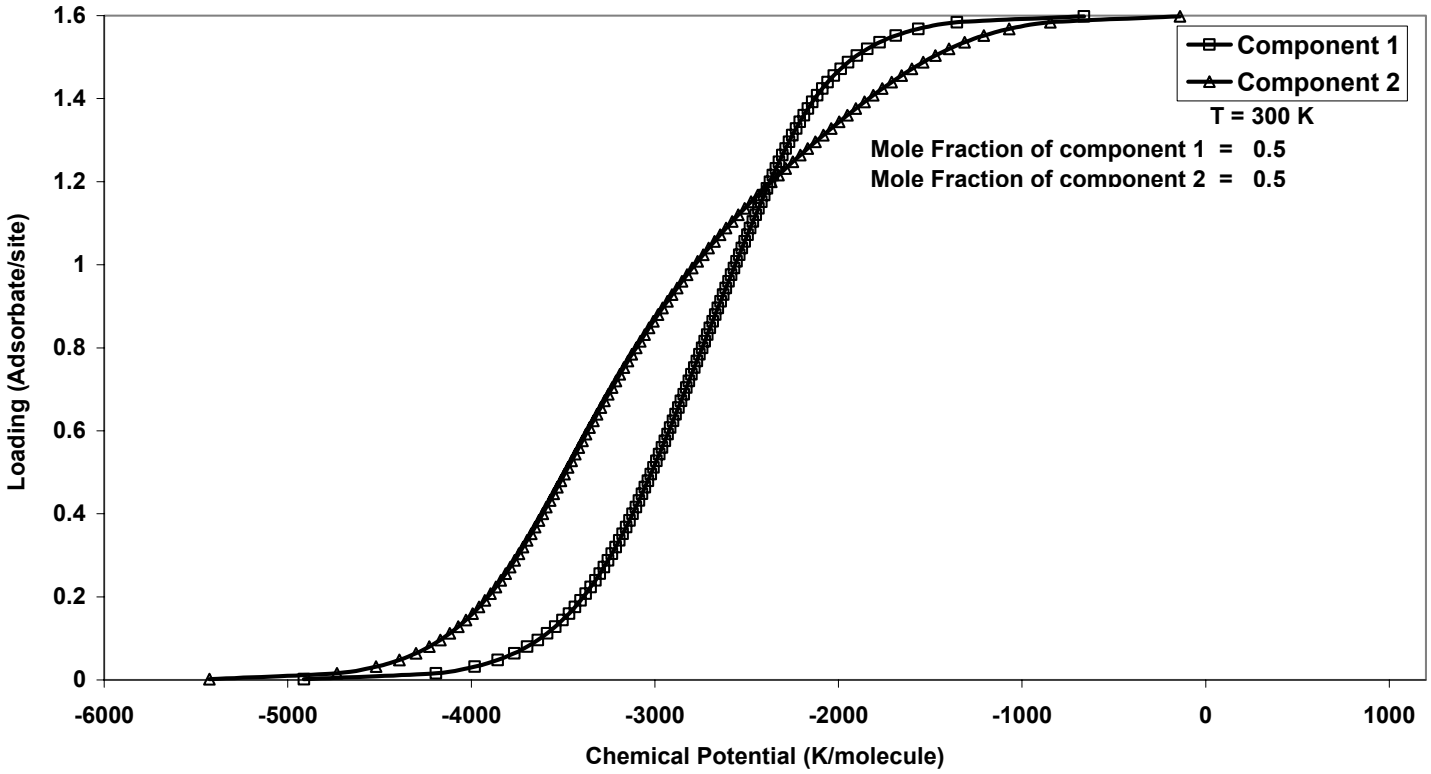

Figure 2: Chemical Potential as a function of loading

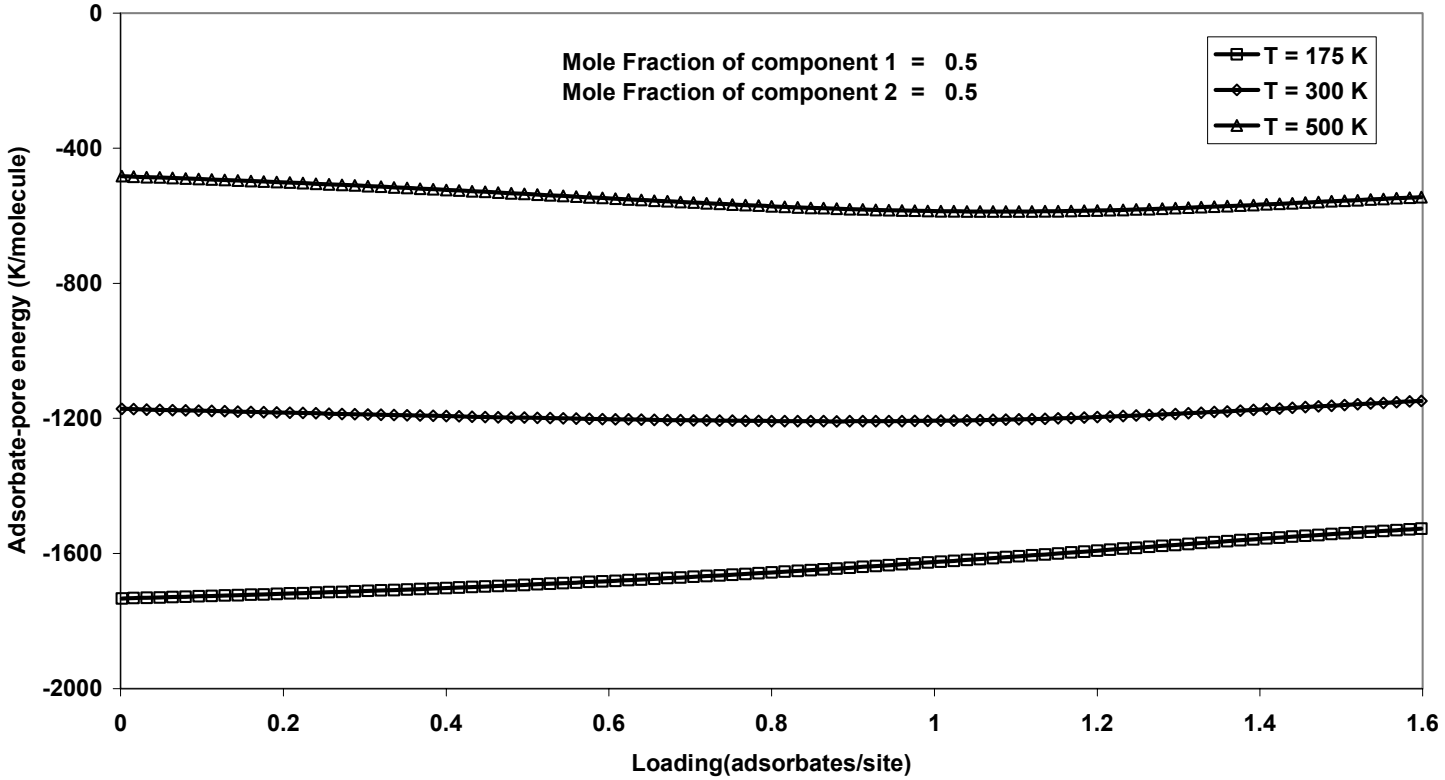

Figure 3: Adosorbate-pore energy as a function of loading

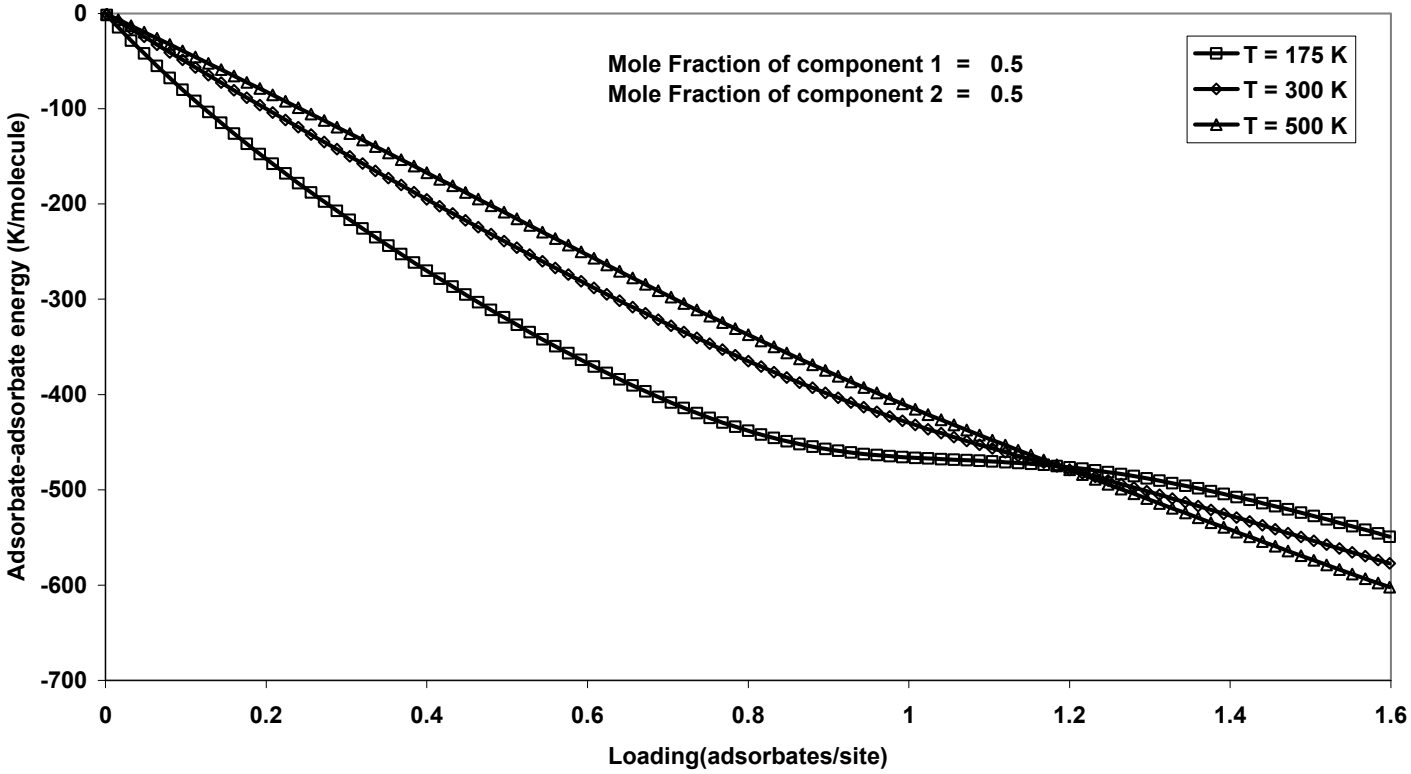

Figure 4: Adsorbate-adsorbate energy as a function of loading

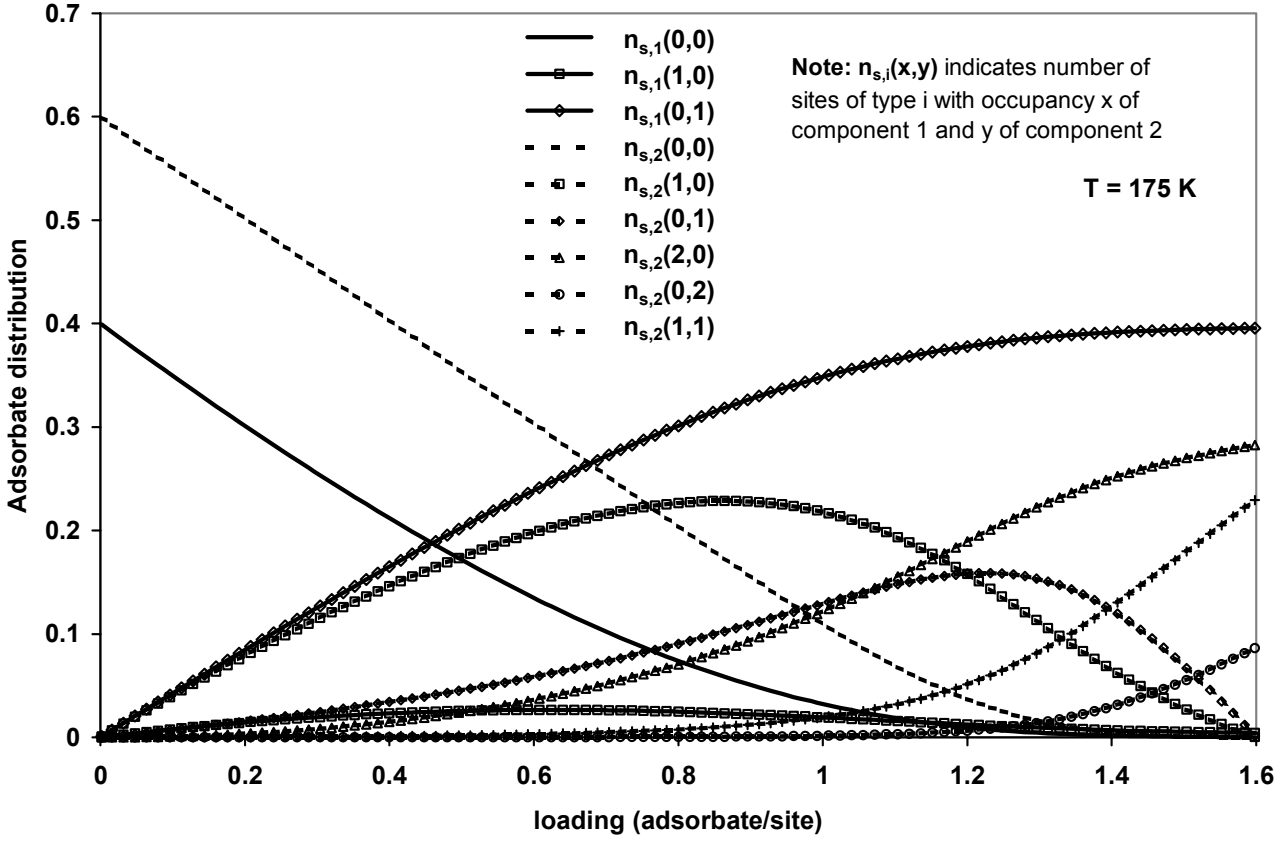

Figure 5: Adsorbate distribution as a function of loading

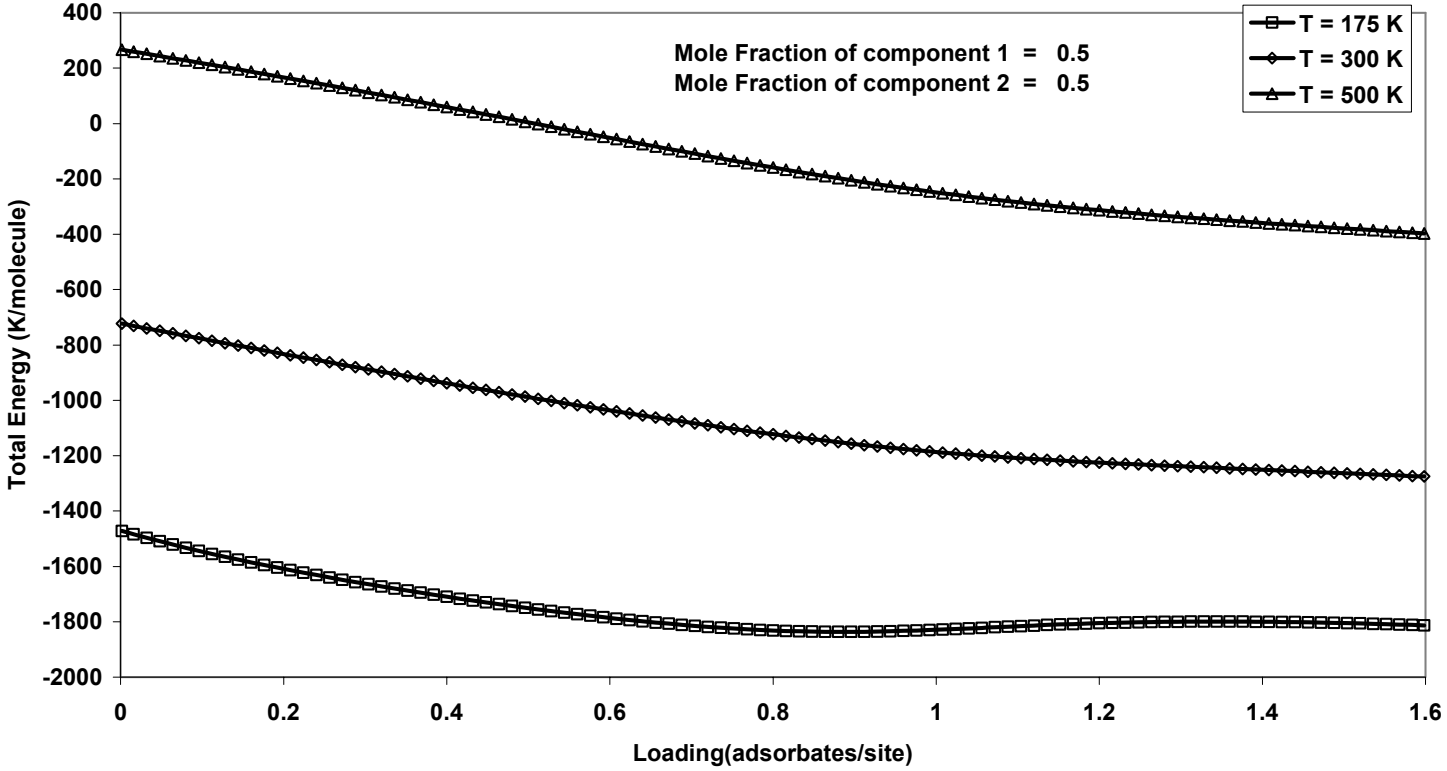

Figure 6: Total energy as a function of loading

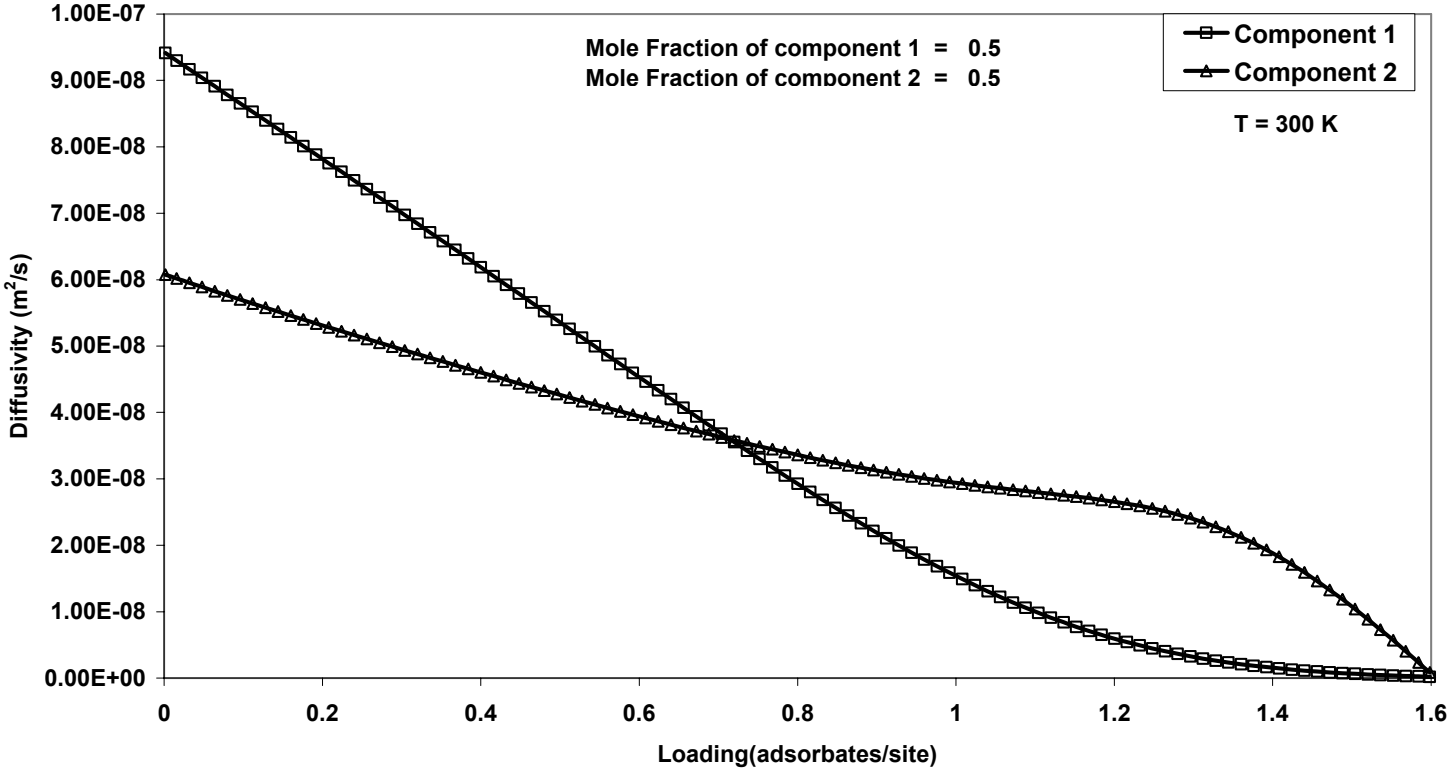

Figure 7: Diffusivity as a function of loading

Part 6

Conclusions and Future Work

This thesis presented generic analytical predictive theories that describe adsorption and diffusion of small molecules in nanoporous materials. Based on the material presented, various conclusions can be drawn. This part summarizes the results and applications of the analytical theory. Suggestions for future efforts directed in this area are presented as well.

6.1 SUMMARY AND CONCLUSIONS

Part 2 presented a predictive generalized theory to describe the phenomena of adsorpion and diffusion of fluids confined in nanopores. The theory assumed a lattice composed of different types of sites. The adsorbate molecules are placed in these sites depending upon the various lattice parameters. The lattice theory of adsorption is fundamentally an extension of the Quasi-Chemical Approximation Theory. The theory incorporates the intersite as well as intrasite interactions that play a dominant role in the placement of molecules. The theory showed that competing energetic and entropic effects govern the adsorbate distribution within the lattice. At infinite loading, the energetic effects play a dominant role in the placement of molecules. We noticed that at low loadings, as expected, more molecules are adsorbed in the energetically deeper sites (that are smaller in volume) whereas at high loadings, the entropic effects dictate the placement as it is energetically less favorable for sites to hold two molecules.

Part 3 described a lattice diffusion theory that yielded a self-diffusion coefficient, which is a function of (i) temperature, (ii) adsorbate density, (iii) adsorbate size, (iv) the adsorbate-adsorbate energetic interaction, and (v) the adsorbate-pore energetic interaction. The theory included the nearest neighbor interactions and site blocking in calculating the mean diffusivity.

Part 4 presented comparison of the results predicted by our theory with Molecular Dynamics simulations for system with high degree of non-ideality. We demonstrated that the theory provided very good qualitative as well as quantitative agreement with the simulations. These comparison studies established that the theory behaves well for

systems where the adsorbate and the adsorbent volumes are on the same order of magnitude.

In Part 5, we demonstrated the capabilities of our theory in accurately predicting the behavior of binary fluids in confined geometries. The model presented could be generalized to any binary mixture confined in an arbitrary geometry. We presented plots of the adsorption isotherms, diffusivities and energies for each component in the adsorbed phase.

This work presented a lattice theory from using concepts of fundamental statistical mechanics. The theory established trends and relationships between the microscopic adsorbate and adsorbent parameters, and the macroscopic level thermodynamic properties such as adsorption isotherms, energy, entropy, and Helmholtz free energy. Our lattice adsorption theory incorporated only five lattice parameters whereas the diffusion theory incorporated no fitting parameters.

Furthermore, this work established the superior computational advantage that theoretical modeling possesses compared to the computer simulations. Our analytical theories took approximately a minute to generate thermodynamic properties including the entire adsorption isotherm, as compared to the MD simulations that took 200 hours of parallel super computing time to generate a few points along the isotherm. Our overall aim was to develop a predictive theoretical alternative to simulations in predicting trends and establishing the molecular level mechanisms governing adsorption and diffusion in nanopores. This thesis developed and examined an analytical theory based on fundamental principles of statistical mechanics. The theory has the potential of displacing simulations and integrating into process simulation packages to investigate novel adsorbent-adsorbate systems currently of interest in several industrial applications. However, as mentioned before in this thesis, further efforts need to be directed in certain areas to improve the model and provide better visibility. This topic is addressed in the following section.

6.2 FUTURE WORK

6.2.1 Inclusion of percolative effects in the diffusion theory

Chapter 3 described the diffusion component of our lattice theory. The theory calculated a mean diffusivity that is basically the local diffusivities weighted by their respective distribution of adsorbates. However, we neglected to incorporate the global distribution of adsorbates that can result in a percolation threshold. Our diffusion model assumed "blocking" species, in that an adsorbed molecule sitting in a site provided an activation barrier for the neighbor molecule to diffuse in that direction. To include the percolative effects, an Effective Medium Approximation (EMA) can be conducted which would account for the global diffusivity. It is important to mention here that since our "blocking" species are mobile, we may not see an absolute percolative threshold - instead the diffusivities would merely approach zero.

6.2.2 Development of a novel generalized method to model different geometries

The analytical adsorption theory presented in this thesis was developed for single component and binary mixtures in various confined geometries. However, each time a different nanoporous material is investigated, the equations need to be reformulated to solve for the statistical functions. One of the future projects in this area should be to develop a novel generalized method to formulate and code-up equations for arbitrary geometries.

6.2.3 Extension of adsorption theory to multicomponent fluids with more than two species

Chapter 4 of this thesis developed the lattice theory for binary mixtures of small molecules. Preliminary results were presented and discussed. Based on this work, the next step would be to extend the theory to more complex systems (for instance, ternary mixtures). Extending the theory in this direction is non-trivial due to the relatively complex numerical solution techniques required to solve systems of non-linear algebraic

equations. In this work, we presented a novel method of numerically scaling the unknown variables to dimensionless form before solving the system of non-linear equations. Certainly, this technique can be used as a benchmark while addressing these issues.

6.2.4 Investigation of infinite dilution behavior of adsorbate-pore interactions

Chapters 4 and 5 presented comparisons of our theory with simulation data for two different adsorbate-adsorbent systems. We noticed that the adsorbent-adsorbate interactions at infinite loadings were not entirely captured by our theory. Here, our model suffered from an inadequate characterization of the transition from infinite dilution to low density. There might be several unexplored factors causing this problem. One could be that the site volume needs to be a function of the occupancy. However, this analysis is only preliminary, and efforts need to be drawn in this direction to improve the model.

Vita

Mithun Kamat is a native of Mumbai, India. He was born on 20th December 1978. In 2000, he received his Bachelors in Chemical Engineering from the University of Mumbai.

In August 2000, he entered the University of Tennessee as a Master's Student in Chemical Engineering. In the spring of 2002, he also successfully completed a co-op assignment with UTC Fuel Cells, Connecticut.